PROCESS FOR PREPARATION OF TEREPHTHALIC ACID

By

Kelly Knight Miller

A THESIS

Submitted to
Michigan State University
in partial fulfillment of the requirements
for the degree of

Chemistry – Master of Science

2015

ABSTRACT

PROCESS FOR PREPARATION OF TEREPHTHALIC ACID

By

Kelly Knight Miller

One of the world's most widely produced polymers, poly(ethylene terephthalate) (PET), is synthesized via condensation polymerization of ethylene glycol with terephthalic acid and small amounts of isophthalic acid. Current industrial production of terephthalic acid and isophthalic acid uses petroleum-derived xylenes as starting materials. The cost and availability of petroleum varies wildly and unpredictably. In order to stabilize costs associated with the synthesis of terephthalic acid and isophthalic acid, alternative feedstocks must be made available.

A reaction sequence has been elaborated that addresses this need. The starting materials, acrylic acid and isoprene, are reacted in a solvent-free cycloaddition catalyzed by an inexpensive Lewis acid catalyst. Vapor phase aromatization of the resulting cycloadducts affords *para*- and *meta*-toluic acid, which are oxidized to terephthalic acid and isophthalic acid, respectively. Both acrylic acid and isoprene are commercially synthesized from petroleum or shale gas but may also be synthesized from biobased feedstocks. Thus, by diversifying available feedstocks, costs associated with commercial terephthalic acid and isophthalic acid synthesis are stabilized. Moreover, this reaction sequence is the only one reported in the literature to produce both terephthalic acid and isophthalic acid for the manufacture of PET.

TABLE OF CONTENTS

LIST OF TABLES

LIST OF FIGURES

LIST OF SCHEMES

KEY TO ABBREVIATIONS

ATP	adenosine triphosphate
BSTFA	*N,O*-bis(trimethylsilyl)trifluoroacetamide
BTX	benzene, toluene, xylene
4-CBA	4-carboxybenzaldehyde
DCM	dichloromethane
DEHP	di-(2-ethylhexyl)phthalate
DINCH	diisononyl cyclohexane-1,2-dicarboxylate
DMAPP	dimethylallyl pyrophosphate
DMF	2,5-dimethylfuran
DMT	dimethylterephthalate
EMP	Embden-Meyerhof-Parnas
FDCA	2,5-furandicarboxylic acid
GC	gas chromatography
h	hour
HMF	hydroxymethylfurfural
HOMO	highest occupied molecular orbital
3-HP	3-hydroxypropionic acid
3-HPA	3-hydroxypropionaldehyde
HPLC	high performance liquid chromatography
HTI	high temperature isomerization
IPA	isophthalic acid

IPP	isopentenyl diphosphate
LTI	low temperature isomerization
LUMO	lowest unoccupied molecular orbital
MAO	methylaluminoxane
MEP	5-methyl erythritol phosphate
min	minute
MVA	mevalonic acid
PBT	poly(butylene terephthalate)
PEF	poly(ethylene furandicarboxylate)
PEP	phosphoenolpyruvate
PET	poly(ethylene terephthalate)
PK	phosphoketolase
PP	pentose phosphate
PS	polystyrene
PTA	purified terephthalic acid
PTFE	polytetrafluoroethylene
PVC	poly(vinyl chloride)
SAPO	silicoaluminophosphate
STDP	selective toluene disproportionation process
THF	tetrahydrofuran

CHAPTER ONE

1. INTRODUCTION

> "Je désignerai le premier de ces acides, celui qui est insoluble, sous le nom d'*acide téréphtalique*. (I will refer to the first of these acids, one that is insoluble, as the *terephthalic acid*; translation mine)."[1]
>
> - Amédée Cailliot, 1847, discoverer of terephthalic acid

Purified terephthalic acid (PTA, Figure 1) is an aromatic diacid used in the manufacture of poly(ethylene terephthalate) (PET) by condensation polymerization with ethylene glycol.[2-4] It was first synthesized in 1847 by the French chemist, Amédée Cailliot, by treating turpentine with nitric acid.[1] Since its discovery, terephthalic acid has become one of the most important large-volume commodity chemicals in the world. In 2012, the global consumption of terephthalic acid was around 47 million tons, nearly all of which went into the manufacture of PET.[5] Poly(ethylene terephthalate) is one of the most ubiquitous industrial polymers with applications in clear bottles for beverages, molded containers and other packaging materials, as well as polyester films and fibers.[5]

Terephthalic acid is commercially prepared via the oxidation of *para*-xylene. Xylene isomers, *ortho*-, *meta*-, and *para*- (Figure 1), are dimethylated aromatic compounds that make up part of a highly valued cut of fossil fuel-derived aromatics called BTX (benzene, toluene, xylenes). The isolation of BTX from fossil fuel resources will be discussed later in this chapter. Xylenes are typically oxidized to higher value products which means the importance of a particular xylene isomer parallels the market value of the oxidized product. Terephthalic acid is the most valuable chemical made from xylenes, thus *p*-xylene is the most highly desired isomer.

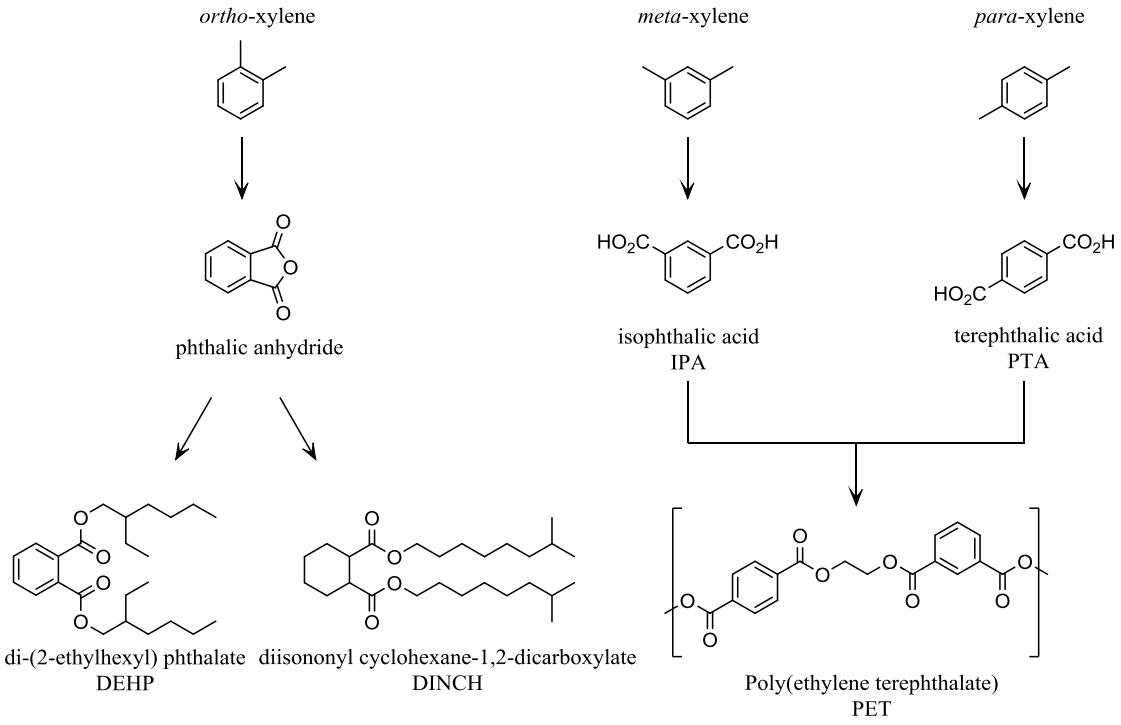

Figure 1. Oxidation of petroleum derived xylene isomers.

2. PRODUCTS FROM OXIDATION OF XYLENES

2.1. *ortho*-xylene

ortho-Xylene is principally used in the manufacture of plasticizers via its oxidation to phthalic anhydride (Figure 1).[6,7] Vapor phase oxidation of the *ortho*-substituted methyl groups occurs between 375-410°C over a heterogeneous Lewis acid catalyst in multitubular fluidized bed reactors. Fluidized bed reactors, in which a high velocity gaseous feed stream suspends catalyst particles in the reactor bed as though they were a fluid, offers better temperature control and less risk of explosion than one in which a fixed bed of solid catalyst is used.[6] Early catalysts developed by BASF and Oronite Chemical Co. (Standard Oil) were based on vanadium pentaoxide (V_2O_5). Modern catalysts are composed of 2-15 wt% V_2O_5 supported on titania (TiO_2)-coated spherical pellets made from porcelain, magnesium silicate, quartz, and silicon carbide.[8] These catalysts are often doped with potassium sulfate (K_2SO_4) to improve selectivity. Liquid phase oxidation is also known and typically offers high selectivity and conversions. However, as it involves purification steps and large amounts of solvents, this method is less attractive than vapor phase oxidation.[8]

Phthalic anhydride is used to make plasticizers which help to make resins more flexible and easier to process.[6,7] Phthalate esters satisfy the broadest range of performance and processing requirements at the lowest cost compared to other types of plasticizers and are therefore one of the more commonly utilized plasticizer classes.[7] Phthalic anhydride is esterified with two equivalents of a short-chain diol to produce several general-purpose phthalates including di-(2-ethylhexyl) phthalate (DEHP, Figure 1) and diisononyl phthalate.[6,7] Although DEHP was once the international standard PVC plasticizer, it is scheduled to be phased out of the European Union by February 2015 due to toxicity issues.[7] Many *ortho*-substituted, short-

chain aromatic polyesters have toxicity associated with their binding to endocrine receptors. Generally, the shorter the alkyl ester, the more toxic the phthalate plasticizer. Diisononyl cyclohexane-1,2-dicarboxylate (DINCH, Figure 1), produced by BASF and Evonik, is synthesized by hydrogenating the aromatic core of diisononyl phthalate.[6,7] Saturated polyesters of this type are nontoxic and becoming more prevalent in consumer products. The American toy company Mattel, for instance, has begun replacing phthalate plasticizers with DINCH.[7]

2.2. *meta*- and *para*-xylene

Both *meta*- and *para*-xylenes are used in the manufacture of polyester resins upon being oxidized to isophthalic acid (IPA) and PTA (Figure 1). Isophthalic acid is commonly used in unsaturated resins because of its ability to provide stronger, more corrosion resistant polymers than phthalic acid.[8] PET contains approximately 3-5% by weight of IPA.[9] The glass-like clarity of PET is due to the incorporation of a small amount of a 1,3-substituted diester into an otherwise linear polymer chain. This creates a geometrical deformation in the chain that partially inhibits crystallization, which improves transparency and lowers the melting point of PET.

Liquid phase oxidation of *meta*- and *para*-xylenes is commercially performed using modified conditions from a patent by the Mid-Century Corp. (Amoco).[10] A high pressure reactor is charged with xylene substrate and catalyst mixture in acetic acid before being pressurized to 15-30 bar with compressed air and heated to 175-225°C.[11] The catalyst system is a mixture of cobalt and manganese acetates with a bromine compound such as sodium bromide.[11,12]

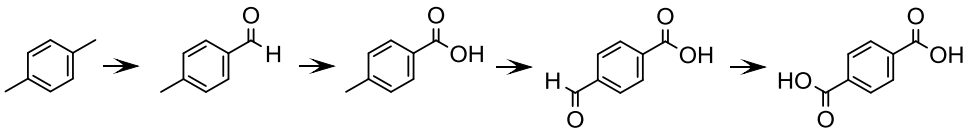

1 **2** **3** 4-CBA PTA

Scheme 1. Reaction scheme of Amoco Mid-Century oxidation of *p*-xylene **1** to terephthalic acid.

Oxidation of *p*-xylene **1** to PTA involves several intermediates as shown in Scheme 1. Most oxidations of aromatic methyl groups follow the Hammett structure-reactivity relationship:

$$\log(k/k_0) = (\sigma)(\rho) \quad (1)$$

where k = rate constant for the consumption of a given compound, k_0 = the rate constant for the consumption of toluene, σ = the characteristic constant for a ring substituent, ρ = the characteristic constant for a set of reaction conditions. Many ρ values for metal/bromine catalyzed oxidations have been reported and most fall in the range of -0.6 to -1.3.[11] Industrially, most Amoco Mid-Century oxidations occur in 90% acetic acid solutions with 10% water. These conditions offer ρ values of -0.95.[11] Equation (1) explains why the oxidation of *p*-xylene **1** occurs consecutively, with the complete oxidation of one methyl group occurring before the other. After the first methyl substituent reaches the carboxylic acid stage, the σ value for the *para*-methyl group changes from -0.3 to +0.4, indicating a reduction in the ring electron density which causes the second methyl oxidation to proceed 4.9 times slower than the first.[11,12]

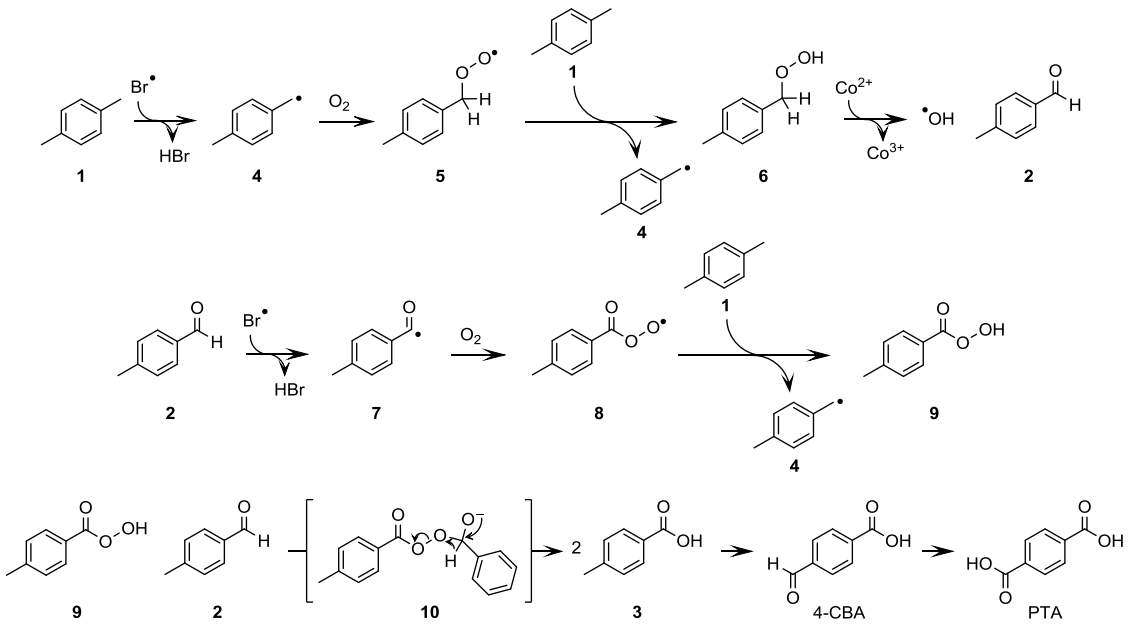

Scheme 2. Aerobic oxidation of *p*-xylene **1** to terephthalic acid.

A detailed mechanism of the oxidation of *p*-xylene **1** to PTA is depicted in Scheme 2. The reaction is a radical process involving peroxy and peracid intermediates.[12] A bromine atom abstracts a methyl group hydrogen atom from *p*-xylene **1** forming a *p*-methylbenzyl radical **4**, a proton, and bromide. This newly formed intermediate **4** reacts with molecular oxygen to form a peroxide intermediate **5**. Co^{II} becomes oxidized to Co^{III} as it decomposes peroxide **6** to *p*-tolualdehyde **2**. A second initiation step is promoted by a bromine radical which abstracts the aldehydic proton from *p*-tolualdehyde **2**. This newly formed radical **7** subsequently reacts with molecular oxygen to afford a peracid **9** which then reacts with another molecule of *p*-tolualdehyde **2** in a Baeyer-Villiger reaction to produce two molecules of *p*-toluic acid **3**. The second aromatic methyl group is oxidized in the same manner as the first to afford PTA.[12] Mn^{II} is oxidized by Co^{III} regenerating the Co^{II} species and affording Mn^{III}. This is reduced back to Mn^{II} in the reaction with bromide to produce a bromine radical (Scheme 3).

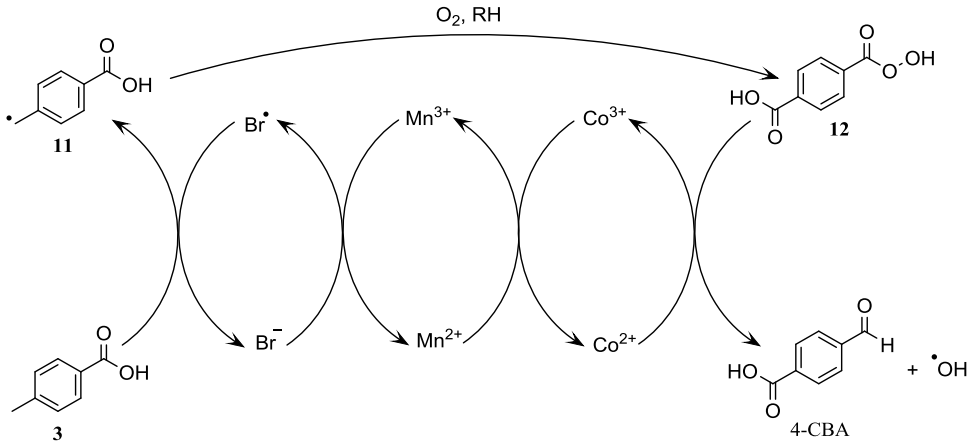

Scheme 3. Catalytic pathway for Amoco Mid-Century oxidation of aryl methyl groups.

Besides PTA, at least thirty two different byproducts have been reported in the Amoco Mid-Century oxidation of *p*-xylene **1** though most occur in less than 0.1% yield. Major byproducts include methane, CO_2, methyl acetate, and two intermediates associated with the incomplete oxidation of the second methyl group: *p*-toluic acid **3** and 4-carboxybenzaldehyde (4-CBA, Scheme 2).[11,12] 4-Carboxybenzaldehyde (4-CBA, Scheme 2) is a problem because it serves as a chain terminator in the polymerization of PTA to PET and therefore significant effort has been expended to eliminate this byproduct. Crude PTA typically containing around 0.3% by weight of 4-CBA is dissolved in water at 285°C and 90 bar and sent into a trickle-bed reactor.[13] The PTA crude flows down a Pd/C catalyst bed while a gaseous H_2 stream moves upward. Hydrogen reduces 4-CBA to *p*-toluic acid **3** which has a higher solubility in water than PTA. Terephthalic acid precipitates from solution outside the reactor while *p*-toluic acid **3** is recycled.[13] The hydrogenolysis of 4-CBA to *p*-toluic acid **3** made the production of PTA of polymer-grade purity possible. Prior to this development, PTA had to be esterified with methanol and the resultant dimethyl terephthalate (DMT) purified by distillation to achieve polymer-level purity. Now, all new facilities produce PTA as DMT is phased out.[14] While PTA

is pushing DMT out of the PET market, DMT still finds use in engineering resins such as polybutylene terephthalate (PBT). In the instance of PBT, terephthalic acid as a Bronsted acid catalyzes the cyclization of 1,4-butanediol to tetrahydrofuran (THF) thus requiring the use of non-acidic DMT.[15]

While the Amoco Mid-Century process of oxidizing aromatic methyl groups is efficient and very widely used, it does have some disadvantages. The most significant problem is the oxidation of the acetic acid solvent to methane and carbon dioxide.[11,13] As shown in Scheme 4, Kolbe chemistry is responsible for the decarboxylation of acetic acid to produce carbon dioxide and a methyl radical. This methyl radical is then able to participate in chain propagation reactions to form methane. The acetic acid that is converted to methane and carbon dioxide must be supplemented with fresh acetic acid added to the reactor.

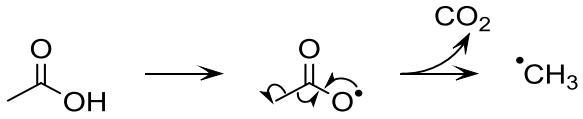

Scheme 4. Kolbe decomposition of acrylic acid.

Not only does this decomposition increase the overall amount of solvent used in the process, but it is an unnecessary waste of carbon. For every 1000 kg of PTA produced, 165 kg of carbon dioxide is generated as a byproduct with 60% of this carbon dioxide generation due to degradation of acetic acid.[13] Furthermore, the highly corrosive reaction medium requires the use of reactors constructed from expensive titanium. It would be advantageous to develop a process to PTA that achieves high selectivity without the challenges of the Amoco Mid-Century oxidation. Important developments in this area will be presented later in the chapter.

3. FOSSIL FUEL FEEDSTOCKS

3.1. Natural and unconventional gas

Table 1. Typical composition of raw natural gas.

Component	Percentage
Methane	70-98
Ethane	1-10
Propane	0-5
Butanes	0-2
Pentanes	0-1
H_2	0-15
CO_2	0-1
H_2S	0-5
Noble gases	0-8

Gaseous sources of hydrocarbons including natural gas and shale gas are rich sources of hydrocarbons suitable for the manufacture of commodity chemicals such as PTA. Natural gas is used for heating and generating electricity but can also be used for the manufacture of chemicals. Nearly all of natural gas is methane but ethane, propane, and higher hydrocarbons may also be present (Table 1).[16] Carbon dioxide and hydrogen sulfide are chief contaminants of natural gas wells. Some natural gas reserves are trapped in the pores of underground rock beds far deeper than natural gas reserves. Such reserves are referred to as unconventional gas. Unconventional gas that is trapped in layers of shale rock is called shale gas and is the most prevalent source of fossil fuel hydrocarbons in North America. The composition of shale gas is similar to natural gas but may differ dramatically from one wellhead to another (Table 2).[17] Because shale gas is trapped in impermeable pores of shale rock much deeper in the earth's crust than natural gas plays, new technologies had to be developed to access it. Hydraulic fracturing, or fracking, combined with horizontal drilling was developed explicitly for this purpose.[18] A well is drilled into the earth until it reaches a horizontal layer of shale rock. The well bore is turned ninety

degrees and drilling subsequently proceeds horizontally through the shale layer which ensures a much greater recovery of gas than a vertical well. A cement casing surrounds the vertical portion of the well while the horizontal portion is encased by a steel casing equipped with explosive charges. Detonation of the charges in the horizontal section of the well create large fractures in the shale rock. The fractures would normally immediately close due to high pressures within the earth, but highly pressurized water pumped into the well keeps the fractures open. The water contains fine-grained silica (SiO_2) and other chemicals that prevent the fractures from closing once the water pump is turned off. When the water pressure is reduced, a gas flows through the open fractures and into the well.[18] Hydraulic fracturing has allowed access to some of the most productive gas plays in the world including Marcellus, Utica, Barnett, Eagle Ford, and Bakken plays in North America. However, fracking may be a public safety concern as areas with high concentration of shale gas wells are suspected to be linked to increased seismological activity.[19]

Table 2. Composition of Marcellus shale gas reserve in Appalachia.

Component	Mol percentage
Methane	76.9
Ethane	13.4
Propane	4.5
Butanes	1.6
Pentanes	1.3
CO_2	1.0
N_2	1.0

C_2-C_6 and higher chain length hydrocarbons are valued components of natural and shale gases. They are separated from methane by compressing the raw gas and passing it through cold *n*-hexane to produce a liquid stream that can be fractionated by distillation. The C_2-C_6

compounds that are isolated in this manner are thereafter referred to as gas liquids.[20] Those technologies that produce aromatics from natural gas liquids will be discussed in section 3.3.3. Yields of BTX obtained from shale gas are lower than if obtained from petroleum.

3.2. Petroleum

Crude oil contains a wider distribution of hydrocarbons than natural gas or shale gas. Organic compounds including steroids and fatty acids are held for millions of years under high pressures within the earth to form an oil in which molecules containing forty or more carbon atoms may be present.[21,22] In order for crude oil to serve as a useful source of hydrocarbons for the chemicals industry, it must first be separated into fractions of similar boiling points. Table 3 shows characteristic properties of petroleum fractions from a Middle-Eastern crude oil.[23] Each fraction contains a different distribution of paraffins, aromatics, and naphthenes (cycloaliphatics) than the others.

Table 3. Characteristic data of a Middle-Eastern petroleum reserve.

Primary fraction	Percentage by volume	Boiling range (°C)	Paraffins (vol%)	Naphthenes (vol%)	Aromatics (vol%)
Light naphtha	7.9%	20-100	89.6%	9.5%	0.9%
Heavy naphtha	6.8%	100-150	70.3%	21.4%	8.3%
Kerosene	12.5%	150-235	58.0%	23.7%	18.3%
Light gasoil	16.4%	235-343	--	--	--
Heavy gasoil	26.3%	343-565	--	--	--
Residual oil	26.8%	>565	--	--	--

Prior to distillation, sodium, calcium, and magnesium chlorides and sulfates must be removed in order to prevent corrosion of pipelines and reactor equipment.[22] These salts occupy an aqueous phase that is coproduced with the crude oil as it forms inside the earth's crust. Desalting the petroleum may involve purely thermal or electrical techniques. Thermal desalting

occurs between 90-150°C at 3.5-17.5 bar.[22] Crude petroleum is passed over a sand or gravel bed which promotes rapid separation and settling of the salt-containing aqueous phase and an organic phase. A more preferred desalting method utilizes a fatty acid, sulfonate, soap, or long chain alcohol to enhance separation of the aqueous phase upon application of an electrical gradient.[22]

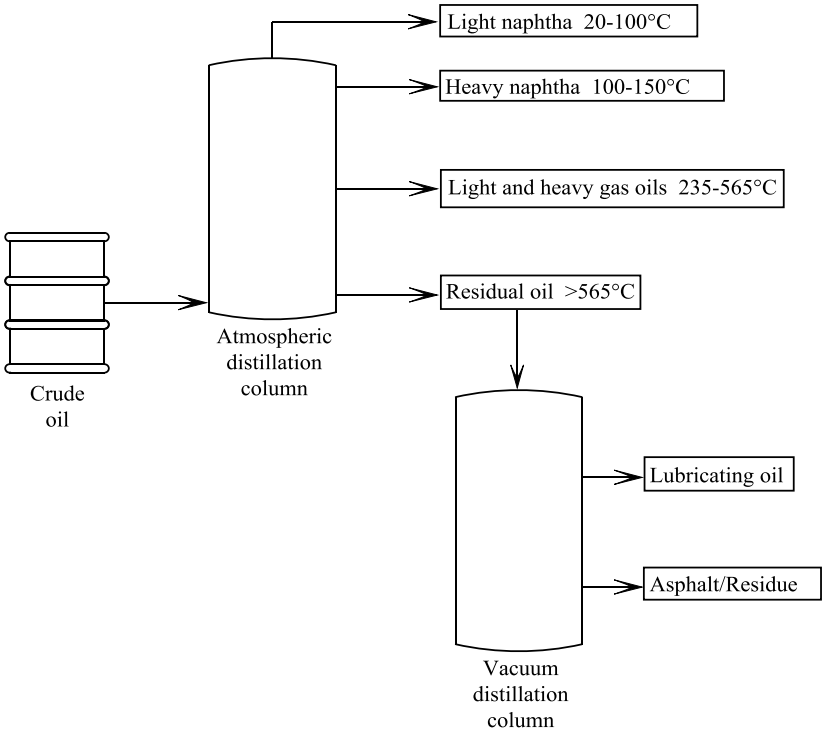

Figure 2. Schematic representation of petroleum distillation.

Once the inorganic contaminants are removed, the crude oil undergoes a primary atmospheric distillation as depicted in Figure 2.[22] The fractionation tower separates light hydrocarbons from heavier gas oils at atmospheric pressure. The crude feed is heated in a preheater to 220-250°C before being injected into a tubular furnace and heated to 360-380°C. This temperature is too low to promote cracking of the heavy hydrocarbon components but does not facilitate their separation from the crude oil. Thus, the heavy bottom products of atmospheric distillation are subjected to further fractionation at pressures below 1 bar.[22]

Vapors coming off the top of the distillation column are composed of methane, and C_2-C_4 hydrocarbons similar to the gas liquids stream that comes off shale gas wells. Methane and ethane may be separated from liquefied petroleum gas (C_3 and C_4 hydrocarbons) under pressure. C_5-C_7 hydrocarbons are referred to as a condensate and may be present in the top vapors or, more commonly, distilled as a side stream.[22] The condensate is primarily composed of aliphatics and mono- and dimethylated cyclopentanes but may also contain other polymethylated cyclopentanes and cyclohexanes (naphthenes, Table 3). Together, C_1 to C_7 hydrocarbons are called light naphtha (Table 3) and although the aromatic content is below 1%, the condensate may be converted to BTX by several processes as will be discussed in section 3.[22]

The side streams of atmospheric distillation, heavy naphtha, kerosene, and light and heavy gas oils, are separated in stripping columns where the lower boiling components are removed by injection of superheated steam. As shown in Table 3, aromatic content increases with higher boiling point. BTX is either isolated or synthesized from fractions boiling at or below 235°C while residual oils, which are separated in a vacuum distillation column, and gas oils contain high concentrations of polynuclear aromatics. Gas oils and the fractions coming from vacuum distillation are used for lubricating oils and bunker fuels while commodity chemicals are made from atmospheric distillation fractions.[22,23]

3.3. Secondary petroleum refining to BTX

Primary petroleum fractions from distillation are further refined in an effort to maximize yields of desired hydrocarbons. Two strategies have been developed for the isolation of BTX from crude oil: thermal or catalytic cracking of naphtha, which is the preferred strategy in

Europe; and catalytic reforming of light naphtha or natural gas, which is the dominant practice in North America.

3.3.1. Thermal and catalytic cracking

Thermal cracking of naphtha with superheated steam is a versatile method to produce a wide variety of hydrocarbons depending on the temperatures used. At 750°C or higher, steam cracking of naphtha favors the production of branched olefins and aromatics while milder temperatures of 450°C-550°C favor branched aliphatics.[24] Figure 3 shows a flow diagram for a naphtha cracker unit. The feed is initially vaporized at 600°C in a series of tubes within a furnace (**1**, Fig. 2) where it is mixed with steam in a 2:1 ratio by weight.

Steam is used to reduce the partial pressures of the hydrocarbons in the feed. Lower partial pressures favor cracking reactions over oligomerization and coke formation.[25] The combined feed stream enters the first of several reactor tubes arranged in parallel inside the furnace heated to about 800°C. Cracked products exiting the reactor must be quickly quenched in heat exchangers (**b**, Fig. 3) to stop the cracking reactions and provide heat that can be used to generate the required superheated steam.[25] Cooled products are separated into light and heavy components in fractionation columns. Primary fractionation (**d** and **e**, Fig. 3) separates water and inorganic acid gases such as hydrogen sulfide from the hydrocarbon effluent.[24,25]

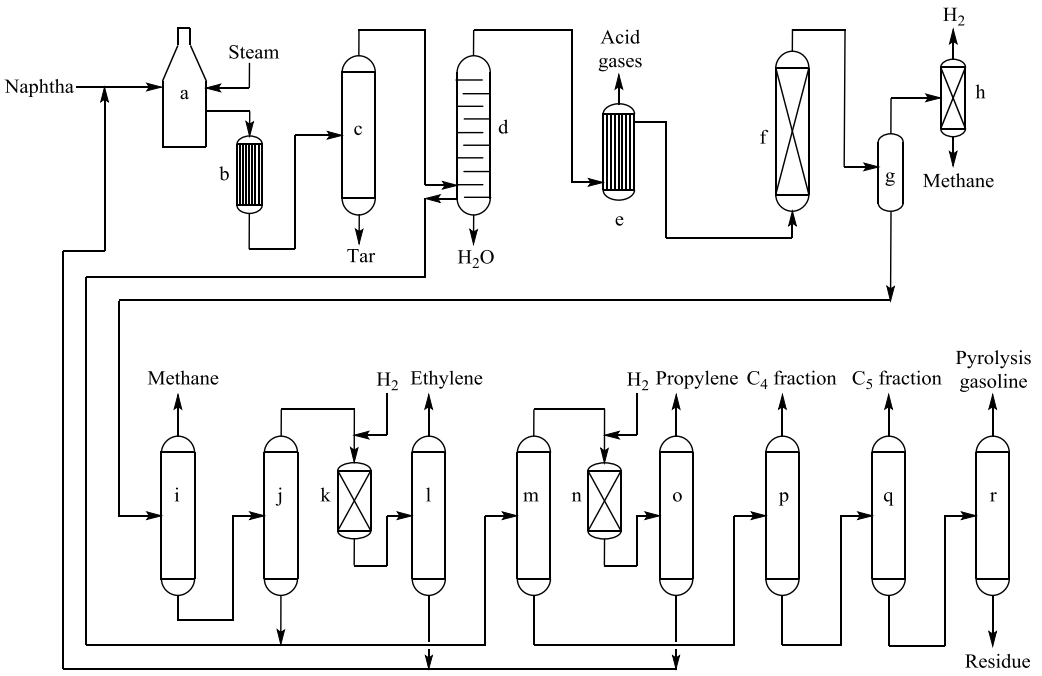

Figure 3. Flow diagram for naphtha steam cracking unit, a) cracking furnace; b) quenching cooler; c) primary fractionation; d) quench column; e) gas purification; f) drier; g) low-temperature cooler; h) hydrogen/methane separation; i) demethanization column; j) deethanization column; k) acetylene hydrogenation; l) ethylene column; m) depropanization column; n) methylacetylene hydrogenation; o) propylene column; p) debutanization column; q) depentanization column; r) residue column.

A series of fractionation columns (**i**-**r**, Fig. 3) selectively isolates compounds based on their carbon content; for example, the depropanation column separates all C_3 compounds from the product effluent.[25] The fraction containing the highest concentration of aromatics is called pyrolysis gasoline or "py gas." As shown in Table 4, the py gas stream is far richer in benzene than in xylenes (40% benzene, 20% toluene, 4% xylenes).[25] Higher aromatics, such as mesitylene and other polyalkylated aromatics, are formed in low yields (around 3%, Table 4) while paraffins make up the second largest component of a steam cracking product stream (around 30%, Table 4).[24,25]

Table 4. Typical composition (wt%) of reformate from catalytic reforming and pyrolysis gasoline from thermal cracking of naphtha.

Product	Reformate gasoline	Pyrolysis gasoline
Benzene	3	40
Toluene	13	20
Xylenes	18	4-5
Ethylbenzene	5	2-3
Higher aromatics	16	3
Paraffins	45	28-31

Because steam cracking is a purely thermal process, heat is used to cleave C-H and C-C bonds. Homolytic bond cleavage is more energetically favorable in the gas phase than heterolytic cleavage, thus the reactions involved in steam cracking are radical reactions.[24] At sufficiently high temperatures (around 750°C) alkyl radicals may eliminate a hydrogen radical to produce an olefin, or may polymerize to form larger hydrocarbons. At more mild temperatures (around 500°C) alkyl radical coupling is more prevalent than hydrogen radical abstraction to form olefins. Paraffinic products exhibit a high degree of branching due to radical termination between alkyl radicals. Furthermore, olefins may cyclize and dehydrogenate to form aromatic products.[24]

Catalytic cracking produces a similar distribution of aromatic, olefinic, and branched aliphatic products to steam cracking but operates under milder conditions than steam cracking.[26,27] Naphtha is passed over a zeolite catalyst in a fluidized bed reactor (Figure 4) operating at 480-530°C. Unlike steam cracking, reactions involved in catalytic cracking operate via a carbonium ion mechanism. However, both steam and catalytic cracking produce highly branched paraffins and aromatic products.[24] In a typical procedure, the naphtha feed and steam mixture is directed into a riser (**d**, Fig. 4) where it meets hot regenerated catalyst delivered through a standpipe ($\mathbf{e_1}$, Fig. 4) from the catalyst regenerator (**c**, Fig. 4).[27] The catalyst and feed

admixture rises into the reactor (**a**, Fig. 4) whereupon spent catalyst is removed from the hydrocarbon effluent in a stripping section (**b**, Fig. 4). Spent catalyst is passed through a standpipe (**e**$_2$, Fig. 4) to the regenerator where any remaining hydrocarbons are removed in a cyclone separator (**f**, Fig. 4).[27]

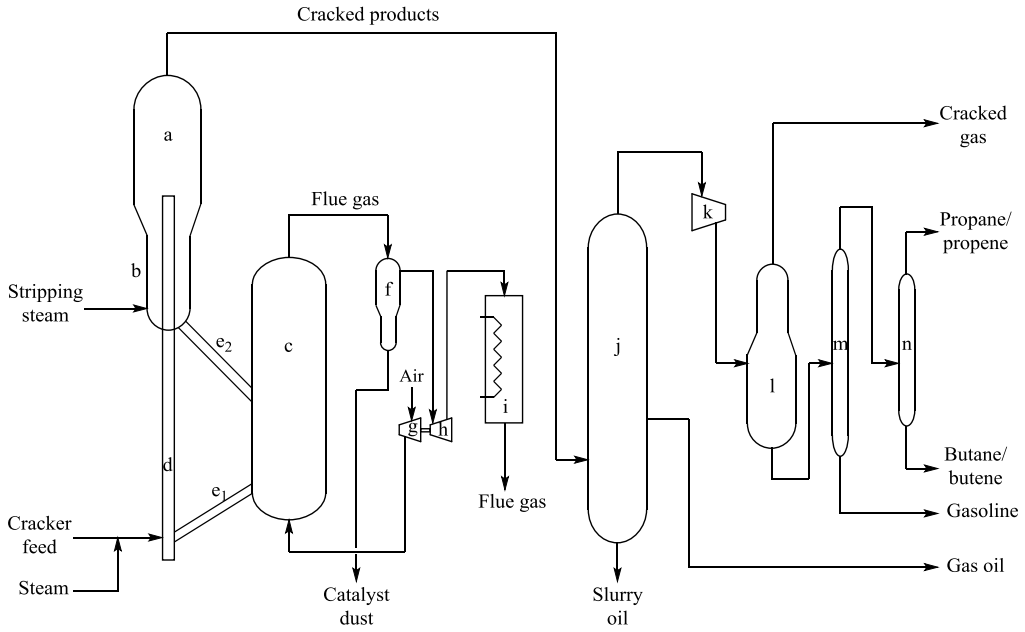

Figure 4. Conventional catalytic cracking unit, a) reactor; b) stripper; c) regenerator; d) riser; e_1) regenerator standpipe; e_2) stripper standpipe; f) cyclone vessel; g) air blower; h) flue gas expander; i) waste-heat boiler; j) fractionating column; k) compressor; l) absorber; m) debutanizer; n) depropanizer.

Cracked products from the top of the reactor are passed into a series of fractionation reactors that separate the effluent into flue gas (hydrogen, methane, ethane, ethylene, hydrogen sulfide), liquefied petroleum gases (propane/propene and butane/butene), gas oils and slurry oils.[27] Gas oil fractions contain aromatic products while the slurry oil is recycled as it contains small amounts of catalyst dust. Gasoline fractions contain C_5 and C_6 compounds analogous to the condensate from petroleum distillation. The presence of a catalyst allows the process to be operated at lower temperatures than those used in steam cracking, from around 800°C to around

500°C.[24,26,27] This potential advantage is somewhat offset by the problem of coking which requires periodic shutdown of the reactor to regenerate the active catalyst.[26,27]

3.3.2. Catalytic reforming

Naphtha may be catalytically reformed to aromatics and small olefins in a manner complementary to the cracking technologies mentioned above.[26,28,29] Naphtha is first heated to 510-540°C and pressurized to 15-25 bar before being passed over a bimetallic catalyst in a series of reactor zones. Figure 5 depicts a process employed by UOP.[28,29] Naphthenic compounds with six or more ring carbons are dehydrogenated to aromatics in the first reactor (**c**, Fig. 5). Methylated cyclopentanes undergo isomerization and dehydrogenation to aromatic compounds in a second reactor (**e**, Fig. 5). Acyclic alkanes are isomerized and cracked in a third reactor (**g**, Fig. 5) to afford branched alkanes and olefins.

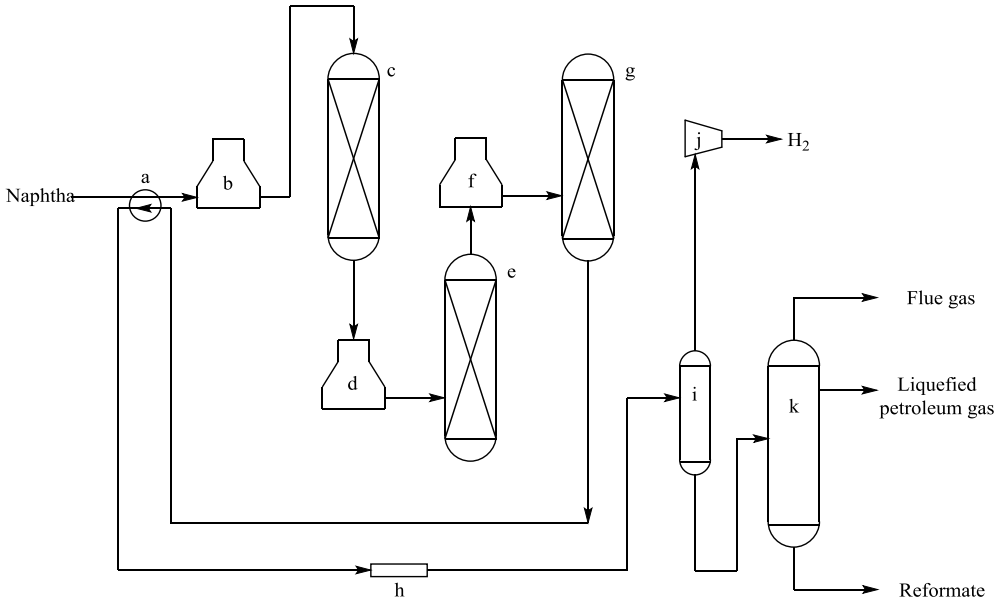

Figure 5. Flow diagram for a catalytic reformer, a) heat exchanger; b) feed heater; c) first reactor; d) first intermediate heater; e) second reactor; f) second intermediate heater; g) third reactor; h) product cooler; i) product separator; j) recycle gas compressor; k) stabilizer.

Reformed products are separated downstream in fractionation columns to afford hydrogen and flue gas, C_3 and C_4 compounds that make up liquefied petroleum gas, and a reformate. The reformate is the cut which contains the highest concentration of aromatic products. Contrary to pyrolysis gas, BTX within the reformate is rich in xylenes (13%) and poor in benzene (3%) (Table 4). This difference is important because most of the methods available to increase overall xylene yields from a BTX cut utilize toluene or xylene isomers rather than benzene (see section 3.4.2).[26,28]

Catalysts used in naphtha reforming are heterogeneous solids comprising an acid component such as silica-alumina (SiO_2/Al_2O_3) and a dehydrogenating metal such as Pt.[24] Chevron has developed a Rheniforming process in which Pt is doped with Re to promote dehydrogenations and prevent sintering of Pt under the reaction conditions.[30] Though the catalysts used in naphtha reforming are robust, coking does occur and the catalyst must be regenerated by burning in air.[30] A swing reactor is commonly used in which spent catalyst is regenerated in a second reactor chamber that runs in tandem with the reforming reactor. This keeps the reforming process continuous.

3.3.3. Cyclar and Aromax reforming of light hydrocarbons

Aromatic materials are isolable from light (C_1-C_6) and heavy (C_7-C_{10}) naphtha cuts. Two important technologies in this field are the Cyclar process[31-34] (BP and UOP) and the Aromax process[35-37] (Chevron-Phillips). In the Cyclar process, ultralight naphtha (C_1-C_4) and naphtha condensate (C_5-C_6) is passed over a gallium-containing ZSM-5 zeolite catalyst at temperatures of at least 425°C in a series of radial-flow reactors (Figure 6) in which the feed is distributed along the entire reactor and flows radially across several circular catalyst beds.[31-34]

Reactor chambers are arranged in a vertical stack (**c**, Fig. 6) with multiple circular catalyst beds.[38] The feed is distributed along the length of the stack but initially is confined to the center of the catalyst beds. The feed moves radially across the beds of catalyst toward the reactor walls. The effluent is kept at the reaction temperature using a series of interheaters (**b**, Fig. 6). The product stream exiting the last reactor is split into gaseous and liquid products in a gas-liquid separator (**e**, Fig. 6). Vapor products are captured in a cryogenic recovery unit (**g**, Fig. 6) and are comprised of methane and ethane from hydrocracking side reactions, hydrogen from dehydrogenation reactions, and a recycle stream of unconverted propane and butane. Liquid products are sent to a stripper column (**f**, Fig. 6) to remove light olefins from aromatic products.[38]

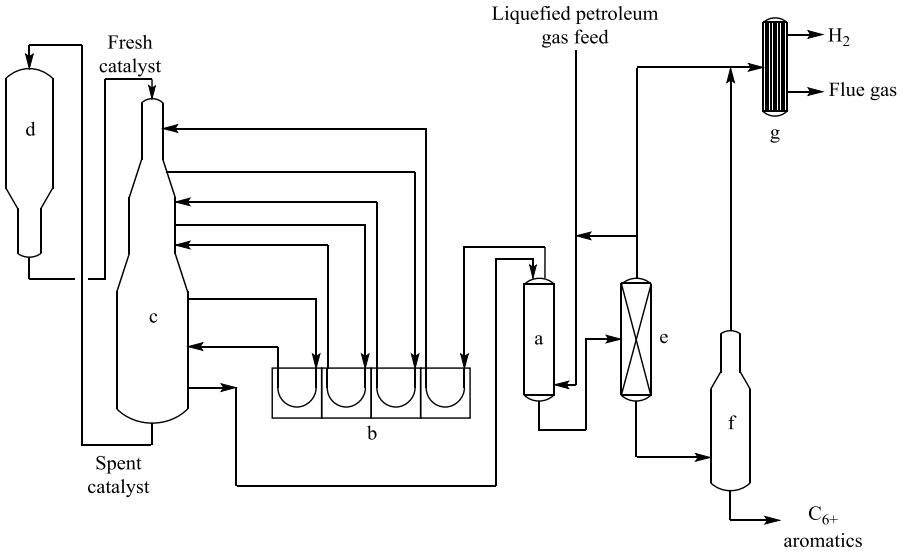

Figure 6. Flow diagram for Cyclar reforming of light naphtha, a) feed exchanger; b) fired heaters; c) stacked reactor; d) catalyst regenerator; e) product separator; f) stripper; g) acid recovery.

A series of reactions collectively termed dehydrocyclodimerization are responsible for the conversion of C_4 and smaller hydrocarbons to BTX.[34] The first reaction of the series is a rate limiting dehydrogenation of alkanes to mono-olefins. These olefins quickly oligomerize to form

larger intermediates that then cyclize to naphthenic compounds. Dehydrogenation of the naphthenic intermediates affords 58-60% yield by weight of BTX.[34] Aromatic yield increases with increasing carbon number of the feed. As such, a 66% yield of BTX can be achieved with an all butane feed. For a more usual mixed feed stream, aromatic product composition is around 43% toluene, 28% benzene, 22% xylenes, with the remaining 7% comprising C_{9+} aromatics and bicyclic compounds.[39] An advantage of the Cyclar process is its ability to use naphtha from petroleum as well as the large amounts of methane and liquefied petroleum gas from natural gas or shale gas.[31-34]

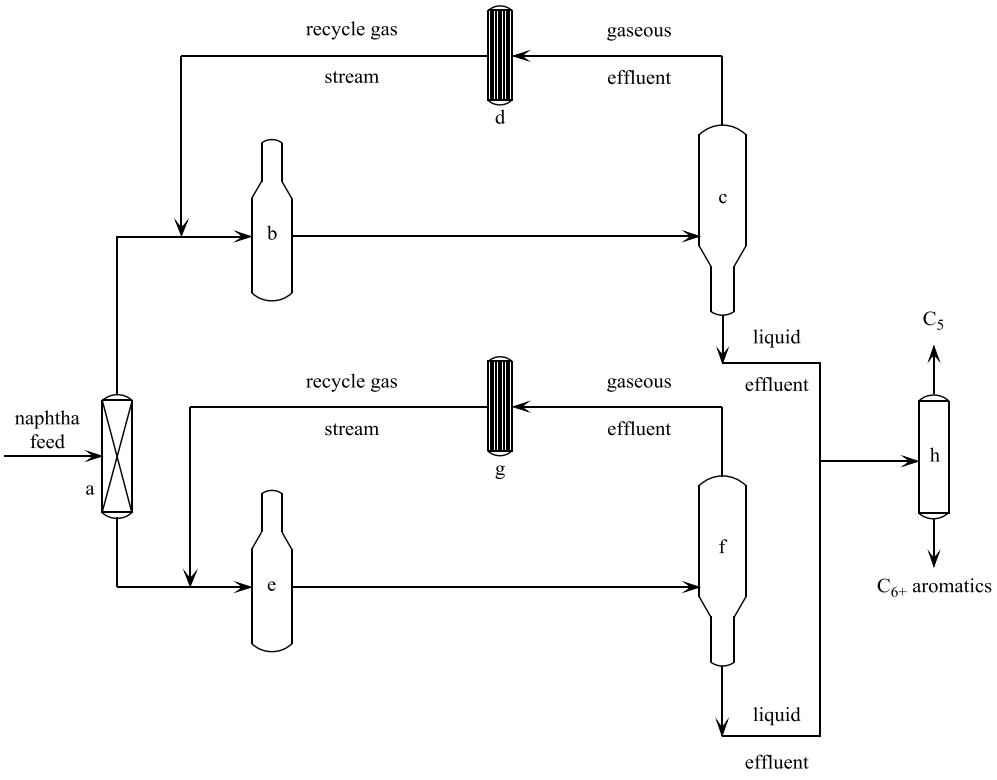

Figure 7. Flow diagram for Aromax reformer, a) C_7/C_8 splitter; b) Aromax reformer; c) gas-liquid separator; d) recycle gas compressor; e) secondary reformer; f) gas-liquid separator; g) recycle gas compressor; h) depentanizer.

The Aromax process (Chevron-Phillips) is also based on a zeolite catalyst and is capable of reforming C_6-C_{10} hydrocarbons to a BTX stream rich in benzene (40-60% by weight).[35-37,40]

This methodology converts a broad boiling range C_6 to C_{10} naphtha to a product stream comprised of 40-60% by weight of benzene.[40] Toluene is also produced but the yield of xylenes is low, hence, this process is best suited for recovery of benzene from naphtha. Figure 7 depicts the reactor flow diagram for the Aromax process.[35] The C_6 to C_{10} feed is first fed into a C_7/C_8 splitter column (**a**, Fig. 7). The overhead stream is predominantly C_6 and C_7 hydrocarbons that are sent to an Aromax reformer (**b**, Fig. 7) containing a Pt/K/Ba-doped L-zeolite catalyst (Aromax trademark).[35-37]

The effluent is sent to a separator (**c**, Fig. 7) to separate a gaseous effluent from the liquid stream before compressing the gaseous effluent in a recycle compressor (**d**, Fig. 7). The bottom stream from the C_7/C_8 splitter is principally a C_8 to C_{10} feed and is passed to a secondary reformer (**e**, Fig. 7) containing a Pt-Sn-Cl/Al_2O_3 catalyst.[35] Effluent from this reformer is sent to a gas-liquid separator (**f**, Fig. 7). Gaseous effluent is passed to a recycle compressor (**g**, Fig. 7) and combined with the gas stream from the Aromax reformer and the C_8 to C_{10} gas feed from the C_7/C_8 splitter before being recycled into the secondary reformer. The liquid effluent from the gas-liquid separator (**f**), is combined with the liquid effluent from the Aromax reformer and ultimately passed to a depentanizer (**h**, Fig. 7). The depentanizer removes the C_5 fraction overhead while the C_6 and higher aromatics are passed on for further processing (not shown).[35]

3.4. Isolation of aromatic products

The refining processes described above, thermal cracking, steam cracking, and the various embodiments of catalytic reforming, are used to increase the amount of desired hydrocarbons in a naphtha fraction. These can be considered as secondary refining processes following primary refining via distillation. Irrespective of the refining process used, further

refining is necessary to retrieve the desired products. For the manufacture of PTA, a BTX stream must be separated from nonaromatic hydrocarbons before further refining via processes that maximize yield of *p*-xylene (**1**, Scheme 1) within the BTX stream.

3.4.1. Separation of aromatic compounds from nonaromatic hydrocarbons

After primary fractionation of a fossil fuel feedstock, aromatic products must be separated from C_4-C_{10} non-aromatic hydrocarbons in naphtha before isolation of individual components. Conventional fractional distillation is impractical because certain non-aromatic alkanes, like cyclohexane and *n*-heptane, form azeotropes with aromatic compounds such as benzene and toluene. Furthermore, there is a very small difference in boiling point between C_8 aromatics (Table 5) which makes separation of each of these components very difficult by conventional distillation.[41]

Table 5. Boiling points of C_8 aromatic compounds.

Product	b.p. (°C)
Ethylbenzene	136.2
p-xylene	138.3
m-xylene	139.1
o-xylene	144.4

Several techniques for the separation of aromatic and non-aromatic hydrocarbon products have been developed and one of the most common is azeotropic distillation of pyrolysis gas.[41] Polar solvents such as amines, ketones, alcohols or thiols, or water are added to the feed mixture in order to selectively remove non-aromatic alkanes as low boiling azeotropes.[41,42] These distill overhead while the aromatic components remain on the bottom of the distillation chamber. Acetone or methanol are the most widely used solvents and are ultimately removed from the non-aromatic cut by extraction with water. The advantage of this process lies in the fact that the

bulk material does not need to be volatized, thus is best suited for fractions with high aromatic content ($\geq$90%).[41]

Extractive distillation, whereby a solvent selectively solubilizes aromatic compounds instead of aliphatics, is utilized when the pyrolysis gas is richer in non-aromatic compounds (65-90% aromatic content). Suitable solvents include *N*-methylpyrrolidine, *N*-formylmorpholine, dimethylformamide, sulfolane, di- and trichlorobenzenes, benzyl alcohol, polyglycols, phenols, amines, and nitriles.[41-44] Non-aromatic compounds are distilled overhead as the solvent and aromatic components are removed at the bottom. The solvent is extracted in a stripping column with the use of steam. Isolated aromatics are treated with Fuller's earth to improve color and remove traces of olefinic material.[41-44]

Liquid-liquid extraction is a more common method of isolating aromatic material and is suited for reformates with low aromatic content (20-65%).[41,45,46] In a liquid-liquid extraction, two solvents are used, one to extract the aromatic components and the other to solubilize non-aromatic hydrocarbons. The properties of each solvent must be such that a readily separable system of two liquids is maintained.[45,46] Liquid-liquid extraction operates by countercurrent extraction wherein a solvent selective toward aromatic compounds flows upward inside a tall column as a nonselective solvent and hydrocarbon mixture flows downward. Aromatics will be solubilized by the selective solvent while the paraffins and naphthenic compounds remain in the nonselective solvent.[41] Often an aromatic reflux is used in which a small amount of pure aromatic material is introduced into the selective solvent prior to extraction. This will force residual non-aromatic compounds out of the extracting solvent thereby enhancing separation.[41] The aromatic extract is either directly distilled or is removed from the selective solvent by stripping into a light hydrocarbon such as *n*-heptane and then separated via distillation.[45,46]

Several different methods of liquid-liquid extraction are used industrially including the Udex process (UOP-Dow) and Tetra process (UCC). A summary of these processes with extraction conditions and solvents used is presented in Table 6.[41]

Table 6. Commercial solvent extraction processes for isolation of aromatic compounds.

Process	Company	Solvent	Conditions
Udex	UOP/Dow	mono-, di-, tri-, tetraethylene glycol/H_2O and mixtures	130-150°C, 5-7 bar
Tetra	UCC	tetraethylene glycol/H_2O	not disclosed
Sulfolane	Shell/UOP	tetrahydrothiophene dioxide (sulfolane)	50-100°C
Arosolvan	Lurgi	*N*-methylpyrrolidone/H_2O	20-40°C, 1 bar
DMSO	IFP	dimethyl sulfoxide/H_2O	20-30°C
CIS	--	propylene carbonate	20-50°C
Duo-Sol	Milwhile Co.	propane/cresol or phenol	not disclosed
Formex	Snamprogetti	*N*-formylmorpholine/H_2O	40°C, 1 bar
Aromex	Koppers	*N*-formylmorpholine/H_2O	80°C, 2 bar
Morphylex	Krupp/Koppers	*N*-formylmorpholine/H_2O	not disclosed
Mofex	Leuna/Werke	monomethylformamide/H_2O	20-30°C, 0.1-0.4 bar
Arex	Leuna/Werke	*N*-methyl-ε-caprolactam	60°C

3.4.2. Maximizing para-xylene yields of a BTX fraction

3.4.2.1. Converting toluene to xylene: disproportionation and transalkylation

As mentioned above, petroleum is distilled into primary fractions that undergo further refining to separate out useful components. BTX is produced by cracking or reforming naphtha feedstocks to afford pyrolysis gas or a naphtha reformate, respectively. As shown above in Table 3 (section 3.3.1), pyrolysis gas and naphtha reformates differ in the concentrations of benzene, toluene, and xylene. To boost the overall yield of xylene, which is the most important component of a BTX stream, toluene may be converted to a mixture of xylene isomers by disproportionation or transalkylation reactions.[47-51] There is, however, no commercial process

for the conversion of benzene to xylene. Therefore, pyrolysis gas, mostly composed of benzene, and any reforming process leading to high yields of benzene, such as the Aromax process, are not ideal for production of xylene.

Crude BTX containing some amounts of ethylbenzene and mesitylene is passed over a zeolite catalyst, usually ZSM-5, at 80-125°C and 35-70 bar.[47] Transalkylation and disproportionation of methyl groups both occur under these conditions. The mol ratio of toluene to C_9 aromatics determines the final ratio of benzene to xylenes.[47-51] Reactions are commonly quenched with hydrogen and the addition of $HCl/AlCl_3$, HF/BF_3, or 1,2-dichloroethane.[47] In practice, conversions of toluene are kept low (<40%) in order to minimize undesired side reactions.[48-51] The Mobil STDP (selective toluene disproportionation process), for example, achieves a mixture of xylenes with 87% selectivity to the *para* isomer in a 30% conversion of toluene.[48] Any benzene that forms in these reactions is separated by distillation and unreacted starting material is recycled.[47-51]

3.4.2.2. Isomerization of meta-xylene

Table 7. Melting points of C_8 aromatic compounds.

Product	m.p. (°C)
p-xylene	13.3
o-xylene	-25.2
m-xylene	-47.9
Ethylbenzene	-95.0

The total amount of *para*-xylene (**1**, Scheme 1) that can be isolated from a single BTX fraction can be enhanced by any one of the known *m*-xylene (Figure 1) isomerization methods.[47,52-57] Though there is a small difference in boiling point between the C_8 aromatics (Table 5, section 3.4.1), the differences in melting points are greater (Table 7) and thus can be

exploited to separate a mixture of *para*- and *meta*-xylene by crystallization at low temperatures. To prevent ice blockages in the crystal lattice, the xylene mixture must first be dried over SiO_2 or Al_2O_3.[47] After drying, the mix is cooled to -75 to -20°C whereupon *p*-xylene separates as a crystal sludge on the cold reactor walls. This sludge is scraped off and either filtered or centrifuged to obtain 70% pure *p*-xylene in a filter cake and 80% pure *m*-xylene in the filtrate. Further purification is achieved through multistage crystallization followed at each stage by separation, washing, and remelting until 99.5% pure *p*-xylene is achieved. This process necessitates a predistillation to remove the lower boiling *ortho* isomer and ethylbenzene.[47,52-54]

At an 85% concentration of *m*-xylene in a mixture of *para* and *meta* isomers, a eutectic mixture forms that prevents further isolation of *p*-xylene.[47] This mixture ultimately forms in the mother liquor during purification by crystallization and would otherwise limit the amount of *p*-xylene that can be extracted. However, hydrocatalytic isomerization can convert the eutectic mixture into an equilibrium mixture of xylene isomers that can then be resubjected to *p*-xylene purification. A mixture of *meta*- and *para*-xylene is combined with hydrogen and passed over a Pt/Al_2O_3-SiO_2 catalyst at 400-500°C and 10-25 bar.[47,52] Acidic oxide supports are responsible for the isomerization reactions while the Pt component promotes hydrogenation of the intermediates. Often, ammonia will be added to the feed in order to block acidic sites of the support oxides that would otherwise cause unwanted dealkylation. Simply using a SiO_2/Al_2O_3 mixture without any metal dopant can isomerize *m*-xylene under cracking conditions of 400-500°C and 1 bar.[47] This is a less expensive method than formal hydrodealkylation but runs the risk of unwanted side reactions such as disproportionation, transalkylation, and excessive coke formation. A milder catalytic isomerization of *m*-xylene occurs at 100°C and 1 bar using hydrogen fluoride-trifluoroborane ($HF-BF_3$) as a catalyst.[55] Hydrogen fluoride-trifluoroborane

selectively forms a complex with *m*-xylene facilitating near complete extraction from a C_8 aromatic mixture. The raffinate, *ortho*- and *para*-xylenes along with ethylbenzene, can be separated by distillation.[55]

Mobil has optimized two different sets of conditions for the hydrocatalytic isomerization of *m*-xylene process using zeolite catalysts.[56,57] The LTI (low temperature isomerization) method uses a fixed bed reactor at 200-260°C and 14 bar to isomerize *m*-xylene to 95-98% of an equilibrium mixture without any loss of C_8 aromatics.[56] The HTI (high temperature isomerization) method uses an H-ZSM-5 catalyst that has been partially exchanged with Pt. Isomerization takes place at 427-460°C and 14-18 bar.[57] The shape selectivity of their zeolite catalyst affords *p*-xylene at 4% above equilibrium concentrations.[56,57]

Once the yield of *para*-xylene has been enhanced by disproportionation and transalkylation of toluene and/or isomerization of *meta*-xylene, *p*-xylene must be isolated. The most widely practiced isolation technique involves adsorption on molecular sieves.[58-60] In the liquid phase, *p*-xylene is adsorbed onto mordenite zeolites at 200°C and 15 bar. After the hydrocarbon feed has been introduced, a desorption solvent such as toluene or *p*-diethylbenzene is used to remove the *p*-xylene from the acidic zeolite sites. Upon distillation, 99.5% pure *p*-xylene is isolated.[58,59] This method can be made continuous by holding the zeolite catalyst in a fixed bed and alternating between xylene feed and desorbant. This process has largely replaced the crystallization approach for the purification of *p*-xylene.[47,58-60]

4. ROUTES TO BIOBASED TEREPHTHALIC ACID

Commercial production of PTA from *p*-xylene is subject to unpredictable changes in the cost of fossil fuels. In order to provide additional starting materials for PTA manufacture in times of increased petroleum prices, synthetic routes involving biobased starting materials may be advantageous. By widening available starting materials, PTA production costs can be stabilized regardless of changes in the cost or availability of fossil fuel feedstocks.

4.1. Biobased starting materials for terephthalic acid synthesis

Several methods have been developed for the synthesis of PTA from biobased starting materials. These starting materials are extracted directly from plant sources or are isolated from fermentation media. This section will focus on the production of the most important starting materials for the synthesis of biobased PTA. Synthetic routes to PTA from the materials discussed in this section will be presented in sections 4.2 and 4.3.

4.1.1. Succinic acid

Succinic acid is an intermediate for the commercial production of lacquers, surfactants, dyes, and green solvents as well as biodegradable plastics and ingredients for stimulating plant and animal growth.[61] Chemical preparation of succinic acid involves hydrogenation of maleic anhydride which affords succinic acid in high yields with good selectivities.[62]

Bioproduction of succinic acid offers an alternate route for commercial synthesis relying on carbohydrate starting materials rather than fossil fuels. Succinate **18** is a key intermediate in the tricarboxylic acid cycle and may be produced via three pathways: the reductive branch of the tricarboxylic acid cycle[63] (***a*-*d***, Scheme 5), the oxidative branch of the tricarboxylic acid cycle[64]

(***f-l***, Scheme 5), and the glyoxylate pathway[65] (***m*** and ***n***, Scheme 5). Operational under anaerobic conditions, the reductive branch of the tricarboxylic acid pathway is the primary mode of succinic acid production in bacteria such as *Actinobacillus succinogenes*.[61] In this pathway, glucose **13** is metabolized to phosphoenolpyruvate **14** via glycolysis (see section 4.1.2) which is converted to oxaloacetate **15** by phosphoenolpyruvate carboxylase. Oxaloacetate **15** is further converted to malate **16** by malate dehydrogenase before going on to fumarate **17** driven by fumarase. Fumarate reductase catalyzes the final conversion of fumarate **17** to succinate **18**.[61,63]

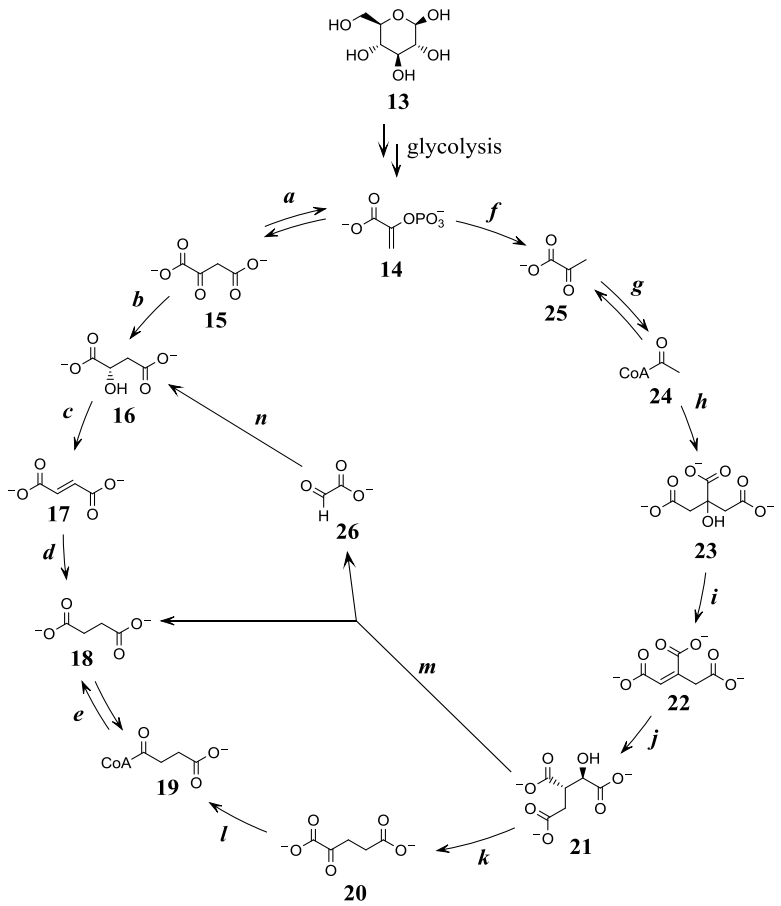

Scheme 5. Microbial production of succinate **18** from glucose via the tricarboxylic acid cycle. Steps ***a-d*** comprise the reductive branch, steps ***f-l*** make up the oxidative branch, and steps ***m*** and ***n*** represent the glyoxylate pathway, a) phosphoenolpyruvate carboxylase (EC4.1.1.31); b) malate dehydrogenase (EC1.1.1.37); c) fumarase (EC4.2.1.2); d) fumarate reductase (EC1.3.5.4); e) succinyl-CoA synthetase (EC6.2.1.5); f) pyruvate kinase (EC2.7.1.40); g) pyruvate synthase (EC1.2.7.1); h) citrate lyase (EC2.3.3.8); i) citrate hydrolyase (EC4.2.1.3); j) D-*threo*-isocitrate hydrolyase (EC4.2.1.3); k) isocitrate dehydrogenase (EC1.1.1.42); l) 2-oxoglutarate synthase (EC1.2.7.3); m) isocitrate lyase (EC4.1.3.1); n) malate synthase (EC2.3.3.9).

E. coli have been shown to produce succinic acid under anaerobic conditions as described above or aerobic conditions.[61] In the presence of oxygen, pyruvate **25** is converted to acetyl-CoA **24** which enters the oxidative branch of the tricarboxylic acid cycle.[64] Acetyl-CoA **24** is converted into citrate **23** by citrate synthase which passes through several intermediates to 2-oxoglutarate **20**. 2-Oxoglutarate **20** is dehydrogenated to succinyl-CoA **19** which is converted to succinate **18** by succinyl-CoA synthetase. In wild-type *E. coli*, succinate **18** is subsequently converted to fumarate **17** by succinate dehydrogenase, thus, succinate **18** does not accumulate within the cell under aerobic conditions. Stopping the oxidative pathway at succinate requires the inactivation of *sdhA* gene which results in blocking the conversion to fumarate **17**.[61]

The glyoxylate pathway is also operational under aerobic conditions and, like the oxidative branch of the tricarboxylic acid cycle, begins with the conversion of acetyl-CoA **24** to citrate **23**.[65] Citrate **23** is then converted into *cis*-aconitate **22** followed by hydration to D-*threo*-isocitrate **21**. Isocitrate lyase converts D-*threo*-isocitrate **21** into glyoxylate **26** and succinate **18**. Malate synthase converts glyoxylate **26** into malate **16** which can be isolated as malic acid (section 4.1.2) or further converted to succinate **18** in the reductive branch of the tricarboxylic acid cycle.[61,65]

4.1.2. Malic acid

Malic acid is industrially produced by catalytic hydration of maleic anhydride to afford a racemic mixture of D-, and L-malic acid.[62] Its primary use is as an acidulant and taste enhancer for the food and beverage industries. Like succinic acid (section 4.1.1.), malic acid is also a key intermediate in the citric acid cycle for a wide range of microorganisms. The simplest and highest yielding pathway for malic acid biosynthesis is the reductive branch of the tricarboxylic

acid pathway (***a*-*d*** Scheme 5, Scheme 6).[66] This metabolic route begins with pyruvate **25** (Scheme 6) (synthesized from glucose **13** by the Embden-Meyerhof-Parnas pathways of glycolysis) which is carboxylated by pyruvate carboxylase to oxaloacetate **15**. Malate dehydrogenase reduces oxaloacetate to malate **16**.

Species in the *Aspergillus* genus of fungi are known to produce malic acid by the reductive tricarboxylic acid pathway.[67] They have also been used in large-scale production of industrial enzymes, organic acids, and pharmaceuticals. *Aspergillus* is thus a well-studied microorganism about which an extensive toolkit of genetic markers, promoters, and gene information has been developed.

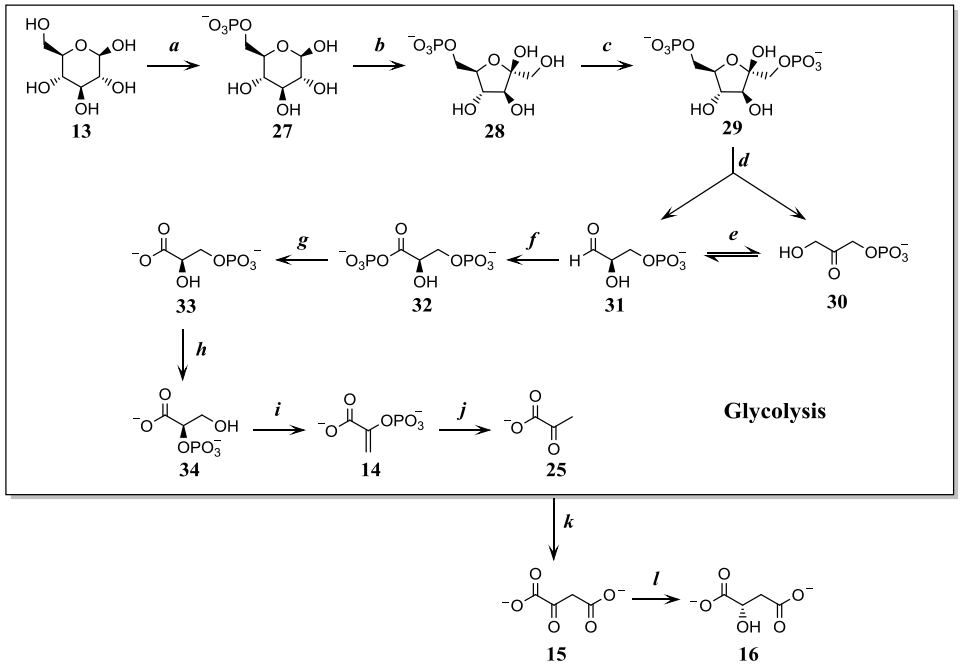

Scheme 6. Microbial synthesis of malate **16** from glucose, a) glucokinase (EC2.7.1.2); b) glucose-6-phosphate isomerase (EC5.3.1.9); c) 6-phosphofructokinase (EC2.7.1.11); d) fructose-1,6-bisphosphate aldolase (EC4.1.2.13); e) triose phosphate isomerase (EC5.3.1.1); f) glyceraldehyde-3-phosphate dehydrogenase (EC1.2.1.12); g) phosphoglycerate kinase (EC2.7.2.3); h) phosphoglycerate mutase (EC5.4.2.12); i) enolase (4.2.1.11); j) pyruvate kinase (EC2.7.1.40); k) pyruvate carboxylase (EC6.4.1.1); l) malate dehydrogenase (EC1.1.1.37).

Research from Novozymes in Denmark has resulted in the engineering of a recombinant strain of *Aspergillus oryzae* that is capable of producing 154 g/L of malic acid from glucose in

164 h of batch fermentation which translates to a 69% yield of malic acid.[67] The *A. oryzae* microorganism was engineered to overexpress the native genes making up the reductive tricarboxylic acid pathway in conjunction with a C_4 dicarboxylic acid transporter.[67] Overexpression of a transporter gene has been shown to increase production of malic acid threefold in *Saccharomyces cerevisiae* by enhancing the transport of malate **16** from the cytosol into the extracellular environment.[66] The modified *A. oryzae* microbe reported by Novozymes produces the highest yields so far for malic acid biosynthesis.[67]

4.1.3. Muconic acid

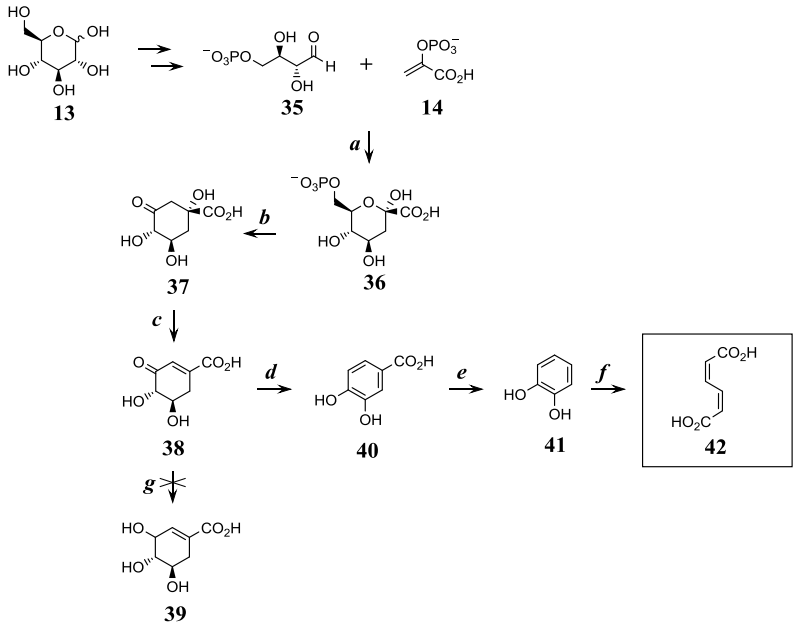

Scheme 7. Microbial production of *cis,cis*-muconic acid **42**, a) 3-deoxy-D-arabino-heptulosonic acid phosphate synthase (EC2.5.1.54); b) 3-dehydroquinate synthase (EC1.4.1.24); c) 3-dehydroquinate dehydratase (EC4.2.1.10); d) 3-dehydroshikimate dehydratase (EC4.2.1.118); e) protocatechuate decarboxylase (EC4.1.1.63); f) catechol 1,2-dioxygenase (EC1.13.11.1); g) shikimate dehydrogenase (EC1.1.1.25).

Muconic acid is an additional candidate as a substrate for the production of biobased PTA. *cis,cis*-Muconic acid may be synthesized using a recombinant microorganism from any

genera of bacteria possessing the common pathway for aromatic amino acid biosynthesis (Scheme 7).[68] The aromatic amino acids, tryptophan, tyrosine, and phenylalanine, are produced from a common intermediate: chorismate, which is derived from shikimic acid **39**.[68,69] In order to produce muconic acid **42**, a microorganism with a mutationally inactivated *aroE*-encoded shikimate dehydrogenase is employed. Such a mutant is unable to convert dehydroshikimate **38** to shikimic acid **39** thereby blocking the aromatic amino acid pathway.[68]

E. coli is the most suitable microbe for the production of *cis*,*cis*-muconic acid **42** from glucose **13**. The strain AB2834 expresses the required *aroE* mutation and is not capable of directing carbon flux beyond dehydroshikimate **38** in the aromatic amino acid synthetic pathway.[68] Instead, a divergent pathway is accessed wherein dehydroshikimate is converted to protocatechuate **40** via 3-dehydroshikimate dehydratase. Protocatechuate decarboxylase catalyzes the decarboxylation of protocatechuate **40** to catechol **41**. Finally, 1,2-dioxygenase converts catechol **41** into *cis*,*cis*-muconic acid **42**.[68,69]

4.1.4. 5-Hydroxymethylfurfural

5-Hydroxymethylfurfural (HMF) has gained attention as a biobased precursor to a variety of chemicals and fuels. It is readily available from carbohydrates and has been used in the synthesis of biobased PTA via conversion to 2,5-dimethylfuran (DMF) or 2,5-furandicarboxylic acid (FDCA). 5-Hydroxymethylfurfural is obtained via dehydration of monomeric carbohydrates as well as di- and polysaccharides. However, due to the reduced solubility of polysaccharides in most solvents as well as the presence of strong glycosidic bonds, HMF is preferably synthesized from monomeric sugars.[70]

The direct formation of HMF by the dehydration of monomeric carbohydrates may proceed through cyclic intermediates or acyclic intermediates. Proposed acyclic pathways (Scheme 8) assume the formation of a linear 1,2-enediol **43** (Scheme 8) as the rate limiting step.[71,72] This intermediate is widely accepted as the intermediate in aldose-ketose isomerization via the Lobry de Bruyn-Alberda van Ekenstein rearrangement[73] that occurs during isomerization of glucose **13** to fructose **44**. Following the formation of the enediol intermediate **43**, two consecutive β-dehydrations occur prior to a ring closing dehydration step to afford HMF.

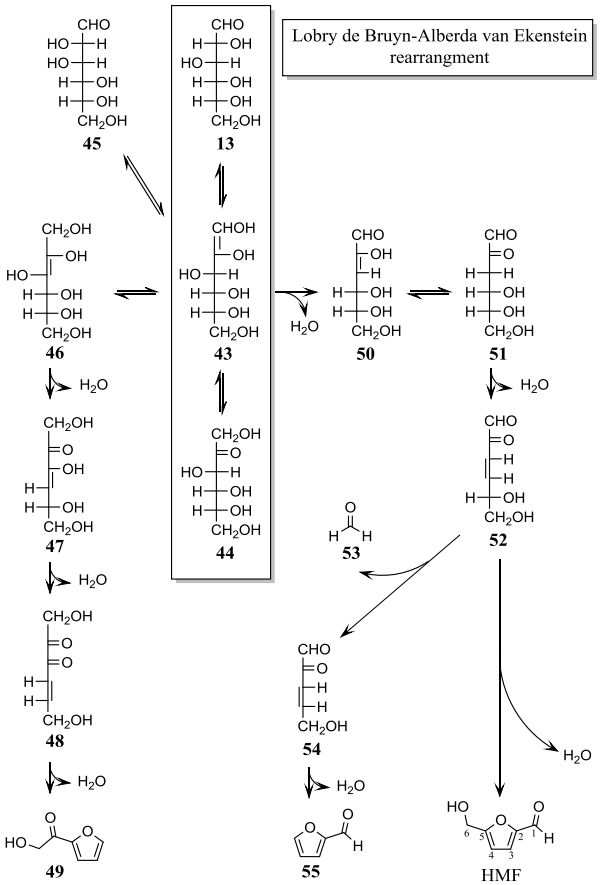

Scheme 8. Proposed acyclic mechanism of glucose **13** dehydration to afford 5-hydroxymethylfurfural and byproducts.

Evidence for an acyclic mechanism in the dehydration of fructose **44** is based on the observation of small amounts of glucose **13** and mannose **45** in the reaction medium.[71,72] This observation

suggests an isomerization of fructose **44** through a 1,2-enediol intermediate **43**.[71] Furfural **55** is generated with the dehydration of an intermediate **53** which arises upon decarbonylation of 3,4-dideoxyglucosone-3-ene **52**. This decarbonylation competes with the ring-closing dehydration that forms HMF. Byproduct 2-hydroxyacetylfuran **49** is generated from two consecutive dehydrations of a 2,3-enediol intermediate **46**, formed after rearrangement of 1,2-enediol **43.**[71,72]

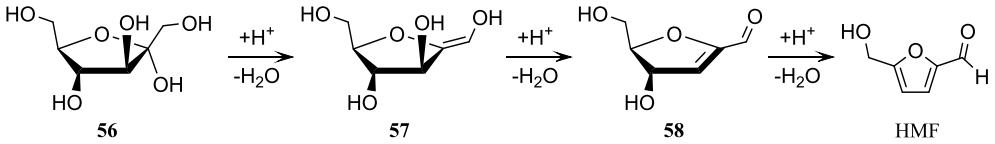

Scheme 9. Proposed cyclic mechanism 5-hydroxymethylfurfural synthesis.

Scheme 9 shows a mechanism involving cyclic intermediates that has also been proposed for the direct formation of HMF from monomeric carbohydrates.[72] Beginning with a cyclic furanose **56**, dehydration of the C_2 hemiacetal forms an enol intermediate **57**. Two consecutive β-dehydrations aromatize the furan ring to afford HMF.[72] Generally, fructose is more reactive and selective toward HMF than glucose, evidenced by higher yields using fructose as a substrate as opposed to glucose. Reports in the literature attribute this decrease of reactivity in glucose to the greater stability of the glucose ring as compared to fructose.[70,72] This stability would limit its ability to form the acyclic enediol intermediate **43**. In the proposed cyclic mechanism, glucose must first isomerize to fructose before dehydration to HMF.[72]

Recent ^{13}C NMR studies have examined the dehydration mechanism of both [$^{13}C_1$]-fructose and [$^{13}C_6$]-fructose.[74] Results show that the C_1 carbon of fructose forms the carbonyl carbon of HMF and the C_6 carbon of fructose forms the hydroxymethyl carbon of HMF. This agrees with both the proposed cyclic and acyclic mechanisms. More significant evidence for a cyclic mechanism is suggested by D_2O studies.[75] Dehydration experiments performed in the

presence of D_2O shows that all steps after the initial dehydration of the hemiacetal are irreversible, explained by the lack of deuterium incorporation into the HMF product.[75] This also suggests that an acyclic mechanism is unlikely because the tautomerization of intermediate **51** in the acyclic mechanism shown in Scheme 8 would lead to deuterium incorporation at C_3 of HMF.[75]

Further evidence for a cyclic dehydration mechanism is found when glucose is used as the substrate. Conventional acid catalysts such as H_2SO_4 or heterogeneous metal oxides such as zirconia (ZrO_2) or TiO_2 afford HMF in low yields (around 30%) when used with glucose but achieve yields around 50-70% when fructose is used.[76] The Zhang group, however, was successful in achieving a 70% yield of HMF from both glucose and fructose by using a system of 10 mol% chromium dichloride ($CrCl_2$) in 1-ethyl-3-methylimidazolium chloride ([EMIm]Cl). Their proposed mechanism describes $CrCl_2$ as an isomerization catalyst for glucose to fructose while the acidic medium catalyzed the dehydration reactions.[76] Similar systems such as tin tetrachloride in 1-ethyl-3-methylimidazolium tetrafluoroborate ($SnCl_4$/[EMIm]BF_4) have also been successful in achieving high yields ($\geq$60%) of HMF from glucose.[77]

Toxicological issues are associated with HMF. It is known that HMF is cytotoxic at high concentrations (80 mM).[78] Irritation to the eyes, upper respiratory tract, skin, and mucous membranes may be caused by overexposure to HMF. However, there have been no reports of carcinogenicity in humans.[78] Because the dehydration of carbohydrates occurs whenever food items are heated, HMF has existed in the human diet for thousands of years.[70] This may have given humans an evolutionary resistance to the cytotoxic effects of furan compounds at concentrations around 150 mg person^{-1} day^{-1}. Recent research has even suggested beneficial

pharmacological activity of HMF including activity against sickle cell anemia, improving blood circulation, and improving antioxidant activity.[78]

While HMF may prove to be less toxic than previously thought, it may be metabolized to mutagenic derivatives. Sulfotransferases metabolize HMF into 5-sulfoxymethylfurfural in vitro.[79] Because the sulfate is a good leaving group, a highly electrophilic carbocation may be produced. Stabilization of this carbocation by the furan ring allows this intermediate to react with cellular nucleophiles such as DNA, RNA, and various proteins. It was recently discovered that administration of 5-sulfoxymethylfurfural to mice leads to acute necrosis and proteinaceous casts in the kidney proximal tubules.[79] It has been found that both HMF and 5-sulfoxymethylfurfural are weak intestinal carcinogens in mice.[79] However, no reports of carcinogenic or genotoxic effects in humans have been developed. This suggests that the toxic potential of HMF in humans is low and current safety margins surrounding the use of this chemical are sufficient.

4.1.5. Ethylene

Ethylene is the simplest unsaturated compound and is used as a precursor to a variety of chemicals such as acetaldehyde, acetic acid, ethylene oxide, and styrene among others. It is also polymerized to produce high and low density polyethylene. Commercial preparation of ethylene uses steam cracking of naphtha.[80] C_5 to C_{12} straight chain paraffins are cracked in the presence of steam at temperatures at or above 650°C to afford ethylene alongside other olefins, isoparaffins, and gaseous products such as CO_2 and H_2.[81,82]

In order to widen available feedstocks for the chemicals industry, biobased ethylene may be utilized. Bio-ethanol is dehydrated at temperatures around 300°C and pressures of 1 bar to 2 bar, often over an acidic catalyst such as Al_2O_3, TiO_2, magnesium oxide (MgO), or zeolites.[80]

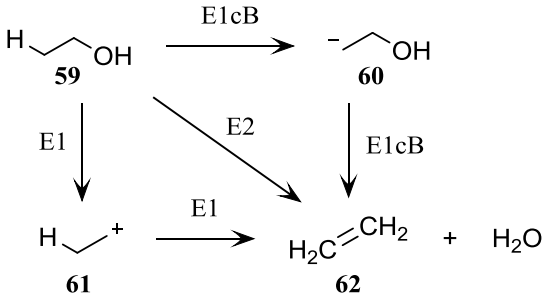

Scheme 10. Possible pathways of dehydration of ethanol **59** to ethylene **62**: E1, E1cB, E2.

The dehydration may follow an E1, E2, or E1cB mechanism as shown in Scheme 10. Diethyl ether **63** is the most prevalent byproduct of ethanol **59** dehydration and may form from ethanol as a co-product or may serve as an intermediate in the synthesis of ethylene **62** (Scheme 11).[80] Other byproducts of ethanol dehydration include alkanes (e.g. methane, ethane, propane), aldehydes (e.g. acetaldehyde), ketones (e.g. acetone), and oligomers.[83] Oligomers are formed from vapor-phase coupling of alkyl fragments. Other byproducts are formed via dehydrogenation, for example the dehydrogenation of ethanol to acetaldehyde. Purification of the ethylene product stream is accomplished by multistage distillation. Polymer grade ethylene of >99% purity is achieved upon purification.[83]

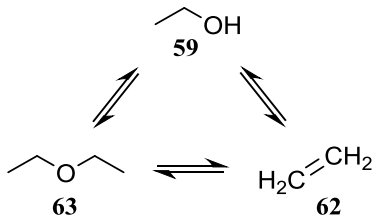

Scheme 11. Parallel series of reactions form ethylene **62** directly from ethanol **59** or involve diethyl ether **63** intermediate.

Chemical companies such as Solvay (Belgium)[83] and Braskem (Brazil)[84] have succeeded in producing ethylene from biobased ethanol. The Braskem Ethylene plant, for instance, was established in 2007 and had a production capability of 200,000 tons of bio-ethylene per annum thus demonstrating the efficacy of producing ethylene from sugar cane.[84] Ethanol itself is obtained from the fermentation of many sources of biomass including agricultural residues, wood, corn and wheat grain, and waste products. These feedstocks contain about 40-50% cellulose, 25-35% hemicellulose, and 15-20% lignin which are processed into glucose.[85,86] Starchy materials such as corn are also important sources of glucose suitable for production of ethanol. Starch processing is a fairly mature technology that uses enzymatic liquefaction and saccharification to break down long chains of starch into glucose monomers which are fermented to ethanol by *Saccharomyces* yeasts (Scheme 12).[86] The production of ethanol from starch is the major source of bio-ethanol in the United States.[85,86]

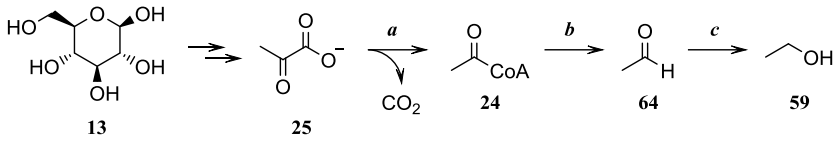

Scheme 12. Fermentation of glucose **13** to produce ethanol **59** in *Saccharomyces cerevisiea*, the enzymes involved are as follows: a) pyruvate formate-lyase (EC2.3.1.54); b) acetaldehyde dehydrogenase (EC1.2.1.10); c) alcohol dehydrogenase (EC1.1.1.1).

Cellulose and hemicellulose are similar to starch in that they are composed of chains of hexose monomers. However, they are constructed out of highly crystalline β-1,4 glycosidic bonds whereas starch is made from less crystalline α-glycosidic bonds.[85] β-Linkages make cellulose and hemicellulose more compact and more resistant to enzymatic attack than starch. Furthermore, lignin, a complex, amorphous polymeric material composed of methoxylated phenylpropane structures, may be covalently linked to hemicellulose via ferulic acid ester

linkages. Thus, the crystalline structure and complex nature of lignocellulose makes it more difficult to enzymatically break down to fermentable carbohydrates than starch.[85,86]

Acidic and basic thermal pretreatment methods have been developed to initially process lignocellulose to improve enzymatic digestibility.[86] Acidic pretreatment uses a strong acid such as H_2SO_4 to hydrolyze hemicellulose while leaving cellulose and lignin intact. Alkaline pretreatments hydrolyze lignin while leaving cellulose and hemicellulose intact. Regardless of the pH of the pretreatment medium, pretreatment will disrupt cell walls and improve enzymatic access to polysaccharides.[86] Cellulases and hemicellulases present in bacteria and other microorganisms break down cellulose and hemicellulose to glucose and other hexose sugars.[85] These carbohydrates are then fermented to ethanol with a range of microorganisms. The ethanol thus produced may be used directly as a fuel or converted to ethylene for chemical manufacture as described above.

4.1.6. Monoterpenes

Monoterpenes are compounds with the formula $C_{10}H_{16}$ and contain two units of isoprene joined together in different ways. Monoterpenes are naturally emitted into the atmosphere by trees and grasses. Some of the principal emitted terpenes include pinene, limonene, myrcene, and 3-carene as well as isoprene itself.[87] Technology has been developed that can utilize limonene as a feedstock for the production of biobased PTA (section 4.3.3.). Though trees and grasses are ubiquitous sources of limonene and other terpenes, atmospheric concentrations range between 0.5-9 parts per billion.[87] This is too low to support an industrial synthesis for a compound produced at a rate of 47 million tons per year[5] and, moreover, isolating these compounds after their emission into the atmosphere is an impractical endeavor.

Limonene is the major component of oil extracted from citrus fruit rinds which are collected as waste products from the juicing industry.[88] The annual production of citrus fruit is around 100 million cubic tons with oranges constituting 60% of the total production.[89] This results in approximately 22 million tons of orange peel waste per annum.[90] This waste product can be used to extract limonene for the production of PTA. Conventional extraction techniques include steam distillation, cold pressing, and solvent extraction.[91] A recent advance using microwave assisted extraction has resulted in an 11% yield of limonene after 30 min at 110°C, which is more than twice as high as conventional techniques.[89] Thus, with recent developments in extraction technology, limonene may prove to be a useful and desirable compound for the production of biobased PTA and an attractive alternative feedstock to supplement petroleum and shale gas. Yet, because of the 1,4-substitution on the cyclohexene ring of limonene, it will not be a suitable substrate for the production of IPA.

4.1.7. Sorbitol

Sorbitol is a polyol with widespread use in nutrition, cosmetics, medicine, and industry. It is used as a low calorie sweetener, a humectant in cosmetic and pharmaceutical products, as well as in paper and tobacco products.[92] Commercially, an aqueous solution of glucose (up to 65% by weight) is catalytically hydrogenated to sorbitol in an autoclave or trickle-bed reactor under high H_2 pressures and low temperatures (around 130°C).[93] Catalysts are usually based on supported Ni but suffer from leaching and deactivation due to loss of crystalline structure.[92] Ruthenium supported on SiO_2 has shown to convert a 40% glucose solution to sorbitol with 99% selectivity and 99.9% conversion under continuous hydrogenation conditions in a trickle-bed reactor. Furthermore, Ru catalysts are less prone to deactivation and do not leach into solution as

conventional Ni catalysts do.[92] Despite the advantages of Ru, Ni remains the catalyst of choice in most applications because it is relatively inexpensive whereas Ru is quite costly.

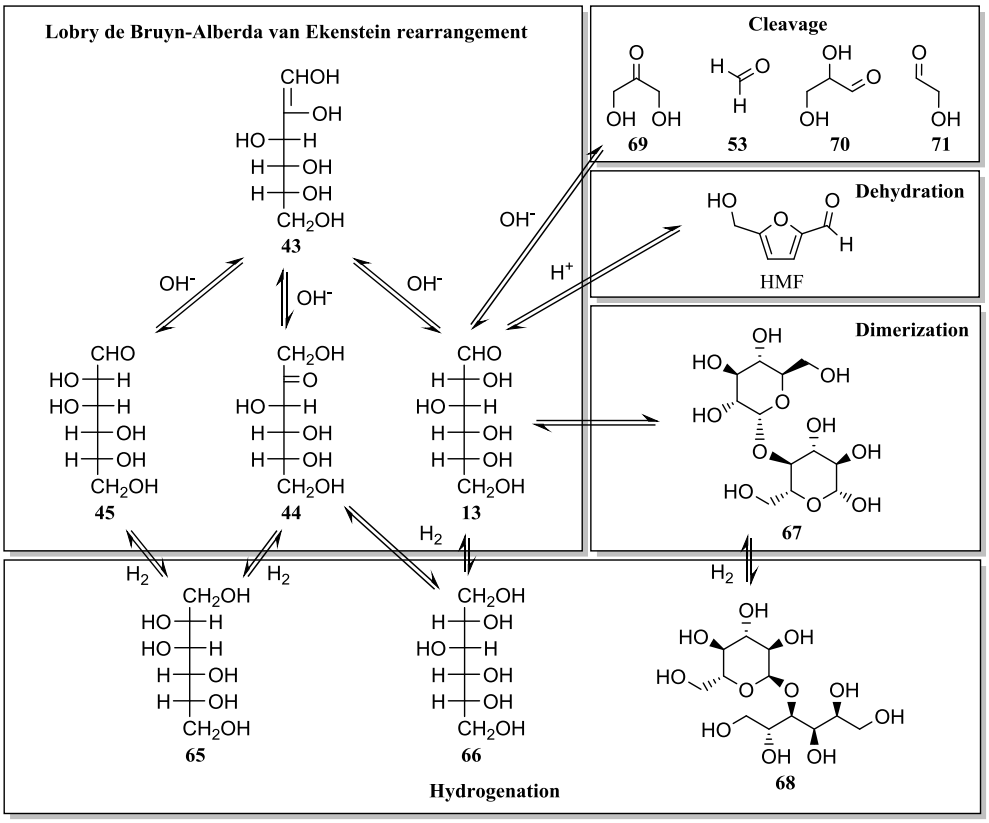

Scheme 13. Reaction network for the hydrogenation of glucose **13** to sorbitol **66**.

The hydrogenation of glucose **13** to sorbitol **66** (Scheme 13) is a one step process but may afford several byproducts including mannose **45**, fructose **44**, maltose **67**, glycerin aldehyde **70**, dihydroxyacetone **69**, glycol aldehyde **71**, formaldehyde **53**, HMF, mannitol **65**, and maltitol **68**.[92,93] As shown in Scheme 13, mannose **45** and fructose **44** are products of the Lobry deBruyn-Alberda van Ekenstein rearrangement with a 1,2-enediol intermediate **43** (section 4.1.4).[73] Hydrogenation of either mannose **45** or fructose **44** will afford mannitol **65**. Glucose **13** may dimerize in solution to afford maltose **67**, which may be hydrogenated to produce maltitol **68**. Small amounts of HMF are formed via in situ dehydration of glucose **13** (section 4.1.4) while dihydroxyacetone **69**, formaldehyde **53**, glycerin aldehyde **70**, and glycol aldehyde

71 are products of alkaline cleavage of C-C bonds.[93] The amount of byproducts is affected by the metal support. An 8% yield of byproducts was obtained with Ni/TiO_2 while Ni/SiO_2 afforded 2-4% of byproducts.[93] Though Ru may promise to be a more effective catalyst for glucose **13** hydrogenation than Ni, both are highly selective to sorbitol **66** and both achieve high conversions of glucose. Whether Ni or Ru is used, continuous hydrogenation of glucose **13** is an efficient means to produce sorbitol **66** for the manufacture of chemicals.[93,94]

4.1.8. Isobutanol

Isobutanol is an alternative candidate as a substrate for the production of biobased PTA. Commercially, isobutanol is produced via the hydroformylation of propylene followed by hydrogenation of the resultant aldehyde.[94] Carbon monoxide and H_2 add across the propylene π bond to afford 2-methylpropanal. Subsequent reduction of the aldehyde affords isobutanol.[94] To widen the available feedstocks for the chemicals industry, native metabolic pathways in microorganisms may be exploited.

Significant quantities of isobutanol are only accessible via engineered microorganisms since native producers only generate isobutanol as a byproduct and not a fermentation end point.[95-97] By overexpressing endogenous amino acid synthesis pathways in *E. coli* and co-expressing the last two steps of the Ehrlich pathway of valine degradation with two exogenous enzymes, ketoisovalerate decarboxylase from *Lactococcus lactis* and alcohol dehydrogenase from *S. cerevisiae*, 22 g/L of isobutanol was produced from glucose. This corresponds to a yield which is 86% of the theoretical maximum.[96]

Wild type *E. coli* convert glucose **13** into valine **77** via 2-ketoisovalerate **74** as shown in Scheme 14.[98] Glycolysis affords pyruvate **25** which is decarboxylated to 2-acetolactate **72** by acetolactate synthase. 2-Acetolactate **72** is converted to 2,3-dihydroxyisovalerate **73** by a ketol-

acid reductoisomerase prior to dehydration to 2-ketoisovalerate **74** by 2,3-dihydroxyisovalerate dehydratase. In typical valine biosynthesis (not shown in Scheme 14), 2-ketoisovalerate **74** is converted to valine **77** upon reaction with glutamate catalyzed by valine transaminase.[98] In order to produce isobutanol **76**, researchers overexpressed 2-ketoisovalerate **74** decarboxylase from *L. lactis* which promotes the Ehrlich pathway of valine degradation via decarboxylation of 2-ketoisovalerate **74** to isobutanal **75**.[95,96] A heterologously expressed alcohol dehydrogenase from *S. cerevisiea* dehydrogenates isobutanal **75** to isobutanol **76**.

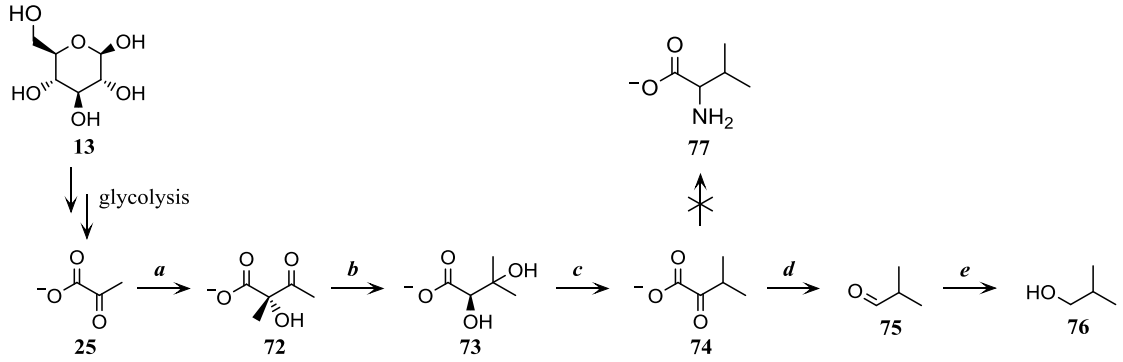

Scheme 14. Fermentation of glucose **13** to afford isobutanol **76**, a) acetolacteate synthase (EC2.2.1.6); b) 2,3-dihydroxyisovalerate reductoisomerase (EC1.1.1.86); c) 2,3-dihydroxyisovalerate dehydratase (EC4.2.1.9); d) 2-ketoisovalerate decarboxylase (EC4.1.1.72); e) alcohol dehydrogenase (EC1.1.1.2).

4.2. Synthetic routes involving *p*-xylene intermediacy

Syntheses of PTA from the starting materials discussed in section 4.1 can be divided into those that involve a *p*-xylene intermediate and those that do not. A summary of those routes involving *p*-xylene intermediacy is presented in Scheme 15. The biobased *p*-xylene **1** produced by these methods will be subjected to established Amoco Mid-Century oxidation. This feature makes integration of these routes into the current chemical manufacture infrastructure easier but does not provide a solution to the challenges associated with the Amoco Mid-Century process (section 2.2).

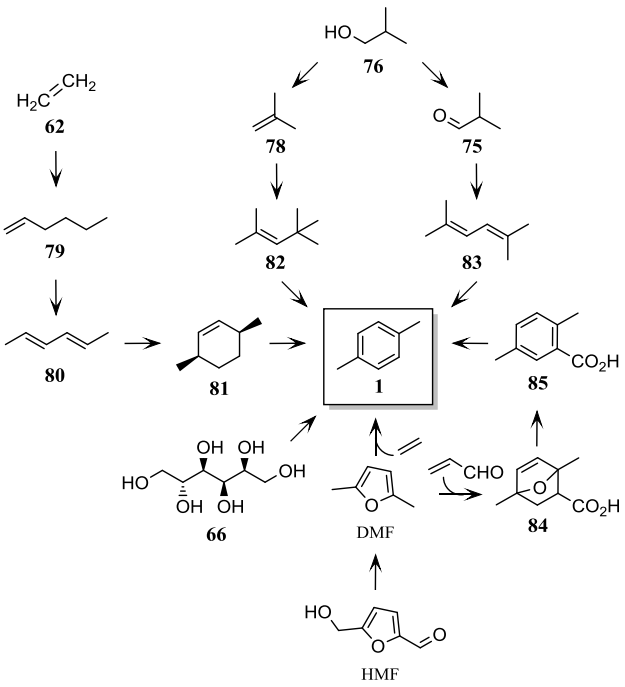

Scheme 15. Synthesis of biobased *p*-xylene **1** from ethylene **62**, isobutanol **76**, sorbitol **66**, and 5-hydroxymethylfurfural.

4.2.1. 5-hydroxymethylfurfural

5-Hydroxymethylfurfural may be a substrate for the synthesis of biobased *p*-xylene upon reduction to DMF. A Diels-Alder cycloaddition between DMF and biobased ethylene or acrolein affords *p*-xylene (Scheme 15). Hydrogenolysis of the hydroxyl group and the aldehyde moiety of HMF is commonly conducted over a solid metal catalyst at mild temperatures and pressures.[99] A system that combines the dehydration of fructose to HMF with the reduction to DMF has been developed (Figure 8).[99-101]

Acid-catalyzed dehydration of fructose **44** to HMF occurs in a biphasic membrane reactor.[99,101] A water-immiscible organic solvent, such as 1-butanol, continuously removes HMF from the fructose-containing aqueous phase. Fructose **44** dehydration is catalyzed by a 0.25 M

solution of HCl with the addition of NaCl to assist in the partitioning of organic and aqueous phases. A conversion of up to 88% based on fructose **44** is achieved with 82% selectivity to HMF in three minutes at 180°C.[101] Continuous extraction of HMF from the medium in which it was generated not only helps drive the dehydration of fructose **44** but also prevents its degradation to levulinic acid and formic acid due to extended residence time in the aqueous phase.[99,101]

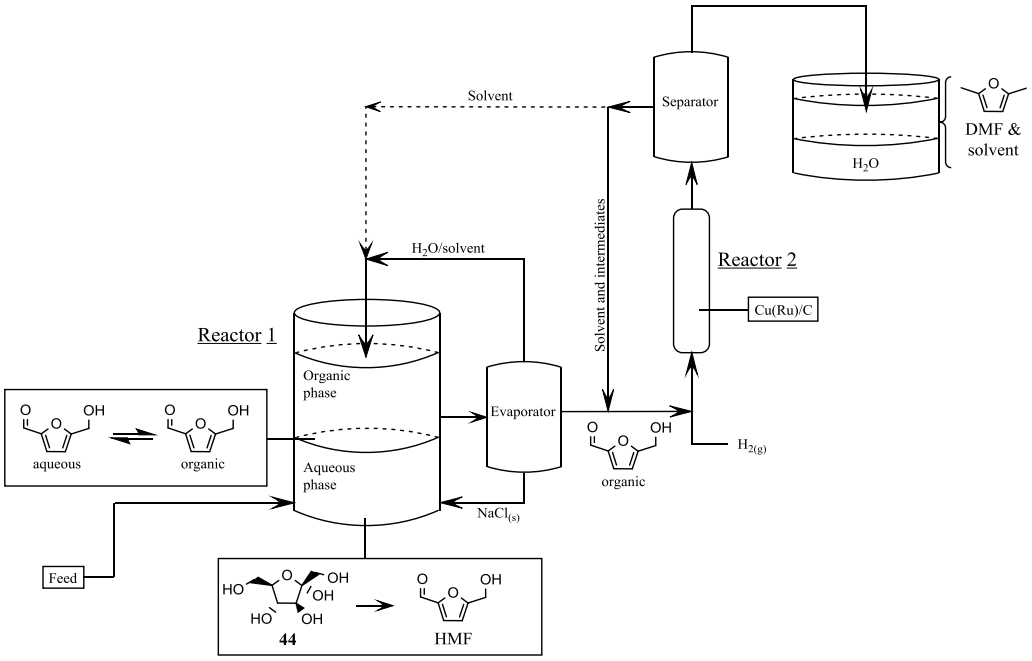

Figure 8. Biphasic reactor for conversion of fructose **44** to 5-hydroxymethylfurfural with vapor phase reduction of 5-hydroxymethylfurfural to 2,5-dimethylfuran.

The extracting solvent containing HMF is then purified by vacuum evaporation at low temperatures (90°C) to remove volatile impurities before being fed into a fixed bed reactor to be converted into DMF.[99,101] Vapor phase hydrogenolysis occurs over a Cu(Ru)/C catalyst at 220°C and around 7 bar H_2 pressure to afford 76-79% yields of DMF.[101] Though there is precedent in the literature that copper chromite ($Cu_2Cr_2O_5$) in air can catalyze the hydrogenation

of furfural into 2-methylfuran and 2-hydroxymethylfurfural,[102-104] this catalyst suffered from deactivation due to loss of crystalline structure upon contact with chlorine contaminants in the HMF feed. A layer of Ru beneath the Cu layer enhances chlorine resistance without affecting hydrogenolysis activity.[99,101]

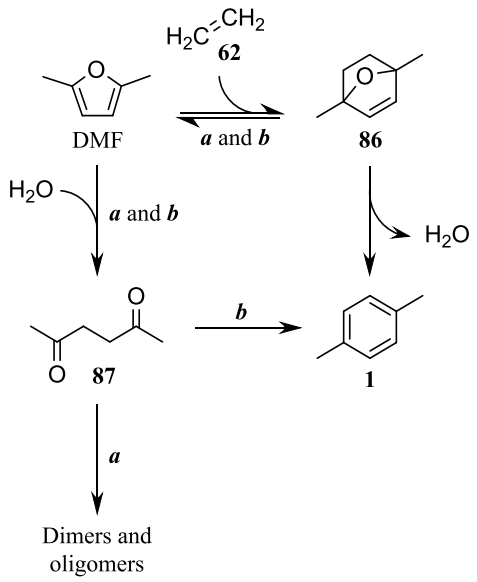

Scheme 16. Conversion of 2,5-dimethylfuran to *p*-xylene **1** by reaction with ethylene **62**, a) H-Beta zeolite, 250°C, 62 bar ethylene; b) $Cu(OTf)_2$, 250°C, 35 bar ethylene. Only pathway (b) converts byproduct **87** to *p*-xylene **1**.

A synthesis of *p*-xylene **1** from the [4+2] cycloaddition of DMF and ethylene **62** has been investigated (Scheme 16).[105-109] The process with the highest yields of *p*-xylene **1** reacts DMF with ethylene **62** in a high pressure reactor using an H-Beta zeolite catalyst at 250°C and 62 bar.[106] The cycloaddition produces 1,4-dimethyl-7-oxabicyclo[2,2,1]hept-2-ene **86** which spontaneously dehydrates to *p*-xylene **1** with >99% conversion and 90% selectivity.[105-109]

2,5-Hexanedione **87** is often an undesired byproduct of acidic catalysis and may oligomerize at moderate conversions. Advantageously, by conducting the cycloaddition of DMF and ethylene in an aprotic solvent with a Lewis acid catalyst, any 2,5-hexanedione **87** that forms

is converted to *p*-xylene **1** (pathway ***b***, Scheme 16).[108] At 250°C and 35 bar, 1 wt% cupric triflate ($Cu(OTf)_2$) in dioxane catalyzes the enolization and subsequent cycloaddition of 2,5-hexanedione with ethylene to afford *p*-xylene **1** with 99% selectivity and 94% conversion.[108] The Cu-catalyzed conversion of 2,5-hexanedione **87** to *p*-xylene **1** can occur in the presence of DMF such that byproduct formation does not negatively affect *p*-xylene yields.[108]

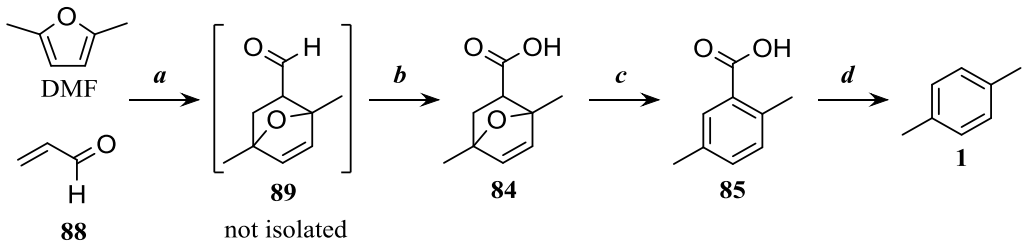

Scheme 17. Conversion of 2,5-dimethylfuran to *p*-xylene **1** by reaction with acrolein **88**, a) $Sc(OTf)_3$, -55°C, 4 Å MS; b) $NaClO_2/CH_3CN$; c) conc. H_2SO_4, 0°C; d) Cu_2O, 210°C.

Acrolein **88** may also serve as a dienophile in a [4+2] cycloaddition with DMF to afford an intermediate that may be aromatized to *p*-xylene **1** as shown in Scheme 17.[110] Bio-acrolein can be isolated from the dehydration of glycerol, which is an overproduced side-product of biodiesel production.[111,112] The cycloaddition between DMF and acrolein **88** is performed at -55°C to -60°C under ambient pressure in a sealed reactor. In the presence of 4 Å molecular sieves, 0.1 mol% scandium triflate ($Sc(OTf)_3$) converts a 3.2:1 mixture of DMF and acrolein **88** into 7-oxabicyclo-[2,2,1]-hept-2-ene **89** at 75% acrolein conversion.[110] The aldehyde cycloaddition adduct **89** decomposes above 0°C so the reaction mixture is quenched at -55°C with aqueous $NaClO_2/CH_3CN$. This quench converts the aldehyde into a carboxylic acid moiety. Aromatization of the carboxylic acid derivative **84** takes place at 0°C with concentrated H_2SO_4 in 48% yield.[110] Lastly, the carboxylic acid group is removed in a copper oxide (Cu_2O) catalyzed decarboxylation at 210°C. After four steps, *p*-xylene **1** is produced in a 34% yield.[110] Though

acrolein **88** can serve as a dienophile in a cycloaddition with DMF to produce *p*-xylene **1**, the low yields cannot compete with the 93% *p*-xylene yields achieved when ethylene was used as the dienophile.

4.2.2. Isobutanol

Biobased *p*-xylene **1** can be produced from isobutanol **76** in one of two pathways (Scheme 18).[113-116] Bio-isobutanol **76** from microbial fermentation of carbohydrates may be dehydrated to isobutylene **78** or dehydrogenated to isobutyraldehyde **75**. C_8 alkenes from the dimerization of isobutylene **78** or the condensation of isobutylene **78** with isobutyraldehyde **75** are converted over a dehydrocyclization catalyst to afford *p*-xylene **1**.

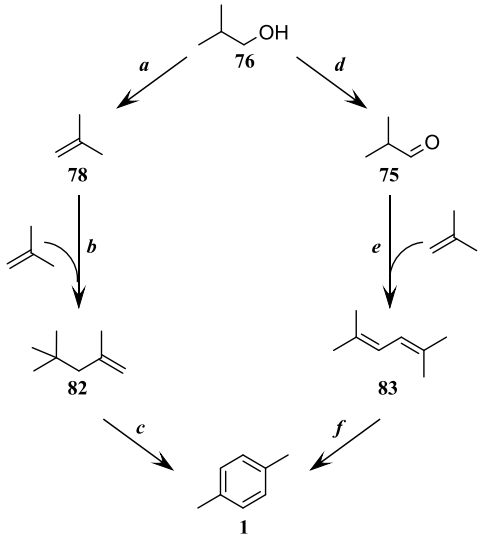

Scheme 18. Conversion of isobutanol **76** to *p*-xylene **1** via two pathways, a) γ-Al_2O_3, 450°C, 4 bar; b) H-ZSM-5, 170°C, 52 bar; c) CrO_3/Al_2O_3, 550°C; d) $Cu_2Cr_2O_5$, 320°C; e) Nb_2O_5, 225°C, 41 bar; f) CrO_3/Al_2O_3, 450°C, 1 bar.

As shown in Scheme 18, isobutanol **76** is dehydrated in the vapor phase over γ-Al_2O_3 at 450°C and 4 bar to afford 95% selectivity to isobutylene **78** at >99% conversion.[113-115] Moderate pressures are used to keep isobutylene **78** in the condensed phase allowing it to be separated from water by decantation. Alternatively, isobutanol **76** may be passed over a copper chromite

($Cu_2Cr_2O_5$) catalyst at 320°C to give isobutyraldehyde **75** at up to 99% selectivity and conversion.[116]

Both pure isobutylene **78** and mixtures of isobutylene **78** and isobutyraldehyde **75** can be converted to *p*-xylene **1**.[113-115] In a continuous flow reactor operating at 225°C and pressurized to 41 bar, isobutylene **78** and isobutyraldehyde **75** are reacted over niobic acid (Nb_2O_5) to produce liquid and gas product streams. The gaseous byproduct is isobutylene **78** and is recycled back into the reactor while the liquid effluent is principally composed of 2,5-dimethyl-2,4-hexadiene **83** at approximately 35% isobutyraldehyde **75** conversion. Hexadiene **83** is then passed over a chromia-alumina (CrO_3/Al_2O_3) catalyst at ambient pressure and 450°C. After 30 minutes of continuous flow, a 70% yield of xylene is produced with 82% selectivity towards the *para* isomer.[113]

In an alternate pathway, isobutylene **78** is dimerized in a fixed bed reactor over an H-ZSM-5 zeolite catalyst at 170°C and 52 bar.[116] At around 50% conversion, dimerization affords octene isomers with 95% selectivity to 2,4,4-trimethylpent-2-ene **82**. The product stream is distilled to remove trimers and tetramers before being fed into a fixed bed reactor and heated to 550°C at ambient pressure. A chromia-alumina (CrO_3/Al_2O_3) catalyst promotes the dehydrocyclization of purified 2,4,4-trimethylpentene **82** to *p*-xylene **1** in 42% yield with 90% selectivity.[116]

Routes to biobased *p*-xylene **1** from isobutanol **76** are promising and particularly successful in the conversion of isobutanol **76** to C_8 intermediates. However, overall selectivity to *p*-xylene **1** in either the isobutylene **78** dimerization (***a*-*c***, Scheme 18) or the isobutylene **78**-isobutyraldehyde **75** (***d*-*f***, Scheme 18) condensation pathways are no more than 80%. For an industrial process to be commercially viable, product selectivities should be 90% or above

particularly if conversions are below 50%. Low conversions characterize the dehydrocyclization of isobutylene **78** dimers (32%)[113] and the reaction between isobutylene **78** and isobutyraldehyde **75** (35%)[114]. Furthermore, aromatization of the C_8 intermediates requires temperatures between 450°C and 550°C.

4.2.3. Sorbitol

Conditions have been optimized for converting sorbitol to an organic product stream that can be further reformed to afford xylene-rich aromatic fraction (Figure 9).[117] Conversion of a 60% solution by weight of sorbitol **66** in water is carried out in a fixed-bed reactor heated to 230°C and pressurized to 18-27 bar. The reactions are driven by a 10% by weight Pt(Re)/C catalyst.[117] When carbohydrates are passed over metal catalysts, C-C and C-O bond scission pathways are possible. Initial adsorption of sorbitol **66** onto the catalyst surface and subsequent dehydrogenation is followed by C-C bond cleavage. This produces adsorbed CO **91** which reacts with water by the water-gas shift reaction to afford H_2 and CO_2. The H_2 thus produced is consumed in deoxygenation reactions promoted by the Re component of the catalyst.[117] C-O bond cleavage forms species with low surface binding energies **92-94** that desorb to form C_4-C_6 alcohols, ketones, carboxylic acids, and heterocyclic compounds. The production of these monofunctional saturated compounds **95-98** is favored at elevated pressures.[117]

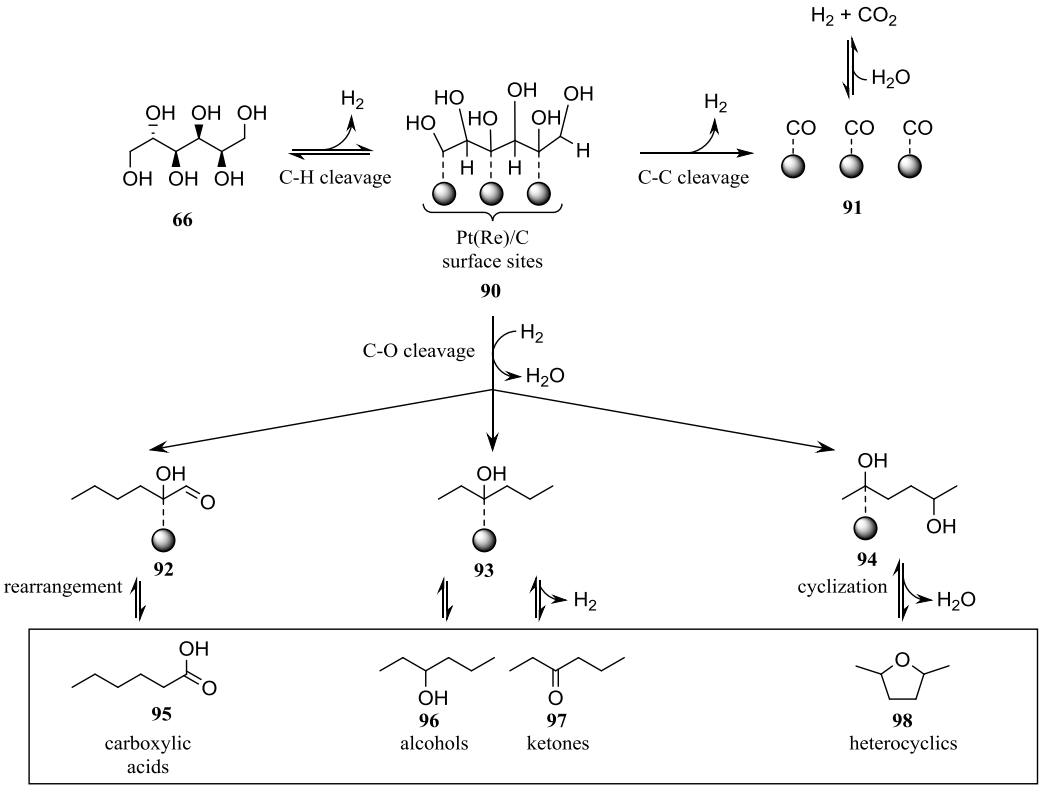

Figure 9. Catalytic conversion of sorbitol **66** to monofunctional product stream.

The liquid organic product stream containing carboxylic acids, alcohols, ketones, and heterocyclic compounds **95-98** can be upgraded to afford good yields of BTX.[117] A 5% by weight Ru/C catalyst reduces carbonyl compounds and oxygen-containing heterocycles to alcohols at 160°C and 55 bar H_2 pressure. The resultant alcohols are dehydrated, oligomerized, and cyclized over an H-ZSM-5 zeolite catalyst at 400°C and 1 bar. Of all the carbon present in the organic phase produced from sorbitol **66**, 25% is converted to C_3-C_4 paraffins, 29% is converted to C_3-C_4 olefins, and 38% is converted to aromatic compounds. Of these aromatic products, 12% is benzene, 37% is toluene, 30% are xylene isomers and ethyl benzene, and the remaining 22% is three to six carbon-substituted benzenes.[117] The conversion of sorbitol to a distribution of hydrocarbons ranging from short chain paraffins to mononuclear aromatics is a potentially useful general strategy for utilizing biomass in the chemical industry.

4.2.4. Ethylene

A route to *p*-xylene **1** using bioethylene **62** as a sole precursor has been developed and is shown in Scheme 19.[118,119] Ethylene is trimerized using an *ortho*-methoxy-substituted aryl phosphine chromium complex developed by British Petroleum to produce 1-hexene with >99% selectivity and 95% yield in a high pressure reactor at 80°C and 8 bar ethylene.[120] C_8 cyclohexenes can then be made from the resultant 1-hexene **79** upon heating to 250°C in mesitylene with 0.32 mol% of an iridium pincer complex under 41 bar ethylene pressure.[118,119] The preferred iridium catalyst is shown in Scheme 19.

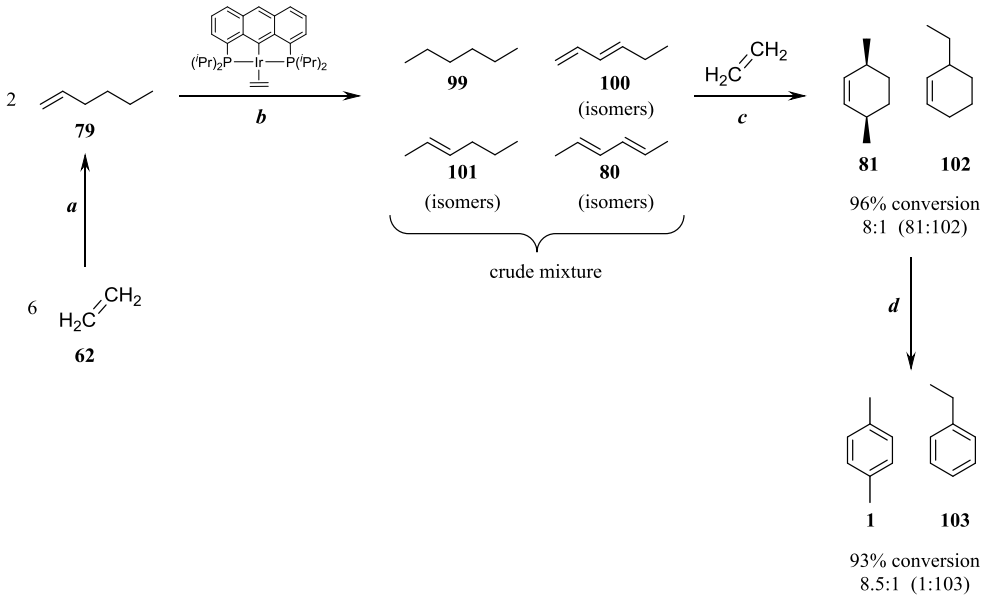

Scheme 19. Synthesis of biobased *p*-xylene **1** from bioethylene **62**, a) [(*o*-$(CH_3O)C_6H_4)_2PN(CH_3)P$(*o*-$(CH_3O)C_6H_4)_2$]$CrCl_2$, 80°C, 20 bar ethylene; b)/c) [Ir] catalyst, 250°C, 41 bar ethylene; d) Pt/Al_2O_3, 400°C.

The iridium species catalyzes the transfer dehydrogenation from hexene **79** to ethylene **62** to afford a mixture of hexadiene isomers **80**,**99**-**101**. Under 41 bar ethylene and 250°C, a 96% conversion of hexadienes is achieved with an 8:1 ratio of 3,5-cyclohexene **83** to 3-ethylhexene **103**.[119] The iridium catalyst is removed under vacuum and the crude mix is degassed before

being fed into a fixed bed reactor.[118,119] Here, it is heated to 400°C and passed over Pt/Al_2O_3 catalyst using N_2 as the carrier gas to afford 93% conversion to an 8.5:1 mixture of *p*-xylene **1** and ethylbenzene **103**.[118,119] High yields of *p*-xylene **1** are achieved in vapor phase dehydrogenation of the crude mixture of cyclohexene products **81** and **102**.

Synthesis of biobased *p*-xylene **1** from bioethylene **62** is an interesting and potentially useful strategy. Conversions at each step are high with an overall 90% selectivity to *p*-xylene **1**. Generally, reaction conditions are mild with the 400°C vapor phase aromatization as the only exception. However, extended reaction times (8 days) are necessary for high conversions in the iridium-catalyzed dehydrogenation and iridium catalysts are expensive.

4.3. Synthetic routes that avoid *p*-xylene intermediacy

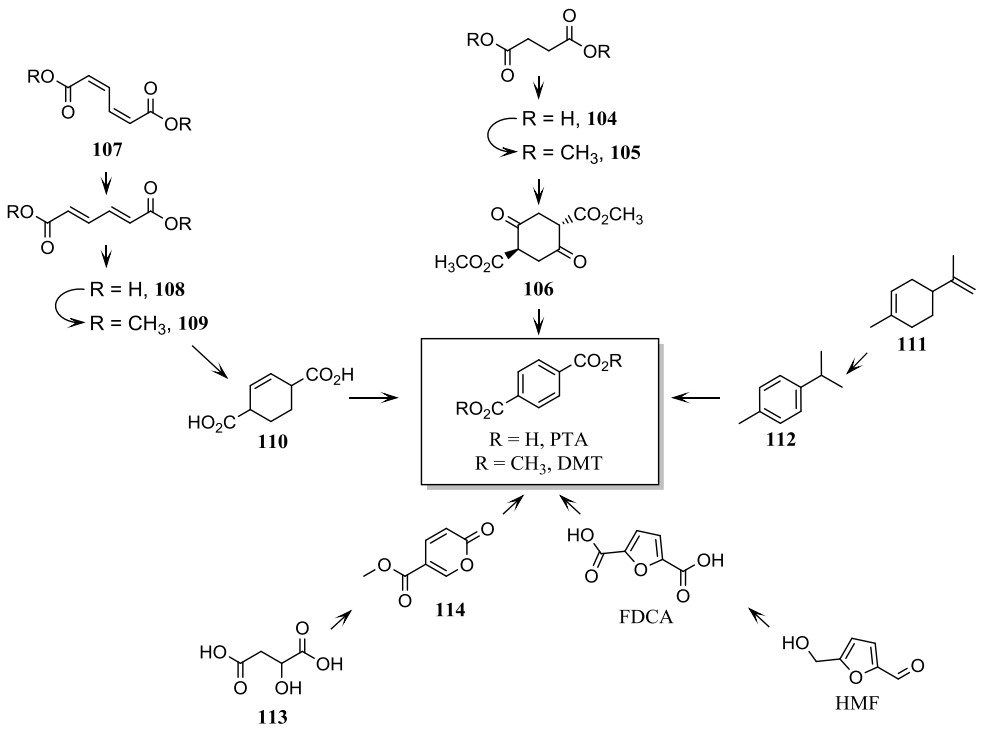

Scheme 20. Synthesis of biobased terephthalic acid from succinic acid **104**, muconic acid **107**, malic acid **113**, 5-hydroxymethylfurfural, and limonene **111**.

Significant effort has focused on the development of synthetic routes toward biobased PTA that avoid *p*-xylene intermediacy (Scheme 20). Four of the proposed routes use substrates that contain the two carboxylic acid moieties present in the structure of PTA and thus avoid an Amoco Mid-Century oxidation. The route beginning with limonene on the other hand, uses an oxidation with stoichiometric potassium permanganate that could likely be supplanted with an Amoco Mid-Century oxidation. This section will focus on those syntheses that prepare PTA without proceeding through a *p*-xylene intermediate.

4.3.1. Diacid substrates

Diacids such as malic acid **113**, succinic acid **104**, and muconic acid **107** (Scheme 20) are interesting candidates as precursors to biobased PTA. Whereas other biobased routes focus on synthesizing *p*-xylene, diacids already contain the two carboxylic acid moieties present in the structure of PTA and thus allow a synthesis that avoids Amoco Mid-Century oxidation. However, each synthesis involves one or more esterification steps and ultimately produce DMT. The ester must be hydrolyzed back to the free acid to afford PTA. Thus, esterification introduces two additional steps to the synthetic route that should be removed before these syntheses become commercially attractive.

4.3.1.1. Succinic acid

A synthetic route to PTA from succinic acid **104** is depicted in Scheme 21.[121,122] Succinic acid **104** is first esterified to dimethyl succinate **105** prior to the addition of a 30% solution of sodium methoxide in anhydrous methanol to liquid dimethyl succinate **105** at 105°C and around 0.5 bar.[121] The vacuum removes methanol as it forms to drive the condensation reaction toward the dimethylsuccinylsuccinate disodium salt **115**. Following the addition, the

vacuum is replaced by ambient N_2 pressure and the slurry is cooled below 30°C before filtering and washing with methanol to isolate the solid salt. The methanol-wet filter cake is transferred into a neutralization vessel containing 15% solution of aqueous H_2SO_4 and stirred for one hour at 30-35°C to afford pure dimethylsuccinylsuccinate **116** in 86% isolated yield.[121]

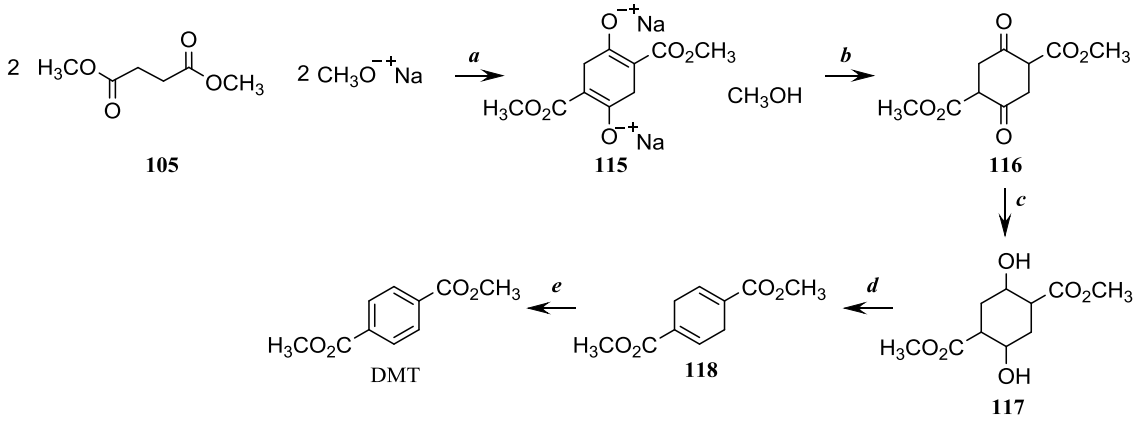

Scheme 21. Conversion of dimethyl succinate **105** to dimethyl terephthalate, a) $NaOCH_3$, CH_3OH, 105°C, 0.5 bar; b) H_2SO_4, 30°C; c) Ru/C, CH_3OH, 120°C, 69 bar H_2; d) NaOH, CH_3OH, 195°C, 3 bar; e) Ru/C, 195°C, 3 bar.

Dimethylsuccinylsuccinate **116** is then reduced and dehydrogenated to DMT in a one pot reaction sequence.[122] The substrate is taken up into methanol and 5% by weight Ru/C is added in a high pressure autoclave. The reactor is purged with H_2 three times before being pressurized to 69-76 bar H_2 and heated to 120°C. A pressure drop from 69 bar to around 55 bar is observed, indicating the consumption of H_2. Maintaining the reactor at the appropriate pressure throughout the reaction requires recharging the reactor to 69-76 bar H_2 several times over a 5 h period, after which no further consumption of H_2 is observed.[122] The reaction mixture is stirred for a total of 16 h after which time the reactor is vented, cooled, and 3% by weight of sodium hydroxide in methanol is added. The reactor is charged with N_2 at 3 bar and heated to 195°C. Sodium hydroxide in methanol promotes the dehydration of the intermediate dimethylcyclohexane-2,5-diol-1,4-dicarboxylate **117**, while the Ru/C catalyst facilitates the dehydrogenation of

dicarboxylate **118** to DMT .[122] The reactor is cooled to ambient temperature and a grey-white slurry is observed. This slurry is washed with methanol and an insoluble white solid is filtered off. The solvent is removed under reduced pressure to afford 89% of a crude mixture containing DMT, dimethyl dihydroterephthalate **118**, and dimethyl tetrahydroterephthalate in a 1:2:1 ratio. Low temperature (-20°C) crystallization affords two crops of DMT crystals at 24% yield.[122]

DMT produced from succinic acid must be hydrolyzed in a final step of the process to produce PTA. However, DMT yields (24%)[122] are too low to be of commercial significance for PTA or PBT manufacture. Unless dimethylsuccinylsuccinate **105** can be reduced and dehydrogenated in a more selective manner to improve DMT yields to 95% or above, the following malic acid **113** route will be preferable to the succinic acid **104** route. Neither method, however, will be ideally suited to PTA production if esterification and hydrolysis steps are involved.

4.3.1.2. Malic acid

Malic acid **113** (Scheme 22) self-condenses in oleum to afford coumalic acid **124** in around 70% yield, which is then esterified to methyl coumalate **125**.[123] Under solvent-free conditions and the absence of a catalyst, methyl coumalate **125** and 1.5 to 3 equivalents of methyl pyruvate **126** are allowed to react for 16 h at 200°C.[124,125] This reaction proceeds through a bicyclic intermediate **127** that undergoes spontaneous decarboxylation and oxidation to DMT in 59% yield after 16 h. Any known hydrolysis protocol leads to PTA. Biobased methyl pyruvate **126** is produced by esterification of pyruvic acid, which is the major product of the glycolysis cycle in plants and microbes (Scheme 6, section 4.1.2).[124,125]

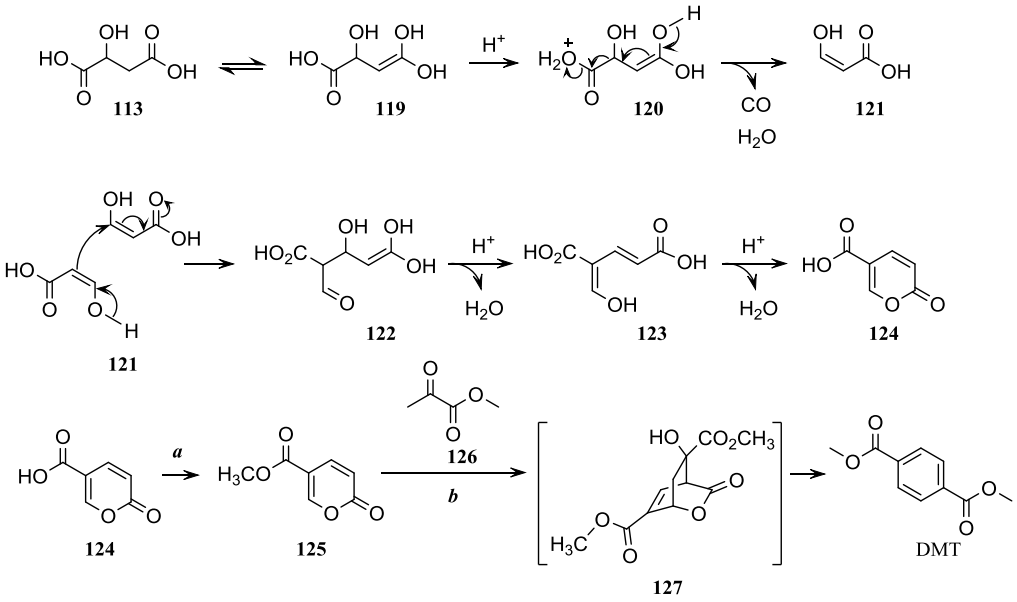

Scheme 22. Synthesis of terephthalic acid from malic acid **113**, a) H_2SO_4, CH_3OH, Δ; b) 200°C.

One of the principal drawbacks of this process is the 70% yield of coumalic acid **124** from malic acid **113** condensation. Without a high yield (>90%) in this step, the overall yield of PTA from malic acid **113** is significantly reduced. An additional challenge to address in this synthesis is the need to esterify both coumalic acid **124** and pyruvic acid. A solvent and catalyst-free reaction would indeed be advantageous in an industrial synthesis of PTA in terms of reducing material costs. However, esterification of both substrates followed by hydrolysis of DMT introduce three additional synthetic steps that diminish the appeal of this route. Before the malic acid route to PTA becomes commercially feasible, progress must be made on converting the free acid forms of coumalic and pyruvic acid.

4.3.1.3. Muconic acid

Muconic acid is an alternative diacid substrate for the synthesis of biobased PTA. A cycloaddition with ethylene **62** affords cyclohex-2-ene-1,4-dicarboxylic acid **110** which is

dehydrogenated over a supported catalyst to PTA.[126] The fermentation of glucose **13** to muconic acid (section 4.1.3) affords pure *cis,cis*-muconic acid **107**. This isomer does not possess the required *s*-cis geometry for a [4+2] cycloaddition and therefore must be isomerized to the *trans,trans* isomer **108** (Scheme 23). Heating to 150°C in water or methanol, or by treating with ultraviolet radiation initially produces *cis,trans*-muconic acid **128**.[126] Further isomerization requires the use of an isomerization catalyst such as elemental iodine.

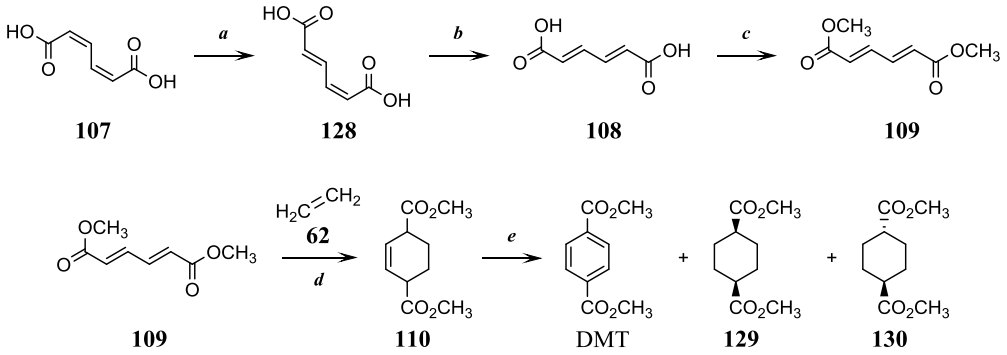

Scheme 23. Synthesis of dimethyl terephthalate from muconic acid **107** and ethylene **62**, a) H_2O, 150°C; b) I_2, 150°C; c) CH_3OH, H_2SO_4, Δ; d) 150°C, 16 bar ethylene; e) Pt/C, 17 bar air, 150°C.

Following isomerization, *trans,trans*-muconic acid **108** is esterified to *trans,trans*-dimethylmuconate **109**. The esterification allows the subsequent cycloaddition to proceed at high conversions (96%).[126] *trans,trans*-Dimethylmuconate **109** reacts with ethylene **62** in a high pressure autoclave at 16 bar ethylene and 150°C in diglyme to afford cyclohex-2-ene-1,4-dicarboxylate **110**.[126] Dehydrogenation to DMT is catalyzed by 1 mol% Pt/C in cyclohexane under 17 bar air and 150°C. After three days, a 59% yield of DMT is obtained alongside 18% dimethyl cyclohexane-1,4-dicarboxylate (both *cis*- **129** and *trans*- **130** isomers) and 23% unreacted starting material. The dehydrogenation to DMT may also be conducted in the same solvent as the cycloaddition to afford 77% yield of DMT, 17% dimethylcyclohexane-1,4-

dicarboxylate **129** and **130**, and 5% tautomerized dimethylcyclohex-2-ene-1,4-dicarboxylate.[126] Without initial conversion of muconic acid to dimethylmuconate, the π bond in the cyclohexene ring of cyclohex-2-ene-1,4-dicarboxylic acid will migrate to be in conjugation with either of the carboxylic acid moieties during the aromatization step. The conjugated species resides in a thermodynamic well that prevents its conversion to PTA. Utilizing dimethyl muconate instead of free muconic acid avoids this undesired π bond migration during the aromatization step of dimethylcyclohex-2-ene-1,4-dicarboxylate to DMT.

The advantage of muconic acid over malic and succinic acid in the production of biobased PTA is that it provides a shorter synthetic route than either of the other substrates. However, muconic acid must also be esterified to dimethyl muconate **109** and the DMT produced must be hydrolyzed to PTA. This disadvantage faces all three routes beginning with diacid substrates. While these routes appear promising with the route from muconic acid as the most attractive, esterification steps must be eliminated before they can become commercially attractive.

4.3.2. 5-Hydroxymethylfurfural

5-Hydroxymethylfurfural has been used as a substrate in the synthesis of biobased PTA that avoids a *p*-xylene intermediate. By oxidizing the hydroxymethyl and aldehyde groups to carboxylic acid moieties, FDCA is obtained.[127,128] 2,5-Furandicarboxylic acid, like the diacid substrates discussed in section 4.3.1, does not require an Amoco Mid-Century oxidation of aryl methyl groups. This can then be converted to PTA in a Diels-Alder cycloaddition with ethylene (Scheme 24). Advantageously, no esterification steps are required.

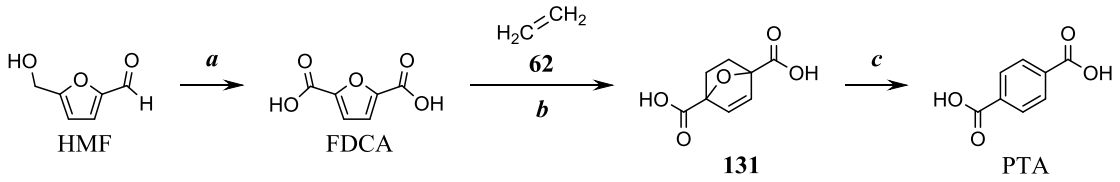

Scheme 24. Conversion of 5-hydroxymethylfurfural to terephthalic acid by oxidation to 2,5-furandicarboxylic acid followed by reaction with ethylene **62**, a) Pt(Bi)/C, O_2, rt; b) 200°C, 14 bar ethylene; c) spontaneous.

5-hydroxymethylfurfural is readily oxidized to FDCA via several methods.[127-130] Stoichiometric oxidants such as $KMnO_4$, dinitrogen tetraoxide (N_2O_4), and nitric acid (HNO_3) are commonly used.[127] The cobalt/manganese/bromine catalyst system used in the Amoco Mid-Century oxidation has also been used to oxidize HMF to FDCA. Other methods have been developed that are more attractive than stoichiometric oxidation or Amoco Mid-Century conditions. Oxidation may be combined with dehydration in the presence of molecular oxygen over Pt/C.[128] Even enzymatic oxidation of HMF has been reported. An oxidoreductase from *Cupriavidus basilensis* was introduced into *Pseudomonas putida* to afford 30 g/L of FDCA at a 97% yield based on HMF.[130]

Following oxidation, FDCA is dissolved in water in a high pressure autoclave at 200°C with 14 bar ethylene pressure for 2 h to afford 0.1 mol% yield of PTA.[128,129] Though the reaction is highly selective (only PTA, unreacted FDCA, and the intermediate bicyclic ether, 7-oxabicyclo[2,2,1]hept-2-ene-1,4-dicarbocylic acid **131**, are detected by HPLC) a product yield of 0.1% suggests this is not a useful method for producing PTA.[128,129] To achieve even a 10% isolated yield of PTA with 0.1% yield per pass, unreacted starting material would have to be recycled over one hundred times.

Thus, HMF only appears to be a useful precursor to biobased PTA if it is used to produce *p*-xylene via its conversion to DMF. Terephthalic acid would then be synthesized using current

Amoco Mid-Century technology which necessitates expensive reactors and involves significant carbon loss through the decomposition of the acetic acid solvent. Avoiding this oxidation by converting HMF to FDCA prior to a cycloaddition with ethylene is unproductive (0.1% yield of PTA). Furthermore, FDCA itself is showing promise as a replacement for PTA in the production of polyester resins as a condensative polymer with ethylene glycol or propylene glycol.[131]

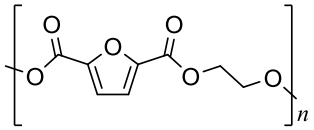

Figure 10. Structure of poly(ethylene furandicarboxylate) (PEF).

Poly(ethylene furandicarboxylate) (PEF) has shown several advantages over poly(ethylene terephthalate) including ten-fold better barrier properties and easier processability.[131] Therefore, current research surrounding FDCA, and by extension HMF, seeks to produce PEF. Terephthalic acid production routes from HMF are adjunct to intense efforts directed toward commercialization of PEF.

4.3.3. Monoterpenes

SABIC Innovative Plastics has elaborated a synthetic route to PTA using a single terpene or a mixture of terpenes in a mild oxidation sequence (Scheme 25).[132-134] In a preferred example of this method, α-limonene **111** is dehydrogenated in the presence of 20 mol% sodium, 70 mol% ethylenediamine, and 1 mol% anhydrous ferric chloride ($FeCl_3$) at 100°C under a N_2 atmosphere for 8 h, to afford 99% yield of *p*-cymene **112** with 99% selectivity.[132] The resultant *p*-cymene **112** is separated from the reaction mixture and added to an aqueous solution of HNO_3. After 24 h of reflux, the reaction crude is extracted intro dichloromethane (DCM) and oxidized further by

reflux in the presence of $KMnO_4$ for an additional 16 h. After filtration, PTA is isolated in 85% yield. Any terpene may be used in this process but preferred substrates possess a six-member ring such as pinene and limonene.[132-134]

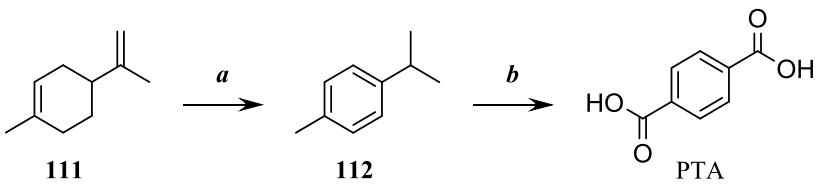

Scheme 25. Synthesis of terephthalic acid from limonene **111**, a) ethylenediamine, $FeCl_3$, Na, 100°C, 99%; b) 1. HNO_3, 100°C, 2. NaOH, $KMnO_4$, 100°C.

The route to biobased PTA from limonene **111** produces the highest yield of PTA (85%) but suffers from the use of stoichiometric oxidation catalysts. Aryl methyl and isopropyl groups of *p*-cymene **112** are effectively oxidized by $KMnO_4$ but unlike the commercial Amoco Mid-Century cobalt/manganese/bromine system, require stoichiometric manganese. Significant costs will be associated with the use and recovery of $KMnO_4$ in the oxidation of monoterpenes to PTA. This route would be substantially more attractive if a mild oxidation catalyst could be used at 1 mol% loading or below.

5. THE ALDER ROUTE

A novel route to PTA has been elucidated that involves three steps: a cycloaddition, aromatization, and aryl methyl oxidation.[135] In 1952, Kurt Alder developed this reaction sequence to trap isoprene formed in the ring opening of methylenecyclobutane **132** using a [4+2] cycloaddition with acrylic acid **134**.[136] After aromatization of the cycloadducts *para*-**135** and *meta*-**136** followed by methyl group oxidation, PTA and IPA are obtained (Scheme 26).[136]

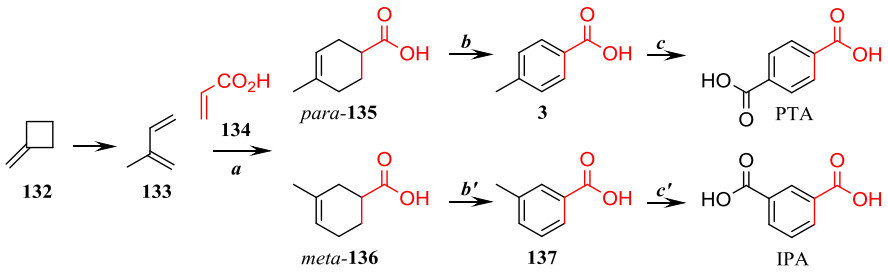

Scheme 26. Alder reaction sequence to terephthalic acid and isophthalic acid, a) 95°C, 13.8 bar; b)/b') H_2SO_4, 230-235°C; c)/c') $KMnO_4$.

One of the most attractive features of this route to PTA and IPA is that the acrylic acid **134** and isoprene **133** starting materials are readily obtainable from either petroleum, shale gas, or biological sources (sections 6 and 7). Commercial production of commodity chemicals that rely solely on petroleum as a feedstock is subject to drastic changes in the availability and prices of crude oil. Alternate sources of starting materials such as shale gas are abundant and cost-effective feedstocks. With the ability to access all three sources of feedstock for the synthesis of isoprene and acrylic acid, the Alder route is a promising and economically robust synthesis of PTA.

Another advantage of the Alder route is its ability to afford both PTA and IPA. PET contains 3-5 wt% IPA to provide transparency and lower the melting point, making the polymer easier to process.[9] None of the ten reported syntheses of biobased PTA is capable of producing

IPA.[113-115] A synthesis that makes both PTA and IPA is especially valuable to PET manufacture. An additional advantage is provided by our development of a Lewis acid-catalyzed solvent-free cycloaddition of an unprotected carboxylic acid. Catalyzing reactions of unprotected carboxylic acids has been a long standing problem in synthetic chemistry, often necessitating the use of an ester derivative in place of the free acid. Developments in our laboratory have allowed free acrylic acid **134** to be utilized which eliminates unwanted esterification and hydrolysis steps in the synthesis of PTA and IPA. Because of recent progress towards commercialization of biobased isoprene **133** and biobased acrylic acid **134** and production of acrylic acid and isoprene from both petroleum and shale gas feedstocks, the reaction sequence developed by Alder constitutes an attractive route for manufacture of PTA and IPA.

This chapter will conclude with a discussion of syntheses of acrylic acid and isoprene in sections 6 and 7, respectively. Production of these compounds from petrochemical sources will be discussed before examining synthetic routes from biobased starting materials. The Alder route to PTA begins with a cycloaddition between acrylic acid and isoprene that will be the topic of Chapter 2, while the aromatization of the cycloaddition products will be presented in Chapter 3.

6. SYNTHESIS OF ACRYLIC ACID

6.1. Petrochemical synthesis

6.1.1. Acetylene-based routes

Early syntheses of acrylic acid **134** involved the reaction of acetylene **138** from calcium carbide and stoichiometric amounts of nickel carbonyl ($Ni(CO)_4$) in water or an alcohol.[137] This synthesis was later improved by Rohm & Haas where 60-80% of the required carbon monoxide was supplied by a separate feed stream while the remaining 20-40% was supplied by $Ni(CO)_4$.[137] Commercial production of acrylic acid **134** used agitated reactors operating at 40°C with 20% excess water or alcohol. Reactor effluent is washed with nickel chloride ($NiCl_2$) brine to remove Ni salts and recycle the water or alcohol solvent.[137]

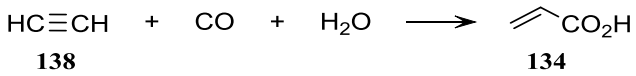

138 **134**

Scheme 27. Synthesis of acrylic acid **134** from acetylene **138**.

Nickel carbonyl is volatile, has little odor, and is highly toxic. Symptoms from overexposure may not appear for several days. Thus, BASF has developed a high pressure synthesis of acrylic acid **134** by reacting acetylene **138** and carbon monoxide at 139 bar and 200°C with a nickel bromide ($NiBr_2$) catalyst with a cupric bromide ($CuBr_2$) promoter.[137] Safety concerns regarding the handling of acetylene **138** are lessened with the use of THF as an inert solvent. The BASF method is complementary to the route developed by Rohm & Haas: BASF forms acrylic acid directly while the Rohm & Haas route is best for producing acrylate esters. However, routes using acetylene **138** as a starting material for the production of acrylic acid are being replaced by oxidation of propylene.

6.1.2. Acrylic acid via oxidation of propane and propylene

The most preferred route for the commercial production of acrylic acid **134** is via the oxidation of propylene **140**. The relatively low cost of propylene **140**, produced as a byproduct of naphtha reforming and ethylene production by steam cracking, and the availability of highly active and selective catalysts has helped make this the dominant strategy for the production of acrylic acid **134**.[138,139] The oxidation of propylene **140** to acrylic acid **134** may proceed by either a one-step or a two-step procedure.[140,141] The one-step oxidation has a reaction enthalpy of -142.1 kcal/mol and is conducted between 325-350°C in order to efficiently promote the oxidation of propylene **140**.[141] However, acrolein **88** is more reactive than propylene **140** and easily decomposes under these conditions. Due to the difference in kinetics between the oxidation of propylene **140** to acrolein **88** and the oxidation of acrolein **88** to acrylic acid **134**, a two-stage process was developed to optimize reaction conditions for each oxidation step.[140,141]

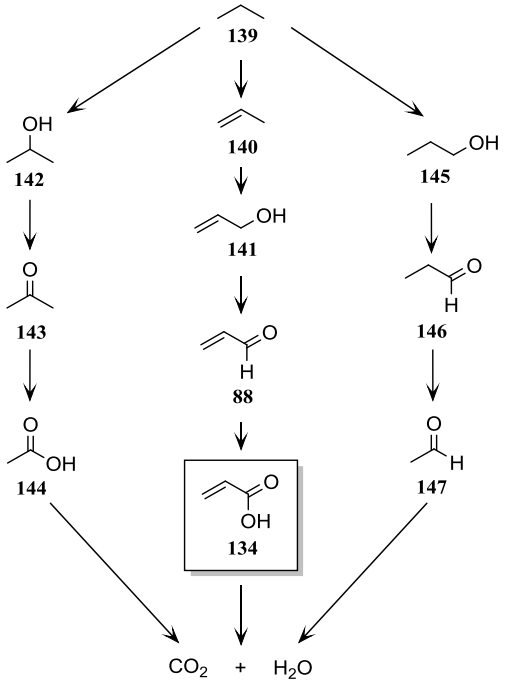

Figure 11. Propane **139** oxidation pathways including over-oxidation of reaction species to CO_2 and H_2O.

As shown in Figure 10, acrolein **88** is formed from propylene in a conversion that involves an allylic alcohol **141** intermediate. This conversion has a reaction enthalpy of -81.4 kcal/mol.[140] In a typical process, propylene **140** is vaporized and mixed with steam and air to generate a stream containing 5-7% by weight propylene **140**, 10-30% steam, and the remainder is air. This feed stream passes over a catalyst bed in a reactor heated to 330-350°C to afford an effluent rich in acrolein **88**.[142] Trace amounts of acrylic acid **134** may also be present in the stream. Catalysts suited for the oxidation of propylene **140** include heteropoly acids and mixed metal oxides, while the best class comprises bismuth molybdates that are modified with another metal such as tungsten or iron.[142,143]

The effluent from the first reactor is fed to a second reactor containing a MoO_3 or V_2O_5 catalyst. The reaction enthalpy for the oxidation of acrolein **88** to acrylic acid **134** is -60.7 kcal/mol,[141] which allows the second reactor to operate at milder temperatures than the first, 210-255°C. Separating the reaction of propylene **140** to acrolein **88** and acrolein **88** to acrylic acid **134** allows for better temperature control and limits the amount of overoxidation to carbon oxides. Propylene **140** conversions for the entire process are high (around 87-98%) with selectivities to acrylic acid **134** around 90-97%.[140-144] Kinetic studies have suggested a Mars van Krevelen-type mechanism as shown in Scheme 28. Lattice oxygen atoms partially oxidize the organic reactant while gas phase oxygen reoxidizes the reduced catalyst.[145] Such a mechanism produces water rather than H_2. This feature not only makes the process safer than conventional dehydrogenations but also helps lower the reaction enthalpies of dehydrogenation steps.

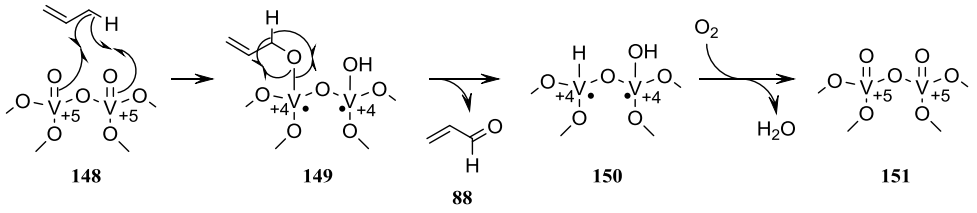

Scheme 28. Mars van Krevelen oxidation of propylene **140** to acrolein **88** over V_2O_5 catalyst.

Propane **139** (Figure 10), naturally present in natural gas and light naphtha streams, may alternatively be oxidized to acrylic acid **134** in a similar manner as propylene **140**. However, it is much less selective due to the significantly lower reactivity of propane **139** relative to propylene **140**.[140,146] Multicomponent mixed metal oxides are the favored catalysts for the oxidation of propane **139**. The most highly active catalyst is a molybdenum-vanadium-tellurium-niobium oxide (Mo-V-Te-Nb-O) that achieves an 80% conversion with 60% selectivity to produce acrylic acid **134** in 48% yield at 380°C.[140]

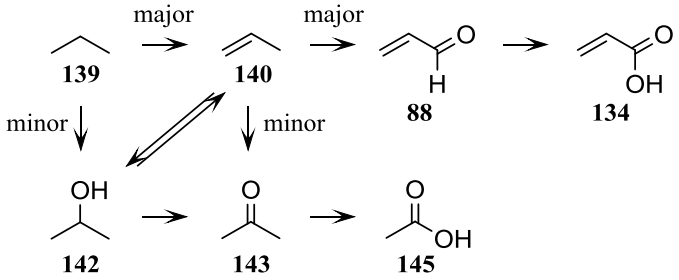

Figure 12. Proposed oxidation pathways over Mo-V-Te-Nb-O catalysts.

Proposed pathways for the production of acrylic acid from propane over Mo-V-Te-Nb-O catalysts are shown in Figure 11.[140,141] Two key steps that determine the selectivity to acrylic acid **134** are the oxidative dehydrogenation of propane **139** to propylene **140** and the allylic oxidation of propylene **140**. Propylene **140** is formed from the direct oxidation of propane **139** but may proceed via a two-step pathway involving 2-propanol **142**. Propylene **140** is then

converted to acrolein **88** via insertion of an oxygen atom into a C-H bond to produce an allylic alcohol **141** (Figure 10) followed by dehydrogenation of the formed C-O bond to produce acrolein **88**. Acrolein **88** is then oxidized to acrylic acid **134**. Though propane **139** can be isolated directly from fossil fuel sources and thus is more abundant than propylene **140** as a byproduct of petroleum refining, the yields of acrylic acid **134** from propane **139** cannot compete with those from propylene **140**.[140,141,142,146]

6.2. Biobased acrylic acid

Production of acrylic acid from petroleum is subject to drastic increases and decreases in the availability and cost of crude oil. Due to the volatility in the economics surrounding the feedstock, acrylic acid prices rise and fall in turn. In order to provide economic stability to acrylic acid production, alternate sources of feedstocks are required. To that end, biological sources of acrylic acid may prove to be highly beneficial.

The CoA ester of acrylic acid, acryloyl-CoA **156** (Scheme 30, section 6.2.1.) is a fairly common metabolic intermediate and is produced as a metabolite in β-alanine biosynthesis, methylthiopropionate degradation, and acrylonitrile degradation.[147] Free acrylic acid, on the other hand, has only been observed as a product of the degradation of dimethylsulfoniopropionate ($C_5H_{10}O_2S$) which helps to maintain fluid balance in a marine bacterial cell by affecting the rate of osmosis.[148]

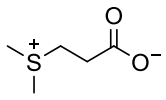

Figure 13. Dimethylsulfoniopropionate.

Dimethylsulfoniopropionate may be directly cleaved to acrylic acid and dimethylsulfide or may undergo initial demethylation followed by cleavage to afford methanethiol and acrylic acid. Unfortunately, pathways involving free acrylic acid **134** or acryloyl-CoA **156** do not produce these metabolites in high concentrations. For example, blocking the enzyme that converts acryloyl-CoA into propanoyl-CoA during β-alanine biosynthesis by using 3-butynoic acid as an inhibitor could not produce acrylic acid titers above 1% of initial glucose concentrations.[149] The most significant problems for the microbial synthesis routes is a lack of a driving force for the production of acrylic acid.[149] Thus, biobased routes to acrylic acid have targeted lactic acid or 3-hydroxypropionic acid (3-HP) as biological intermediates which are chemically converted to acrylic acid.

6.2.1. Dehydration of 3-hydroxypropionic acid

3-Hydroxypropionic acid (3-HP) is readily dehydrated to acrylic acid under mild conditions.[150] It is easily solvated in aqueous media and forms dimers in solution, therefore, fermentation broth containing biologically produced 3-HP may contain dimers and oligomers as well as the free acid (Scheme 29).

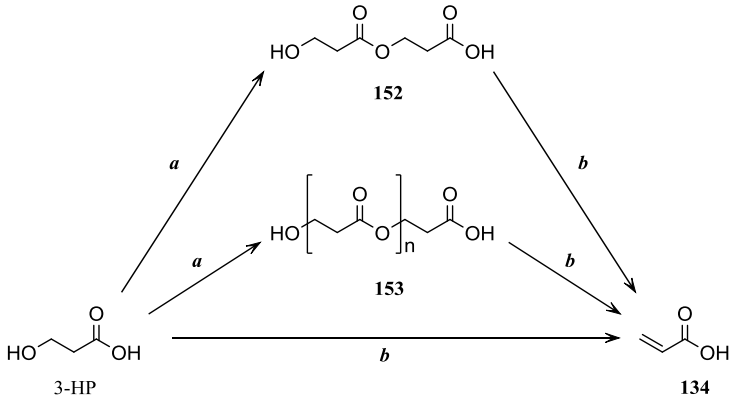

Scheme 29. Dehydration of 3-hydroxypropionic acid, dimers **152**, and oligomers **153** to acrylic acid **134**, a) microbial fermentation (e.g. *E. coli*); b) TiO_2, 180°C.

Using a mixed feed stream containing 9.19% by weight 3-HP and 2.70% dimers in water, acrylic acid was produced with 98% conversion of 3-HP and >99% selectivity to acrylic acid **134**.[150] The feed stream was passed over a 16-30 mesh TiO_2 catalyst bed at 180°C. The results suggest that dimers as well as 3-HP monomer was converted to acrylic acid under the reaction conditions.

Table 8. Proposed pathways for biosynthesis of 3-hydroxypropionic acid from glucose **13**.

Entry	Pathway
1	pyruvate **25** → lactate **154** → lactoyl-CoA **155** → acryloyl-CoA **156** → 3-HP-CoA **157** → 3-HP
2	pyruvate **25** → acetyl-CoA **24** → malonyl-CoA → 3-oxopropanoate **162** → 3-HP
3	pyruvate **25**/PEP **14** → oxaloacetate **15** → aspartate **163** → β-alanine **159** → 3-oxopropanoate **162** → 3-HP
4	pyruvate **25**/PEP **14** → oxaloacetate **15** → aspartate **163** → β-alanine **159** → β-alanyl-CoA **160** → acryloyl-CoA **156** → 3-HP-CoA **157** → 3-HP
5	pyruvate **25**/PEP **14** → succinate **18** – propionate **164**/propionyl-CoA **165** → acryloyl-CoA **156** → 3-HP-CoA **157** → 3-HP
6	pyruvate **25** → α-alanine **158** → β-alanine **159** → 3-oxopropanoate **162** → 3-HP
7	pyruvate **25** → α-alanine **158** → β-alanine **159** → β-alanyl-CoA **160** → acryloyl-CoA **156** → 3-HP-CoA **157** → 3-HP

Several microorganisms have been investigated for the biological production of 3-HP including *Escherichia coli, Klebsiella pneumoniae,* and *Lactobacillus collinoides* using both glycerol and glucose as a carbon source.[151] Seven different biochemical pathways using glucose **13** as a starting material have been proposed (Scheme 30, Table 8).[151]

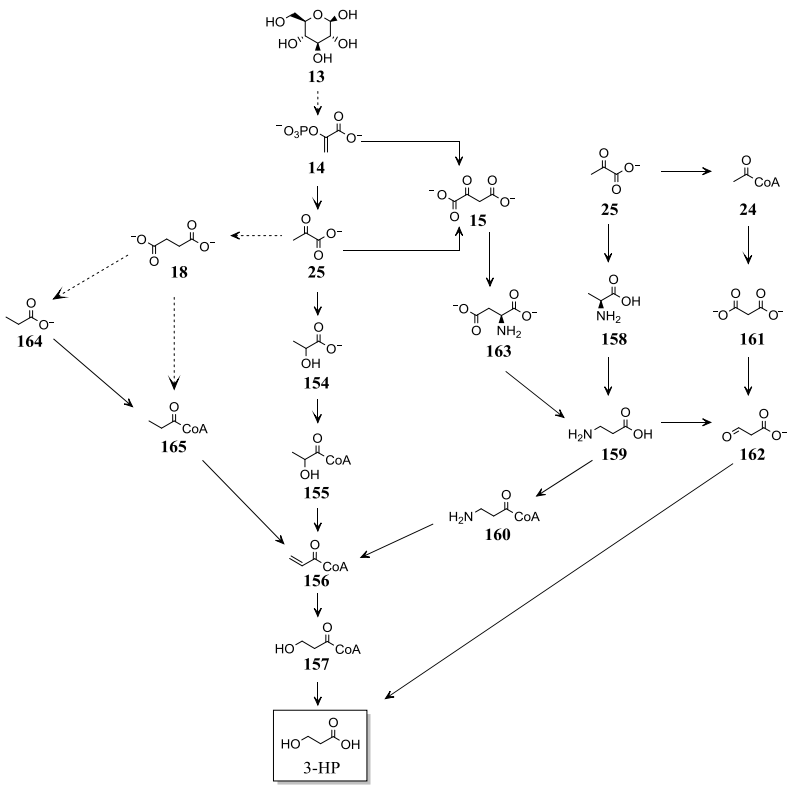

Scheme 30. Biosynthetic pathways for the synthesis of 3-hydroxypropionic acid from glucose **13**. Dashed arrows indicate multiple steps.

All seven pathways involve pyruvate **25** or phosphoenolpyruvate **14** as the core intermediate. Pathways 4 and 5 (Table 8) are energy intensive and involve a net loss of ATP.[151] This limitation will likely prevent these pathways from being utilized in a commercial process. However, the production of 3-HP via malonyl-CoA (Pathway 2, Table 8) has been realized in a recombinant *E. coli* strain.[152] Overexpression of malonyl-CoA reductase, nicotinamide nucleotide transhydrogenase, and acetyl-CoA carboxylase along with an inhibition of fatty acid synthesis via reduction of the levels of enoyl-ACP reductase resulted in 49 g/L of 3-HP after 69 h with a 0.49 mol mol^{-1} glucose yield. This is the highest yield of 3-HP from glucose **13** reported so far.[152]

Due to the rapid growth of biodiesel production, there is an abundant and inexpensive quantity of crude glycerol **166** (Scheme 31).[151] Two metabolic pathways exist for the biosynthesis of 3-HP from glycerol: one dependent on CoA, and a CoA-independent pathway (Scheme 31). The CoA-dependent pathway was inspired by 1,2-propanediol degradation in *Salmonella enterica*.[153] The same enzymes used in the native host can be expressed for the production of 3-HP and are all found in a contiguous cluster called the propanediol utilization (*pdu*) locus.[151,153] The production of 3-HP begins with the conversion of glycerol **166** to 3-hydroxypropionaldehyde (3-HPA) **170** catalyzed by a coenzyme B_{12}-dependent diol dehydratase.[153] The resultant 3-HPA **170** is converted to 3-HP-phosphate **179** and ultimately 3-HP by several enzymes such as propanol dehydrogenase, CoA-dependent propionaldehyde dehydrogenase, phosphotransacylase, and propionate kinase.[153] Although this pathway has been known for many years, it has not been applied to commercial processes.[151]

The CoA-independent pathway is simpler than the CoA-dependent pathway and can utilize multiple alcohol dehydrogenases present in many microbes. Glyceraldehyde dehydratase catalyzes the conversion of glycerol **166** to 3-HPA **170**, which is further transformed to 3-HP by an alcohol dehydrogenase. The difficulty with this pathway lies in the oxygen sensitivity of the coenzyme-B_{12}-independent glycerol dehydratase.[151] Because 3-HP production is generally aerobic, the coenyme-B_{12}-dependent glycerol dehydratase must be utilized. *K. pneumoniae* naturally produces coenzyme-B_{12} and are therefore often studied as hosts for production of 3-HP from glycerol **166**.[154] A recombinant microorganism was developed by overexpressing the γ-glutamyl-γ-aminobutyraldehyde dehydrogenase of *K. pneumoniae* and disrupting two major oxidoreductases. In a glycerol-fed fermentation, 3-HP was produced at 28 g/L after 48 h with a yield of 40% based on glycerol **166**.[154] Thus, both glucose **13** and glycerol **166** may be utilized

as starting materials for the biological production of 3-HP. A partnership between OPX Bio and Dow Chemical Co. have already commercialized a process for the production of acrylic acid **134** from biologically derived 3-HP.[155] Cargill, Novozyme, and BASF have also collaborated on the production of acrylic acid from biobased 3-HP, though as of January 2015, BASF has left the partnership.[156]

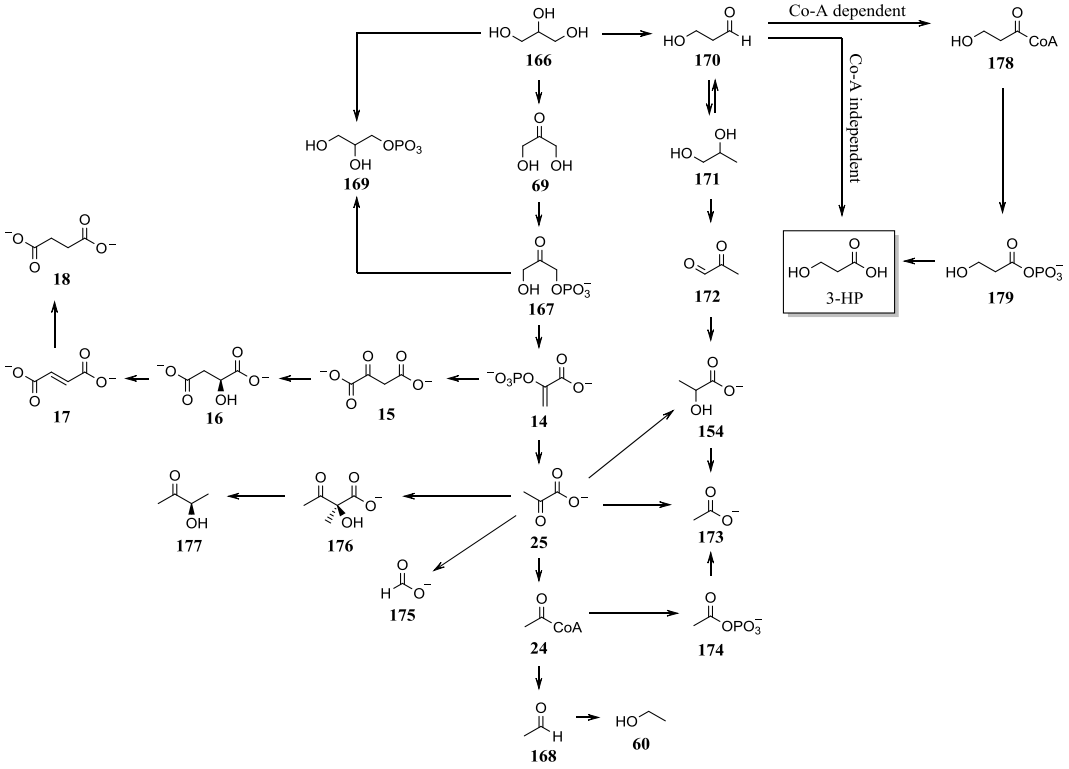

Scheme 31. Pathways for glycerol **166** metabolism including Co-A dependent and Co-A independent pathways for 3-hydroxypropionic acid biosynthesis.

6.2.2. Dehydration of lactic acid

The dehydration of biologically derived lactic acid is an alternate strategy for the production of biobased acrylic acid. Lactic acid is often used to make poly(lactic acid), a biodegradable polymer, but petroleum derived lactic acid is always produced as a racemate.[157] However, biologically produced lactic acid is made as a pure L- or D- isomer, which helps provide crystallinity to poly(lactic acid). As such, fermentation routes are the preferred means for commercial production of lactic acid.[158]

Microbial synthesis of lactic acid takes place via one of three major metabolic pathways, the Embden-Meyerhof-Parnas (EMP) pathway, the phosphoketolase (PK) pathway, and the pentose phosphate (PP) pathway (Figure 12A, 12B).[158] Many microbes possess the EMP pathway in conjunction with either the PK pathway or the PP pathway, therefore lactate **158** production is dependent on which pathway is accessed according to specific growth conditions.

A wide variety of carbohydrates may be converted to lactate **154**. For the conversion of arabinose **184** to lactate **154**, the phosphoketolase gene in *Lactobacillus plantarum* was substituted for the transketolase gene from *Lactococcus lactis*, thereby shifting carbon flux into the PP pathway.[159] In 27 h, 38.6 g/L of lactate **154** was produced which corresponds to a yield of 1.54 mol mol^{-1} arabinose **184**. In another study, an *E. coli* microbe engineered by a knockout in the sucrose repressor gene (*cscR*) afforded 97 g/L of lactate **154** in 84 h with a yield of 0.9 mol mol^{-1} sucrose, which enters the EMP pathway after conversion to glucose **13** and fructose **44**.[160]

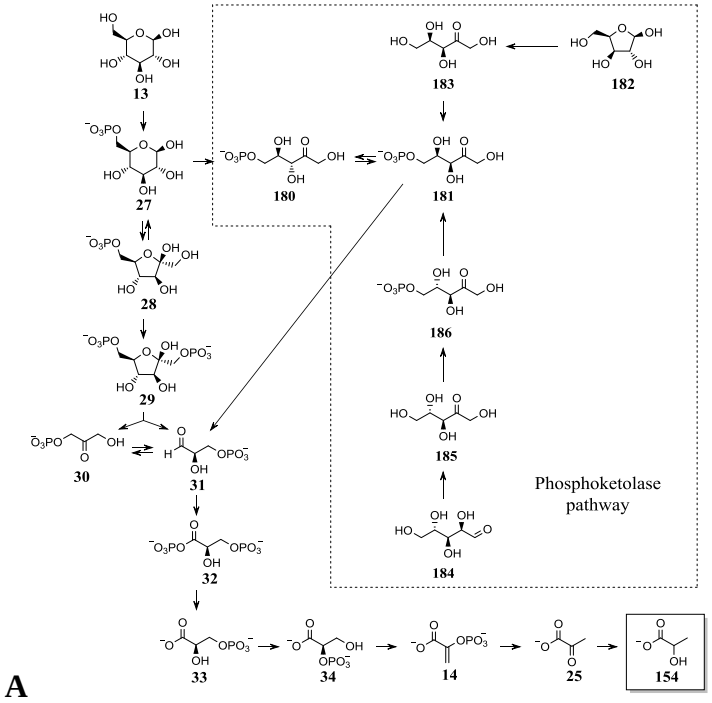

A

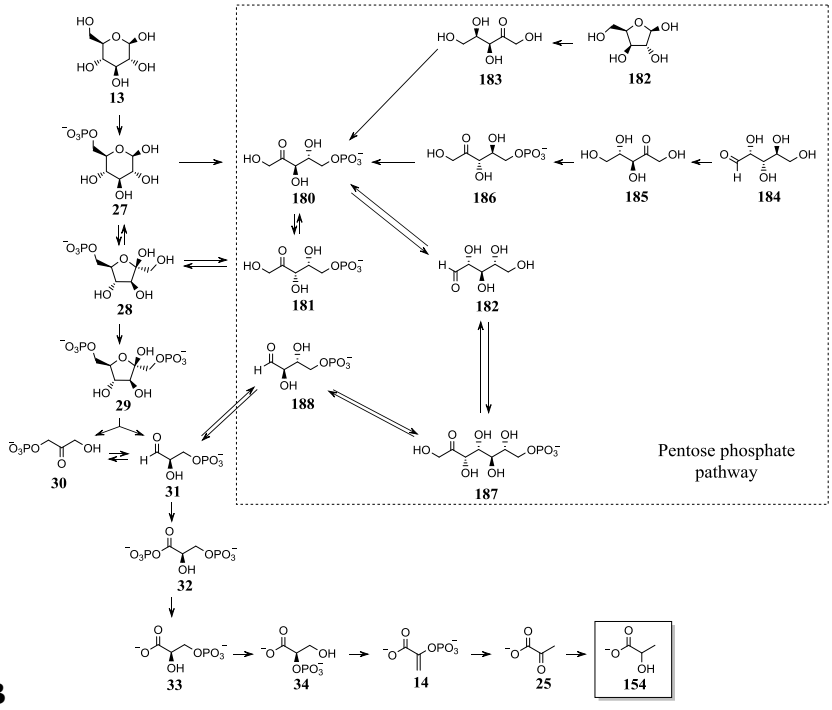

B

Figure 14. Microbial synthesis of lactate from simple sugars. **A.** Embden-Meyerhof-Parnas pathway and the phosphoketolase pathway; **B.** Embden-Meyerhof-Parnas pathway and the pentose phosphate pathway.

In a related experiment, *E. coli* was engineered to accumulate lactate **154** from glucose **13** by knocking out the gene encoding pyruvate formate lyase (*pflB*). By coexpressing a *Streptococcus bovis* lactate dehydrogenase gene in the *pflB* knockout, a titer of 73 g/L of lactate **154** was produced on a complex medium of several carbohydrates.[161] Thus, the production of lactic acid **189** via fermentation is a well-studied, mature technology.

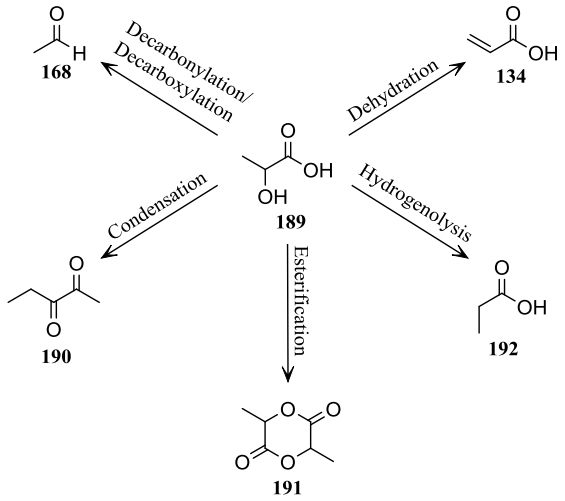

Figure 15. Dehydration of lactic acid **189** and its competing reactions.

The lactic acid **189** (Figure 13) produced by fermentation is readily dehydrated to acrylic acid **134**. Several different types of zeolite or metal oxide catalysts have been investigated in the dehydration of lactic acid **189** but some of the best results so far have been with hydroxyapatites ($Ca_{10}(PO_4)_6(OH)_2$).[162] At 360°C and atmospheric pressure, a 10 mol% solution of lactic acid **189** in water is dehydrated to acrylic acid **134** with 71-74% selectivity to give a total yield of 50-62%. Jackson and Miller of Michigan State University have shown several competing side reactions during the dehydration of lactic acid **189** including decarbonylation/decarboxylation to produce acetaldehyde **168**, condensation reactions to produce 2,3-pentanedione **195**, esterification via dimerization to produce cyclic ester **195**, and hydrogenolysis producing

propionic acid **197**.[163] These side products always occur during chemical dehydration of lactic acid **189** and are responsible for less than quantitative acrylic acid yields. A plausible mechanism for the production of acrylic acid **134** using hydroxyapatite catalysts is presented in Scheme 32.[162]

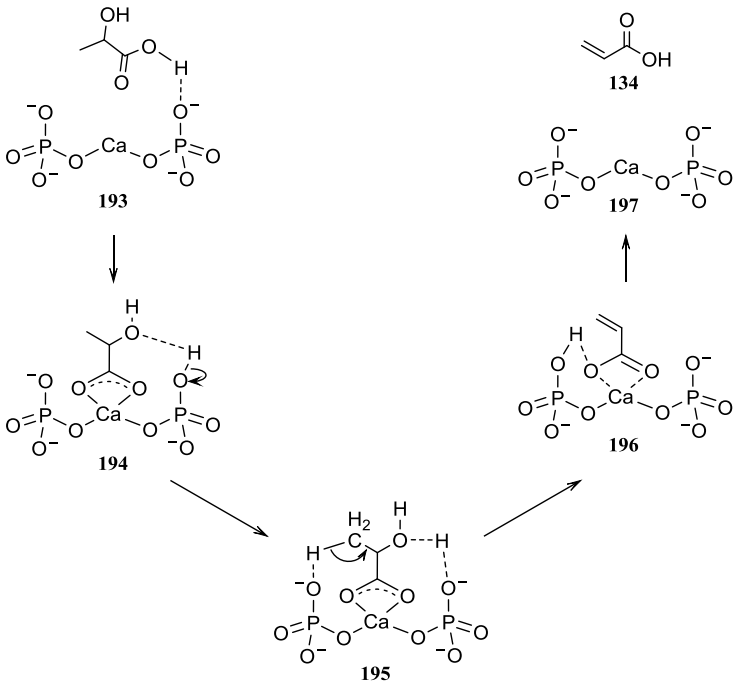

Scheme 32. Possible mechanism for production of acrylic acid **134** over hydroxyapatite catalysts.

The Procter & Gamble Co. have developed a catalyst more active and selective than hydroxyapatites.[164] A catalyst prepared from barium nitrate ($Ba(NO_3)_2$) and dibasic potassium phosphate (K_2HPO_4) catalyzed a vapor phase conversion of a 20 wt% aqueous feed of lactic acid **189** to acrylic acid **134** with 91% conversion and 93% selectivity at 350°C. Myriant has also patented a route to acrylic acid **134** from the dehydration of biobased lactic acid **189** using Na or Cs impregnated zeolites, but the selectivities to acrylic acid **134** for this process are only around 20%.[165]

7. SYNTHESIS OF ISOPRENE

7.1. Petrochemical syntheses

Global production of isoprene **133** (Scheme 26) is in excess of 1.7 billion pounds per year and is largely used for rubber in tires, adhesives, and elastomers.[166] Isoprene is most commonly produced from a crude C_5 hydrocarbon stream from petroleum. It may be isolated directly from a C_5 stream from a cracking plant, or may be produced as a result of isopentane or isopentenes. Several syntheses of isoprene from smaller units have also been developed.

7.1.1. Extractive distillation

Extractive distillation of isoprene from petroleum cracking streams is the major source of fossil fuel-based isoprene. The process is based on a selective solvent such as *N*-formylmorpholine, dimethylformamide, *N*-methylpyrrolidone, or acetonitrile, that solvates and removes isoprene from a complex mixture of hydrocarbons.[167-171] These mixtures typically contain 15-20 wt% isoprene along with tertiary amylenes (isoamylene), and over 15 other C_5 hydrocarbons. The Goodyear Tire & Rubber Co. is the leading producer of isoprene in the US[166] and has developed an extractive distillation method that uses *n*-pentane to form a binary azeotrope with isoprene.[170,171]

Extractive distillation is an effective method for removing isoprene but is limited by the availability of isoprene-containing feed streams. A trend in industry, particularly in North America, is to use light hydrocarbons or shale gas in cracking reactors instead of heavy hydrocarbons.[172] Cracking these lighter feedstocks produces much less isoprene than naphtha crackers, thus making extractive distillation less attractive in the United States than it otherwise would be using traditional petroleum feedstocks.

7.1.2. Dehydrogenation of isoamylenes and isopentane

When isoamylenes (2-methyl-1-butene **200**, 3-methyl-1-butene **198**, and 2-methyl-2-butene **199**) are present in C_5 streams, these may be readily extracted and converted into isoprene (Scheme 33). In an extraction developed by the Sinclair Refining Company,[173] 1,3-pentadiene is removed from a crude C_5 stream by solid adsorption before the C_5 mixture is introduced into a 60-65% aqueous solution of H_2SO_4 at 10-20°C. Under these conditions, isoamylenes **198** and **200** are isomerized to 2-methyl-2-butene **199** before the spontaneous addition of H_2SO_4 to form the sulfuric acid ester **200** (Scheme 33). After splitting the ester **200** at 35°C, distillation affords 2-methyl-2-butene **199** in 93.5% yield and 2-methyl-1-butene **200** in 5.4% yield.[173] Dehydrogenation of 2-methyl-2-butene **199** takes place over an iron oxide-chromium oxide-potassium carbonate (Fe_2O_3-Cr_2O_3-K_2CO_3) catalyst at 600°C to afford an 85% yield of isoprene **133**.[173] This process is used commercially in Russia. Alternatively, isopentane may be dehydrogenated to isoprene.[174] However, this reaction is more thermodynamically unfavorable than the dehydrogenation of isoamylenes and requires temperatures in excess of 600°C to break the C-H bonds. Nonetheless, this can be utilized when isopentane is readily available from C_5 streams.[174]

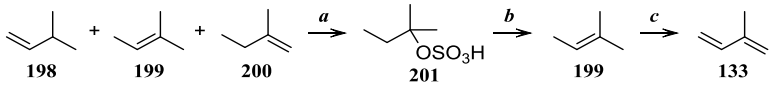

Scheme 33. Sinclair extraction of 2-methyl-2-butene **199** with H_2SO_4 followed by dehydrogenation to isoprene **133**, a) 65% H_2SO_4, 10-20°C; b) 35°C; c) Fe_2O_3-Cr_2O_3-K_2CO_3, 600°C.

Advantageously, isoamylenes may be chemically produced from a stream of butene isomers if a C_5 stream is unavailable.[175] Molecular sieves remove any 1-butene present which must be isomerized to 2-butene over Ru oxide (RuO_2) or to isobutylene over ZrO_2 prior to dehydrogenation. Following isomerization, the product is introduced back into the butene

mixture. This feed is then disproportionated into isoamylenes and propylene over a catalyst comprised of tungsten, molybdenum, Re oxides, or Re phosphates at 340-400°C and 21 bar. The product stream containing isoamylenes and byproduct ethylene and propylene is separated by fractionation before the isoamylenes are dehydrogenated to isoprene as described above.[175]

7.1.3. Isoprene from smaller units

7.1.3.1. Propylene dimerization

Jointly developed by The Goodyear Tire & Rubber Co. and Scientific Design Company, the dimerization of propylene is an alternate route to isoprene **133** that does not require isolation from cracking streams.[176,177] In a three-stage process (Scheme 34) propylene **141** is first dimerized at 200°C over a Ziegler catalyst such as tri-*n*-propylaluminum ($Al(CH_2CH_2CH_3)_3$) to afford 2-methyl-1-pentene **202** with 99% selectivity. This is subsequently isomerized to 2-methyl-2-pentene **203** over a SiO_2/Al_2O_3 catalyst at 100°C. Demethanation of 2-methyl-2-pentene **203** to isoprene **133** occurs in the presence of ammonium sulfide ($(NH_4)_2S$) at 650-680°C or, alternatively, with HBr and superheated steam at 650-800°C. The overall selectivity to isoprene **133** is around 50% based on propylene **141**.[176,177]

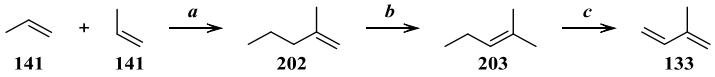

Scheme 34. Isoprene **133** synthesis via dimerization of propylene **141**, a) $Al(CH_2CH_2CH_3)_3$, 200°C; b) SiO_2/Al_2O_3, 100°C; c) $(NH_4)_2S$, 650-680°C.

7.1.3.2. The Snamprogetti Process

An alternative synthesis of isoprene makes use of the reaction between acetone **143** and acetylene **138** (Scheme 35).[176,178] Acetone, a byproduct of the Hock oxidation of cumene, and acetylene, readily obtainable from ethylene or calcium carbide, are reacted in the presence of

KOH in liquid ammonia at 10-40°C and 20 bar to afford 2-methyl-3-butyn-2-ol **204**. This intermediate is hydrogenated to 2-methyl-buten-2-ol **205** before dehydrogenation over Al_2O_3 at 250-300°C and 1 bar to afford isoprene **133**.[176,178] Though this process has seen commercial use, it is no longer employed primarily due to the hazards surrounding the handling of acetylene **138**.

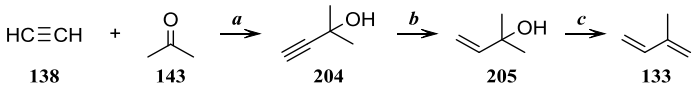

Scheme 35. Snamprogetti synthesis of isoprene **133** from acetylene **138** and acetone **143**, a) KOH, NH_3, 10-40°C, 20 bar; b) H_2, Pt/C; c) Al_2O_3, 250-300°C, 1 bar.

7.1.3.3. Isobutylene condensation with formaldehyde

The Prins condensation of isobutylene **78** with formaldehyde **53** is an alternate synthetic route to isoprene **133** and is practiced by many companies including Bayer, Marathon Oil, the CIS, and Kuraray (Scheme 36).[176,179-181] The most common embodiment makes use of a two-stage, liquid phase process. Formaldehyde **53** reacts with isobutylene **78** in the presence of a strong mineral acid such as H_2SO_4 at 70-95°C and 20 bar to form 4,4-dimethyl-1,3-dioxane **206**. Phosphate catalysts such as H_3PO_4/C or calcium phosphate ($Ca_3(PO_4)_2$) in water catalyze the conversion of the dioxane intermediate **206** to isoprene **133** at 240-400°C in a separate reactor. The selectivity to isoprene **133** is about 77% based on isobutylene **78**.[179-181]

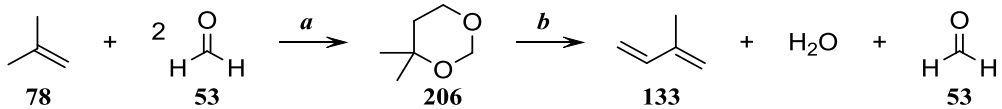

Scheme 36. Synthesis of isoprene **133** from Prins reaction of formaldehyde **53** with isobutylene **78**, a) H_2SO_4, 70-95°C, 20 bar; b) $Ca_3(PO_4)_2$, 240-400°C.

Several companies have developed unique conditions to try to improve this methodology and perhaps the most important development has been a continuous one-step process that does

not require isolation of dioxane **206** prior to dehydration.[176] An aqueous solution of 15-30% by weight of boric acid ($B(OH)_3$) and 0.5-5% by weight of H_3PO_4 catalyzes the conversion of isobutylene **78** to isoprene **133** at 150-200°C in a high pressure reactor. Formaldehyde **53** conversions are high (94-99%) and selectivity to isoprene **133** is 70-78%.[176,181] The addition of a glycol ether to the acidic aqueous solution assists in the gas-liquid contact between isobutylene **78** and the acid solution within the reaction zone. Advantageously, a tertiary alcohol such as *tert*-butanol may be present in the feed which dehydrates to isobutylene **78** in situ. Furthermore, precursors to formaldehyde **53** may be used such as trioxane, paraformaldehyde, and methylal which decompose to formaldehyde **53** under the reaction conditions. Due to the volatility of the isoprene product, continuous distillation of the product stream from the reactor zone helps to drive the reaction forward.[176,181]

7.1.3.4. Olefin metathesis

Both isoprene and acrylic acid can be synthesized by a reaction sequence beginning with ethylene (Scheme 37). Ethylene dimerization to 1-butene is catalyzed by $[Fe(CH_3CN)_6][BF_4]$ in $AlCl_3$/BMIC (1-butyl-3-methylimidazolium chloride) with methylaluminoxane (MAO) as a cocatalyst at 10°C and 20 bar ethylene.[182] A quantitative yield of 1-butene is achieved under these conditions.[182] 1-Butene is then converted to a mixture of isobutene and a mixture of *E*-2-butene and *Z*-2-butene at atmospheric pressure and 470°C using Al^{3+}-doped SBA-15 zeolite.[183] The resultant mixture of 2-butene and isobutene is converted to 2-methyl-2-butene and propylene over a WO_3/SiO_2 catalyst at 430°C.[184] After separation of propylene from 2-methyl-2-butene, the former may be oxidized to acrylic acid as discussed above, while the latter may be dehydrogenated to isoprene as described in section 7.1.2.

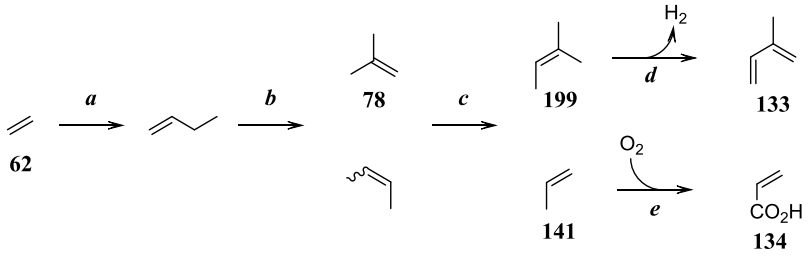

Scheme 37. Reaction sequence of isoprene **133** and acrylic acid **134** synthesis from ethylene **62**, a) $[Fe(CH_3CN)_6][BF_4]$, MAO, $AlCl_3$/BMIC, 10°C, 20 bar; b) Al-SBA-15, 470°C; c) WO_3/SiO_2, 430°C; d) Fe_2O_3-Cr_2O_3-K_2CO_3, 600°C; e) 1. Mo-Bi-Fe-Co-V-K-O, 320°C, 2. V_2O_5, 225°C.

7.2. Biobased isoprene production

Currently, all of the world's isoprene is produced from petroleum-based feedstocks and is thereby subject to volatility in the supply and costs linked to crude oil.[172] Furthermore, there is a trend toward declining availability of naphtha required for cracking and generation of C_5 hydrocarbons streams from which isoprene may be extracted. [172] Alternate sources of isoprene are needed to both meet the global isoprene demand and to stabilize isoprene costs in the face of a volatile crude oil economy.

Plants are by far the largest annual producers of isoprene releasing up to 59 million tons per year into the atmosphere.[185] This is enough isoprene to produce 60 billion tires for cars and trucks, which is 50 times the current worldwide tire production. However, plants are not a viable commercial source of isoprene because there is no practical means to collect biogenic isoprene emissions on a large scale. Alternatively, isoprene has been shown to be produced by microbial sources, though the global contribution of wild-type microorganisms is small when compared to plants.[186,187] The best bacterial producer of isoprene is *Bacillus subtilis*, which, in cell-free studies, has been shown to synthesize isoprene from a common precursor, dimethylallyl pyrophosphate (DMAPP).[188] Other research has demonstrated the efficacy of expressing the plant-derived isoprene synthase enzyme in *E. coli* which can produce isoprene in culture.[189]

These pioneering studies suggest recombinant microbes may be a commercially feasible option for biobased isoprene production and thus provide a means to diversify feedstocks for isoprene manufacture.

The key components for a recombinant microorganism to be successful in producing high titers of isoprene are the isoprene synthase enzyme from plants, and engineered isoprenoid precursor pathways.[189-191] Since isoprene synthase has not been found in microbes, this enzyme must be derived from plants. Plant-based isoprene synthase produces isoprene via elimination of pyrophosphate from DMAPP, which is one of two isoprenoid precursors along with isopentenyl diphosphate (IPP).[189]

DMAPP and IPP are essential to all living organisms and are produced by one of two biosynthetic pathways: the mevalonic acid (MVA) pathway which is native to eukaryotes and some prokaryotes, and the 5-methyl erythritol phosphate (MEP) pathway which is native to prokaryotes and plants (Figure 14A, 14B).[172,190,191] Sources of carbon come from intermediates derived from pathways central to sugar metabolism; MVA uses acetyl-CoA **24**, while MEP uses pyruvate **25** and glyceraldehyde 3-phosphate **31**.[172] While DMAPP can be produced via both pathways, the MVA pathway has been used industrially in both yeast and bacteria and therefore is the best characterized pathway.[172,192] The MEP pathway has been discovered more recently and contains iron-sulfur cluster enzymes which are still poorly characterized.[193,194] Optimization of the MEP pathway is worth investigation, however, as it has a higher theoretical mass yield from glucose than the MVA pathway (30.2% maximum yield for MEP, 25.2% maximum yield for MVA).[172]

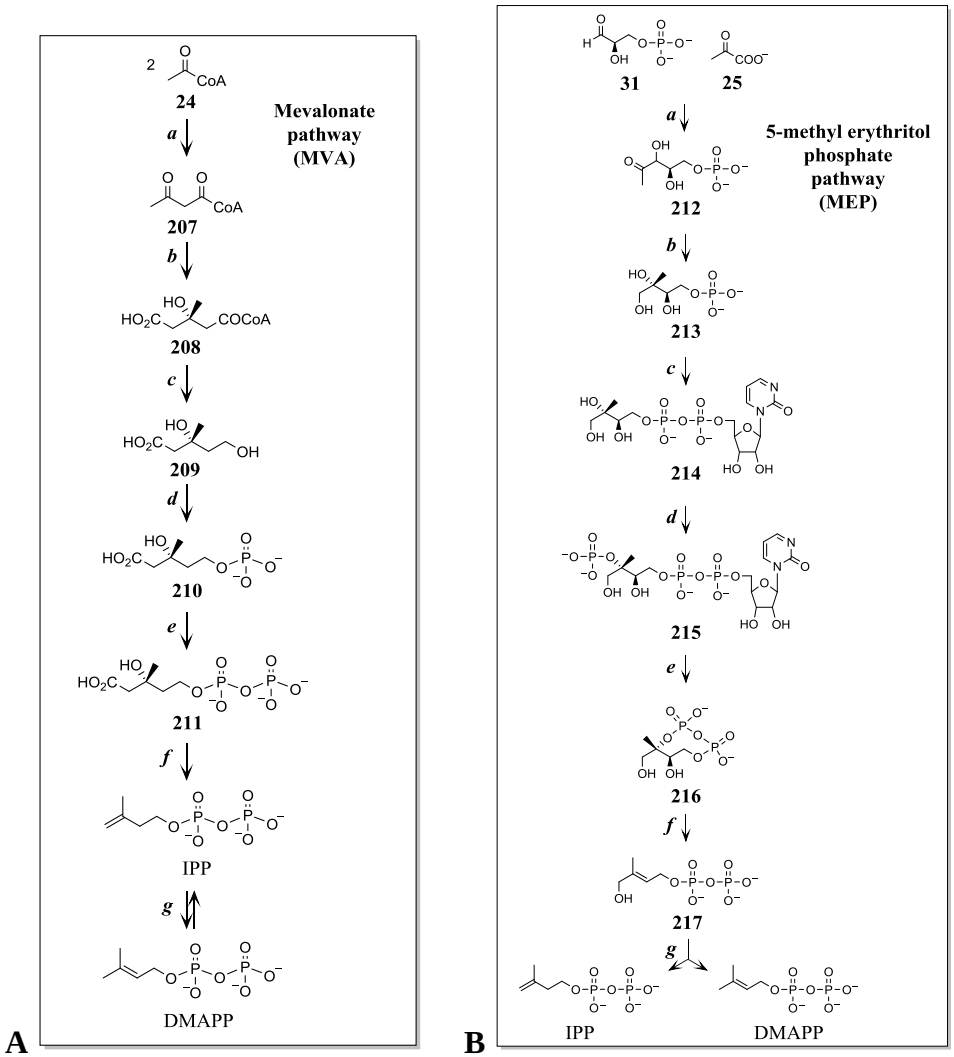

Figure 16. Pathways of isoprenoid biosynthesis. **A.** Mevalonate pathway; enzymes involved are as follows: a) acetyl-CoA *C*-acetyltransferase (EC2.3.1.9); b) hydroxymethylglutaryl-CoA synthase (EC2.3.3.10); c) hydroxymethylglutaryl-CoA reductase (EC1.1.1.34); d) mevalonate kinase (EC2.7.1.36); e) phosphomevalonate kinase (EC2.7.4.2); f) mevalonate diphosphate decarboxylase (EC4.1.1.33); g) isopentenyl diphosphate isomerase (EC5.3.3.2). **B.** 5-Methyl erithritol phosphate pathway; enzymes involved are as follows: a) 1-deoxyxylulose-5-phosphate synthase (EC2.2.1.7); b) 1-deoxyxylulose-5-phosphate reductoisomerase (EC1.1.1.267); c) 4-diphosphocytidyl-2-*C*-methylerythritol synthetase (EC2.7.7.60); d) 4-diphosphocytidyl-2-*C*-methyl-D-erythritol kinase (EC2.7.1.148); e) 2-*C*-methyl-D-erythritol-2,4-cyclodiphosphate synthase (EC4.6.1.12); f) 1-hydroxy-2-methyl-2*E*-butenyl-4-diphosphate synthase (EC1.17.7.b); g) 1-hydroxy-2-methyl-2*E*-butenyl-4-diphosphate reductase (EC1.17.1.2).

Several specialty chemical companies are investigating microbial production of isoprene on a commercial scale including Arkema,[195] GlycosBio,[196] Aemetis,[197] and LanzaTech.[198] Major downstream rubber players have partnered with biochemical companies to develop routes to

biobased isoprene for tires such as Bridgestone and Ajinomoto,[199] Goodyear and DuPont,[200] and Michelin and Amyris with the recent addition of Brazkem in Brazil.[201] Recently, Goodyear and Genencor (a division of Danisco USA) have exploited the MVA pathway in combination with plant isoprene synthases in *E. coli* for high titers of isoprene from glucose.[202] After 60 h, isoprene is produced in titers of 60 g/L with a purity of 99.5% w/w. Unlike many other chemicals produced via fermentation, isoprene is volatile enough to exit the fermentor in the off-gas, thus saving costs of separating it from the fermentation medium.[172] With recent advances in microbial engineering for isoprene production, fermentation may be a very useful strategy to produce isoprene on large scales. This can meet isoprene needs not currently met by petroleum-derived isoprene due to volatility in the cost and availability of crude oil.

REFERENCES

REFERENCES

1. Cailliot, A. Etudes sur L'Essence de Terebenthine. Ann. Chim. Phys. 1847, 3, 27-40.

2. Sheehan, R. J. Terephthalic Acid, Dimethyl Terephthalate, and Isophthalic Acid. In *Ullman's Encyclopedia of Industrial Chemistry, Vol. 36*; Wiley-VCH: Weinheim, 2012; pp 17-28.

3. Sattler, H.; Schweizer, M. Polyester Fibers. In *Ullman's Encyclopedia of Industrial Chemistry*; Wiley-VCH: Weinheim, 2011; pp 1-34.

4. Raghavendrachar, P.; Ramachandran, S. Liquid-Phase Catalytic Oxidation of *p*-Xylene. *Ind. Eng. Chem. Res.* **1992**, *31*, 453-462.

5. Collias, D. I.; Harris, A. M.; Nagpal, V.; Cottrell, I. W.; Schultheis, M. W. Biobased Terephthalic Acid Technologies: A Literature Review. *Ind. Biotechnol*. **2014**, *10*, 91-105.

6. Wittcoff, H.; Reuben, B. G.; Plotkin, J. S. *Industrial Organic Chemicals* 3rd Ed.; Wiley: Hoboken, 2013; pp 386-391.

7. Bizzari, S. N.; Blagoev, M.; Kishi, A. *Plasticizers: CEH Marketing Research Report*, 2007.

8. Franck, H.-G.; Stadelhofer, J. W. *Industrial Aromatic Chemistry*; Springer: Berlin, 1988; pp 265-272.

9. Wittcoff, H. A.; Reuben, B. G.; Plotkin, J. S. *Industrial Organic Chemicals* 3rd Ed.; Wiley: Hoboken, 2013; p 403.

10. Saffer, A.; Barker, R. S. Preparation of aromatic polycarboxylic acids. US 2,833,816, 1958.

11. Tomás, R. A. F.; Bordado, J. C. M.; Gomes, J. F. P. p-Xylene Oxidation to Terephthalic Acid: A Literature Review Oriented toward Process Optimization and Development. *Chem. Rev.* **2013**, *113*, 7421-7469.

12. Partenheimer, W. Methodology and scope of metal/bromide autoxidation of hydrocarbons. *Catal. Today*, **1995**, *23*, 69-158.

13. Tibbitt, J. Personal communication.

14. Park, C.-M.; Sheehan, R. J. Phthalic acids and other benzenepolycarboxylic acids. In *Kirk-Othmer Encyclopedia of Chemical Technology*; Wiley, 2001; pp 1-45.

15. Chanda, M.; Roy, S. K. Industrial Polymers, Specialty Polymers, and Their Applications; CRC: Boca Raton, 2008; p 1-57.

16. Berkowitz, N. *Fossil hydrocarbons: chemistry and technology*; Academic: San Diego, 1997; pp 88-91.

17. Cutler, J. Presented at the West Virginia Marcellus to Manufacturing Conference, Charleston, WV, March 2013.

18. King, H. Hydraulic Fracturing of Oil & Gas Wells Drilled in Shale. http:// geology.com/articles/hydraulic-fracturing/.htm (accessed Feb. 24, 2015).

19. Montgomery, L. Oklahoma worries over swarm of earthwuakes and connection to oil industry. *The Washington Post*, Jan. 28, 2015.

20. Szmant, H. H. *Organic Building Blocks of the Chemical Industry*; Wiley: New York, 1989; pp 33-35.

21. Berkowitz, N. *Fossil hydrocarbons: chemistry and technology*; Academic: San Diego, 1997; pp 91-94.

22. Elvers, B. *Handbook of Fuels: Energy Sources for Transportation*; Wiley-VCH: Weinheim, 2008; pp 29-34.

23. Franck, H.-G.; Stadelhofer, J. W. *Industrial Aromatic Chemistry*; Springer: Berlin, 1988; pp 60-62.

24. Wittcoff, H. A.; Reuben, B. G.; Plotkin, J. S. *Industrial Organic Chemicals* 3rd Ed.; Wiley: Hoboken, 2013; pp 114-119.

25. Franck, H.-G.; Stadelhofer, J. W. *Industrial Aromatic Chemistry*; Springer: Berlin, 1988; pp 76-81.

26. Franck, H.-G.; Stadelhofer, J. W. *Industrial Aromatic Chemistry*; Springer: Berlin, 1988; pp 63-72.

27. Elvers, B. *Handbook of Fuels: Energy Sources for Transportation*; Wiley-VCH: Weinheim, 2008; pp 34-38.

28. Elvers, B. *Handbook of Fuels: Energy Sources for Transportation*; Wiley-VCH: Weinheim, 2008; pp 44-50.

29. Jensen, R. H. Process for conversion of light aliphatic hydrocarbons to aromatics. US 4,642,402, 1987.

30. Kluksdahl, H. E. Reforming a sulfur-free naphtha with a platinum-rhenium catalyst. US 3,415,737, 1968.

31. Bennett, I. C.; Hall, A. H. P. Aromatization of paraffins. US 4,766,264, 1988.

32. McNiff, T. K. Production of aromatics from ethane and/or ethylene. US 4,613,716, 1986.

33. Dilip, D. Gallium ion exchanged zeolites. GB 2,082,157 A, 1982.

34. Guisnet, M.; Gnep, N. S.; Alario, F. Aromatization of short chain alkanes on zeolite catalysts. *Appl. Catal. A: Gen.* **1992**, *89*, 1-30.

35. Nacamuli, G. J. Process for production of aromatics in parallel reformers with an improved catalyst life and reduced complexity. US 6,143,166, 2000.

36. Cheung, T.-T. P. Catalytic reforming. US 20140066676 A1, 2014.

37. Chen, C.-Y.; Miller, S. J.; Ziemer, J. N.; Liang, A. J. Process for the production of para-xylene. US 8,471,083 B2, 2013.

38. Matar, S.; Hatch, L. F. *Chemistry of Petrochemical Processes* 2nd Ed.; Gulf Professional: Woburn, 2001; pp 178-180.

39. Wittcoff, H. A.; Reuben, B. G.; Plotkin, J. S. *Industrial Organic Chemicals* 3rd Ed.; Wiley: Hoboken, 2013; p 471.

40. Chevron Phillips Chemical Company. Aromax Technology Process. http://www.cpchem.com/en-us/rnt/licensing/aromaxtech/Pages/Process.aspx. (accessed on Nov. 16, 2014).

41. Arpe, H.-J. *Industrial Organic Chemistry* 5th Ed.; Wiley-VCH: Weinheim, 2010; p 328-333.

42. Gaile, A. A.; Zalishchevskii, G. D.; Gafur, N. N.; Semenov, L. V.; Varshavskii, O. M.; Fedyanin, N. P.; Koldobskaya, L. L. Removal of Aromatic Hydrocarbons from Reforming Naphtha. Combined Extraction-Extractive-Azeotropic Distillation Process. *Chem. Technol. Fuels Oils*, **2004**, *40*, 215-221.

43. Wytze Meindersma, G.; Podt, A.; de Haan, A. Selection of Ionic Liquids for the Extraction of Aromatic Hydrocarbons from Aromatic/Aliphatic Mixtures. *Fuel Process. Technol*. **2005**, *87*, 59-70.

44. Arce, A.; Earle, M. J.; Rodriquez, H.; Seddon, K. R. Separation of Aromatic Hydrocarbons from Alkanes Using the Ionic Liquid 1-ethyl-3-imidazolium bis[(trifluoromethyl)sulfonyl]amide. *Green Chem*. **2007**, *9*, 70-74.

45. Radwan, G. M.; Al-Muhtaseb, S. A.; Fahim, M. A. Liquid-Liquid Equilibria for the Extraction of Aromatics from Naphtha Reformate by Dimethylformamide/Ethylene Glycol Mixed Solvent. *Fluid Phase Equil*. **1997**, *129*, 175-186.

46. Marawski, P.; Letcher, T. M.; Naicker, P. K.; Domanska, U. Liquid-Liquid Equilibria for Mixtures of Furfuryl Alcohol + an Aromatic Hydrocarbon + an Alkane at T = 298.15 K. *J. Chem. Eng. Data*, **2002**, *47*, 1453-1456.

47. Arpe, H.-J. *Industrial Organic Chemistry* 5th Ed.; Wiley-VCH: Weinheim, 2010; pp 339-345.

48. Haag, W. O.; Olson, D. H. Selective disproportionation of toluene. US 4,097,543, 1978.

49. Das, J.; Bhat, Y. S.; Halgeri, A. B. Transalkylation and disproportionation of toluene and C9 aromatics over zeolite beta. *Catal. Lett*. **1994**, *23*, 161-168.

50. Sulikowski, B.; Rachwalik, R. Catalytic Properties of Heteropolyacid/Zeolite Hybrid Materials: Toluene Disproportionation and Transalkylation with 1,2,4-Trimethylbenzene. *Appl. Catal. Gen.* **2003**, *256*, 173-182.

51. Mikitenko, P.; Hotier, G. Production of para-xylene from an effluent from para selective toluene disproportionation using a crystallization process combined with simulated moving bed adsorption. US 6,060,634, 2000

52. McArdle, E. H., Mason, D. M. Chemical process. US 2,435,792, 1944.
53. Jones, L. R.; Wood, D. C. Isomerization of alkyl aromatics using a gallium containing aluminosilicate catalyst. US 4,245,130, 1981.

54. Martens, J. A.; Perez-Pariente, J.; Sastre, E.; Corma, A.; Jacobs, P. A. Isomerization and Disproportionation of m-Xylene: Selectivities Induced by the Void Structure of the Zeolite Framework. *Appl. Catal*. **1988**, *45*, 85-101.

55. Ueno, T. Japan gas-chemical xylene separation process. *Bull. Jpn. Pet. Inst*. **1970**, *12*, 171-176.

56. Morrison, R. A. Xylene isomerization. US 3,856,872, 1974.

57. Olson, D. H.; Haag, W. O. Xylene isomerization. US 4,159,282, 1979.

58. Broughton, D. B.; Gerhold, C. G. Continuous sorption process employing fixed bed of sorbent and moving inlets and outlets. US 2,985,589, 1961.

59. Kuznicki, S. M.; Bell, V. A.; Nair, S.; Hillhouse, H. W.; Jacubinas, R. M.; Braunbarth, C. M.; Toby, B. H.; Tsapatsis, M. A Titanosilicate Molecular Sieve with Adjustable Pores for Size-Selective Adsorption of Molecules. *Nature*, **2001**, *412*, 720-724.

60. Wu, P.; Debebe, A.; Ma, Y. H. Adsorption and Diffusion of C6 and C8 Hydrocarbons in Silicalite. *Zeolites*, **1983**, *3*, 118-122.

61. Cheng, K.-K.; Zhao, X.-B.; Zeng, J.; Zhang, J.-A. Biotechnological Production of Succinic Acid: Current State and Perspectives. *Biofuels, Bioprod. Bioref*. **2012**, *6*, 302-318.

62. Nexant. Maleic anhydride. Nexant, Inc., White Plains, New York, 2009.

63. MetaCyc Pathway: incomplete reductive TCA cycle. http://metacyc.org/META/NEW-IMAGE?type=PATHWAY&object=P42-PWY (accessed on January 31, 2015).

64. MetaCyc Pathway: TCA cycle I (prokaryotic). http://metacyc.org/META/NEW-IMAGE?type=PATHWAY&object=TCA&detail-level=2. (Accessed on February 1, 2015).

65. MetaCyc Pathway: TCA cycle IV (2-oxoglutarate decarboxylase). http://metacyc.org/META/NEW-IMAGE?type=PATHWAY&object=P105-PWY&detail-level=2. (Accessed on February 1, 2015).

66. Zelle, R.; de Hulster, M. E.; van Winden, W. A.; de Waard, P; Dijkema, C; Winkler, A. A,; Geertman, J. A.; van Dijken, J. P.; Pronk, J. T.; van Maris, A. J. A. Malic Acid Production by Saccharomyces cerevisiae: Engineering of Pyruvate Carboxylation, Oxaloacetate Reduction, and malate export. *Appl. Environ. Microbiol*. **2008**, *74*, 2766-2777.

67. Brown, S. H.; Bashkirova, L.; Berka, R.; Chandler, T.; Doty, T.; McCall, K.; McCulloch, M.; McFarland, S.; Thompson, S.; Yaver, D.; Berry, A. Metabolic engineering of Aspergillus oryzae NRRL 3488 for increased production of L-malic acid. *Appl. Microbiol. Biotechnol*. **2013**, *97*, 8903-8912.

68. Frost, J. W.; Draths, K. M. Bacterial cell transformants for production of cis,cis-muconic acid and catechol. US 5,616,496. 1997.

69. MetaCyc Pathway: chorismate biosynthesis I. http://metacyc.org/META/NEW-IMAGE?type=PATHWAY&object=ARO-PWY&show-citations=NIL&detail-level=2. (Accessed on February 1, 2015).

70. van Putten, R.-J.; van der Waal, J. C.; de Jong, E.; Rasrendra, C. B.; Heeres, H. J.; de Vries, J. G. Hydroxymethylfurfural, A Versatile Platform Chemical Made from Renewable Resources. *Chem. Rev*. **2013**, *113*, 1499-1597.

71. Moreau, C.; Durand, R.; Razigade, S.; Duhamet, J.; Faugeras, P.; Rivalier, P.; Ros, P.; Avignon, G. Dehydration of fructose to 5-hydroxymethylfurfural over H-mordenites. *Appl. Catal. A: Gen.* **1996**, *145*, 211-224.

72. Antal Jr., M. J.; Mok, W. S. L.; Richards, G. N. Mechanism of formation of 5-(hydroxymethyl)-2-furaldehyde from D-fructose and sucrose. *Carbohydr. Res.* **1990**, *199*, 91-109.

73. Angyal, S. J. The Lobry de Bruyl-Alberda van Ekenstein Transformation and Related Reactions. In *Glycoscience: Epimerization, Isomerization, and Rearrangement Reactions of Carbohydrates*; Springer: Verlag Berlin Heidelberg, 2001; pp 1-15.

74. Zhang, J.; Weitz, E. An in Situ NMR Study of the Mechanism for the Catalytic Conversion of Fructose to 5-Hydroxymethylfurfural and then to Levulinic Acid Using ^{13}C Labeled D-Fructose. *ACS Catal.* **2012**, *2*, 1211-1218.

75. Akien, G. R.; Qi, L.; Horvath, I. T. Molecular mapping of the acid catalyst dehydration of fructose. *Chem. Commun.* **2012**, *48*, 5850-5852.

76. Zhao, H.; Holladay, J. E.; Brown, H.; Zhang, Z. C. Metal Chlorides in Ionic Liquid Solvents Convert Sugars to 5-Hydroxymethylfurfural. *Science*, **2007**, *316*, 1597-1600.

77. Hu, S.; Zhang, Z.; Song, J.; Zhou, Y.; Han, B. Efficient conversion of glucose into 5-hydroxymethylfurfural catalyzed by a common Lewis acid SnCl4 in an ionic liquid. *Green Chem*. **2009**, *11*, 1746-1749.

78. *EFSA J*. **2005**, *215*, 1-73.

79. Surh, Y.-J.; Liem, A.; Miller, J. A.; Tannenbaum, S. R. 5-Sulfooxymethylfurfural as a possible ultimate mutagenic and carcinogenic metabolite of the Maillard reaction product, 5-hydroxymethylfurfural. *Carcinogenesis*, **1994**, *15*, 2375-2377.

80. Zhang, M.; Yu, Y. Dehydration of Ethanol to Ethylene. *Ind. Eng. Chem. Res.* **2013**, *52*, 9505-9514.

81. Corma, A.; Mengual, J.; Miguel, P. J. Stabilization of ZSM-5 zeolite catalysts for steam catalytic cracking of naphtha for production of propene and ethene. *Appl. Catal. A: Gen*. **2012**, *421-422*, 121-134.

82. Sohn, S. W.; Rice, L. H.; Kulprathipanja, S. Ethylene production by steam cracking of normal paraffins. US 8,283,511 B2, 2012.

83. Solvay, SA Process for the manufacture of ethylene by dehydration of ethanol. European Patent 2,594,546 A1, 2013.

84. Braskem 'I'm Green' Polyethylene. http://www.braskem.com/site.aspx/Im-greenTM-Polyethylene (accessed Jan. 24, 2015).

85. Gray, K. A.; Zhao, L.; Emptage, M. Bioethanol. *Curr. Opin. Chem. Biol.* **2006**, *10*, 141-146.

86. Zakzeski, J.; Brujnincx, P. C. A.; Jongerius, A. L.; Weckhuysen, B. M. The catalytic valorization of lignin for the production of renewable chemicals. *Chem. Rev.* **2010**, *110*, 3552-3599.

87. Graedel, T. E. Terpenoids in the atmosphere. Rev. Geophys. Space Phys. **1979**, *17*, 937-947.

88. Kerton, F. M.; Marriott, R. *Alternative Solvents for Green Chemistry*, 2nd Ed.; RSC: Cambridge, 2013; p 166.

89. Attard, T. M.; Watterson, B.; Budarin, V. L.; Clark, J. H.; Hunt, A. J. Microwave assisted extraction as an important technology for valorizing orange waste. *New J. Chem.* **2014**, *38*, 2278-2283.

90. Rezzadori, K.; Benedetti, S.; Amante, E. R. Proposals for the residues recovery: Orange waste as raw material for new products. *Food Bioprod. Process.* **2012**, *90*, 606-614.

91. Hull, W. Q.; Lindsay, C. W.; Baier, W. E. Chemicals from oranges. *Ind. Eng. Chem.* **1953**, *45*, 876-890.

92. Kusserow, B.; Schimpf, S.; Claus, P. Hydrogenation of glucose to sorbitol over nickel and ruthenium catalysts. *Adv. Synth. Catal.* **2003**, *345*, 289-299.

93. Davda, R. R.; Dumesic, J. A. Renewable hydrogen by aqueous-phase reforming of glucose. Chem. Commun. **2004**, 36-37.

94. Hahn, H.-D.; Dambkes, G.; Rupprich, N.; Bahl, H.; Frey, G. D. Butanols. In *Ullmann's Encyclopedia of Industrial Chemistry*; Wiley-VCH: Weinheim; **2013**; 1-13.

95. Connor, M. R.; Liao, J. C. Microbial production of advanced transportation fuels in non-natural hosts. *Curr. Opin. Biotechnol.* **2009**, *20*, 307-315.

96. Atsumi, S.; Hanai, T.; Liao, J. C. Non-fermentative pathways for synthesis of branched-chain higher alcohols as biofuels. *Nature*, **2007**, *451*, 86-90.

97. Renny Feldman, R. M.; Gunawardena, U.; Urano, J.; McInhold, P.; Aristidou, A.; Aselson Dundon, C.; Smith, C. Yeast organism producing isobutanol at a high yield. US 8,017,375 B2, 2011.

98. MetaCyc Pathway: valine degradation II. http://metacyc.org/META/NEW-IMAGE?type=PATHWAY&object=PWY-5057&detail-level=4. (Accessed on February 3, 2015).

99. Roman-Leshkov, Y.; Barrett, C. J.; Liu, Z. Y.; Dumesic, J. A. Production of dimethylfuran for liquid fuels from biomass-derived carbohydrates. *Nature*, **2007**, *447*, 982-985.

100. Moliner, M.; Roman-Leshkov, Y.; Davis, M. E. Tin-containing zeolites are highly active catalysts for the isomerization of glucose in water. *Proc. Natl. Acad. Sci.* **2010**, *107*, 6164-6168.

101. Roman-Leshkov, Y. Phase modifiers promote efficient production of hydroxymethylfurfural from fructose. *Science*, **2006**, *312*, 1933-1937.

102. Zheng, H.-Y.; Zhu, Y.-L; Teng, B.-T.; Bai, Z.-Q.; Zhang, C.-H.; Xiang, H.-W.; Li, Y.-W. Towards understanding the reaction pathway in vapour phase hydrogenation of furfural to 2-methylfuran. *J. Mol. Catal. A: Chem.* **2006**, *246*, 18-23.

103. Manly, D. G.; Dunlop, A. P. Catalytic Hydrogenation. I. Kinetics and Catalyst Composition in Preparation of 2-Methylfuran. *J. Org. Chem.* **1958**, *23*, 1093-1095.

104. Rao, R. S.; Baker, T. K.; Vannice, M. A. Furfural hydrogenation over carbon-supported copper. *Catal. Lett.* **1999**, *60*, 51-57.

105. Cheng, Y.-T.; Huber, G. W. Production of targeted aromatics by using Diels-Alder classes of reactions with furans and olefins over ZSM-5. *Green Chem.* **2012**, *14*, 3114-3125.

106. Chang, C.-C.; Green, S. K.; Williams, C. L.; Dauenhauer, P. J.; Fan, W. Ultra-selective cycloaddition of dimethylfuran for renewable p-xylene with H-BEA. *Green Chem.* **2014**, *16*, 585-588.

107. Williams, C. L.; Chang, C.-C.; Do, P.; Nikbin, N.; Caratzoulas, S.; Vlachos, D. G.; Lobo, R. F.; Fan, W. Cycloaddition of biomass-derived furans for catalytic production of renewable p-xylene. *ACS Catal.* **2012**, *2*, 935-939.

108. Masuno, M. N.; Smith, P. B.; Hucul, D. A.; Dumitrascu, A.; Brune, K.; Smith, R. L.; Bissell, J.; Foster, M. Methods of producing para-xylene. US 8,889,938 B2, 2014.

109. Brandvold, T. A. Carboydrate route to para-xylene and terephthalic acid. US 8,314,267 B2, 2012.

110. Shiramizu, M.; Toste, F. D. On the Diels-Alder Approach to Solely Biomass-Derived Polyethylene Terephthalate (PET): Conversion of 2,5-Dimethylfuran and Acrolein into p-Xylene. *Chem. Eur. J.* **2011**, *17*, 12452-12457.

111. Katryniok, B.; Paul, S.; Belliere-Baca, V.; Rey, P.; Dumeignil, F. Glycerol dehydration to acrolein in the context of new uses of glycerol. *Green Chem.* **2010**, *12*, 2079-2098.

112. Katryniok, B.; Paul, S.; Capron, M.; Dumeignil, F. Towards the sustainable production of acrolein by glycerol dehydration. *ChemSusChem,* **2009**, *2*, 719-730.

113. Peters, M. W.; Taylor, J. D.; Jenni, M. M.; Manzer, L. E.; Henton, D. E. Integrated process to selectively convert renewable isobutanol to p-xylene. US 2011/044243 A1, 2011.

114. Taylor, T. J.; Taylor, J. D.; Peters, M. W.; Henton, D. E. Variations on Prins-like chemistry to produce 2,5-dimethylhexadiene from isobutanol. US 8,742,187 B2, 2014.

115. Taylor. J. D.; Jenni, M. M.; Peters, M. W. Dehydration of fermented isobutanol for the production of renewable chemicals and fuels. *Top. Catal.* **2010**, *53*, 1224-1230.

116. Manzer, L.; Kourtakis, K.; Herron, N.; McCarron, E.; VerNooy, P. Process for the preparation of p-xylene. US 7,067,708 B2, 2006.

117. Kunkes, E. L.; Simonetti, D. A.; West, R. M.; Serrano-Ruiz, J. C.; Gartner, C. A.; Dumesic, J. A. Catalytic conversion of biomass to monofunctional hydrocarbons and targeted liquid-fuel classes. *Science,* **2008**, *322*, 417-421.

118. Brookhart, M.; Findlater, M.; Guironnet, D.; Lyons, T. W. Synthesis of para-xylene and toluene. US 2013/0237732 A1, 2013.

119. Lyons, T. W.; Guironnet, D.; Findlater, M.; Brookhart, M. Synthesis of p-xylene from ethylene. *J. Am. Chem. Soc.* **2012**, *134*, 15708-15711.

120. Carter, A.; Cohen, S. A.; Cooley, N. A.; Murphy, A.; Scutt, J.; Wass, D. F. High activity ethylene trimerization catalysts based on diphosphine ligands. *Chem. Commun.* **2002**, 858-859.

121. Campbell, C. D.; Cole, D. T.; Taylor, III, H. R. Process for the preparation of dialkyl succinylsuccinates. US 5,783,723, 1998.

122. Kruper, Jr., W.; Rand, C. L.; Molzahn, D. C. Processes for producing terephthalic acid and terephthalate esters. US 2013345467 A1, 2013.

123. Ashworth, I. W.; Bowden, M. C.; Dembofsky, B.; Levin, D.; Moss, W.; Robinson, E.; Szczur, N.; Virica, J. A new route for manufacture of 3-cyano-1-naphthalenecarboxylic acid. *Org. Process. Res. Dev.* **2003**, *7*, 74-81.

124. Lee, J. J.; Kraus, G. A. One-pot formal synthesis of biorenewable terephthalic acid from methyl coumalate and methyl pyruvate. *Green Chem.* **2014**, *16*, 2111-2116.

125. Lee, J. J.; Kraus, G. A. Divergent Diels-Alder methodology from methyl coumalate toward functionalized aromatics. *Tet. Lett.* **2013**, *54*, 2366-2368.

126. Frost, J. W.; Miermont, A.; Schweitzer, D.; Bui, V.; Wicks, D. A. Terephthalic and trimellitic based acids and carboxylate derivatives thereof. US 8,367,858 B2, 2013.

127. Miura, T.; Kakinuma, H.; Kawano, T.; Matsuhisa, H. Method for producing furan-2,5-dicarboxylic acid. US 7,411,078 B2, 2008.

128. Gong, W. H. Terephthalic acid composition and process for the production thereof. US 7,385,081 B1, 2008.

129. Gong, W. H. Terephthalic acid composition and process for the production thereof. US 8,299,278 B2, 2012.

130. Hanke, P. D. Enzymatic oxidation of hydroxymethylfurfural. US 8,183,020 B2, 2012.

131. PEF Bottles. http://avantium.com/yxy/products-applications/fdca/PEF-bottles.html (accessed Jan. 24, 2015).

132. Berti, C; Binassi, E.; Colonna, M.; Fiorini, M.; Kannan, G.; Karanam, S.; Mazzacurati, M.; Odeh, I. Bio-based terephthalate polyesters. US 8,946,472 B2, 2015.

133. Collona, M.; Berti, C.; Fiorini, M.; Binassi, E.; Mazzacurati, M.; Vannini, M.; Karanam, S. Synthesis and radiocarbon evidence of terephthalate polyesters completely prepared from renewable resources. *Green Chem.* **2011**, *13*, 2543-2548.

134. Kamitsou, M.; Panagiotou, G. D.; Triantafyllidis, K. S.; Bourikas, K.; Lycourghiotis, A. Kordulis, C. Transformation of α-limonene into p-cymene over oxide catalysts: A green chemistry approach. *Appl. Catal. Gen.* **2014**, *474*, 224-229.

135. Miller, K. K.; Zheng, P.; Nishizawa-Brennen, Y.; Frost, J. W. Synthesis of Biobased Terephthalic Acid from Cycloaddition of Isoprene with Acrylic Acid. *ACS Sustainable Chem. Eng.* **2014**, *2*, 2053-2056.

136. Alder, K.; Dortmann, H.-A. Über substituierende addition and dien-synthese beim methylen-cyclobutan. (IX. Mittel über substituierende additionen). *Chem. Berich.* **1952**, *85*, 556-565.

137. Arpe, H.-J. *Industrial Organic Chemistry* 5th Ed.; Wiley-VCH: Weinheim, 2010; pp 299-304.

138. Huang, S.-Y.; Lipp, D. W.; Farinato, R. S. Acrylic acid and derivatives. In *Kirk-Othmer Encyclopedia of Chemical Technology*; John Wiley & Sons, 2004, p. 342-369.

139. Calamur, N.; Carrera, M. Propylene. In *Kirk-Othmer Encyclopedia of Chemical Technology*; John Wiley & Sons, 2001; pp 1-25.

140. Bettahar, M. M.; Costentin, G.; Savary, L.; Lavalley, J. C. On the partial oxidation of propane and propylene on mixed metal oxide catalysts. *Appl. Catal. A: Gen.* **1996**, *145*, 1-48.

141. Lin, M. M. Selective oxidation of propane to acrylic acid with molecular oxygen. *Appl. Catal. A: Gen.* **2001**, *207*, 1-16.

142. Teshigahara, I.; Kinoshita, H. Method for producing composite oxide catalyst. US 7,217,680 B2, 2007.

143. Teshigahara, I.; Kanuka, N. Catalyst for production of unsaturated aldehyde and unsaturated carboxylic acid, and process for its production. US 7,262,148 B2, 2007.

144. Nakazawa, Y.; Matsumoto, S.; Kobayashi, T.; Kurakami, T. Catalyst and method for producing acrylic acid. US 8,877,964 B2, 2014.

145. Lintz, H.-G.; Reitzmann, A. Alternative reaction engineering concepts in partial oxidations on oxidic catalysts. *Catal. Rev.* **2007**, *49*, 1-32.

146. Dubois, J.-L.; Desdevises, F.; Serreau, S.; Vitry, D.; Ueda, W. Method for producing acrylic acid from propane, in the presence of molecular oxygen. US 7,345,198 B2, 2008.

147. MetaCyc: Acrylyl-CoA. http://metacyc.org/META/NEW-IMAGE?type=COMPOUND&object=ACRYLYL-COA. (Accessed on Feb. 12, 2015).

148. Straathof, A. J. J.; Sie, S.; Franco, T. T.; van der Wielen, L. Feasibility of acrylic acid production by fermentation. *Appl. Microbiol. Biotechnol.* **2005**, *67*, 727-734.

149. Danner, H.; Urmos, M.; Gartner, M.; Braun, R. Biotechnological production of acrylic acid from biomass. *Appl. Biochem. Biotechnol.* **1998**, *70-72*, 887-894.

150. Lilga, M. A.; White, J. F.; Holladay, J. E.; Zacher, A. H.; Muzatko, D. S.; Orth, R. J. Method for conversion of β-hydroxy carbonyl compounds. US 7,687,661 B2, 2010.

151. Kumar, V.; Ashok, S.; Park, S. Recent advances in biological production of 3-hydroxypropionic acid. *Biotechnol. Adv.* **2013**, *31*, 945-961.

152. Lynch, M. D.; Gill, R. T.; Warnecke, L. T. Method for producing 3-hydroxypropionic acid and other products. US 8,883,464 B2, 2014.

153. Leal, N. A.; Havemann, G. D.; Bobik, T. A.; PduP is a coenzyme-A-acylating propionaldehyde dehydrogenase associated with the polyhedral bodies involved in B_{12}-dependent 1,2-propanediol degradation by a *Salmonella enterica* serovar Typhimurium LT12. *Arch. Microbiol.* **2003**, *180*, 353-361.

154. Ashok, S.; Raj. S. M.; ko, Y.; Sankaranarayanan, M.; Zhou, S.; Kumar, V; Park, S. Effect of nitrate on glycerol metabolism and anaerobic production of 3-hydroxypropionic acid by recombinant *Klebsiella pneumoniae* overexpressing *puuC*. *Metab. Eng.* **2013**, *15*, 10-24.

155. OPXBIO good chemistry: Dow and OPXBIO Collaborating on Renewable Route to Acrylic Acid. http://www.opxbio.com/news/dow-and-opxbio-collaborating-on-renewable-route-to-acrylic-acid/ (accessed on Feb. 26, 2015).

156. Novozymes News: Novozymes, Cargill continue bio-acrylic acid partnership as BASF exits. http://www.novozymes.com/en/news/news-archive/Pages/Novozymes-Cargill-continue-bio-acrylic-acid-partnership-BASF-exits.aspx. (Accessed on February 16, 2015).

157. Randhawa, M. A.; Ahmed, A.; Akram, K. Optimization of lactic acid production from cheap raw material: sugarcane molasses. *Pakistan J. Bot.* **2012**, *44*, 333-338.

158. Eiteman, M. A.; Ramalingam, S. Microbial production of lactic acid. *Biotechnol. Lett.* **2015**, ePub: Ahead of Print, DOI: 10.1007/s10529-015-1769-5.

159. Okano, K.; Yoshida, S.; Tanaka, T.; Ogino, C.; Fukuda, H.; Kondo, A.; Homo-D-lactic acid fermentation from arabinose by redirection of the phosphoketolase pathway to the pentose phosphate pathway in L-lacteate dehydrogenase gene-deficient *Lactobacillus plantarum*. *Appl. Environ. Microbiol.* **2009**, *75*, 7858-7861.

160. Wang, Y.; Li, K.; Huang, F.; Wang, J.; Zhao, J.; Zhao, X.; Garza, E.; Manow, R.; Grayburn, S.; Zhou, S. Engineering and adaptive evolution of *Escherichia coli* W for L-lactic acid fermentation from molasses and corn steep liquor without additional nutrients. *Biores. Technol.* **2013**, *148*, 394-400.

161. Dien, B. S.; Nichols, N. N.; Bothast, R. J.; Recombinant *Escherichia coli* engineered for production of L-lactic acid from hexose and pentose sugars. *J. Ind. Microbiol. Biotechnol.* **2001**, *27*, 259-264.

162. Yan, B.; Tao, L.-Z.; Liang, Y.; Xu, B.-Q. Sustainable production of acrylic acid: catalytic performance of hydroxyapatites for gas-phase dehydration of lactic acid. *ACS Catal.* **2014**, *4*, 1931-1943.

163. Gunter, G. C.; Miller, D. J.; Jackson, J. E. Formation of 2,3-pentanedione from lactic acid over supported phosphate catalysts. *J. Catal.* **1994**, *148*, 252-260.

164. Godlewski, J. E.; Villalobos, J.; Collias, D. I.; Velasquez, J. E. Process for production of acrylic acid or its derivatives from hydroxypropionic acid or its derivatives. US 8,884,050 B2, 2014.

165. Ozmeral, C.; Glas, J. P.; Dasari, R.; Tanielyan, S.; Bhaga, R. D.; Kasireddy, M. R. Catalytic dehydration of lactic acid and lactic acid esters. US 2013/0157328, 2013.

166. Ormonde, E. V.; Lochner, U.; Nakamura, I. K. Isoprene. In *CEH Product Review* 8; SRI Consulting: Menlo Park, 2008; pp 9-10.

167. Muller, E.; Eisenlohr, K. H.; Klein, H. Process for separating C5 hydrocarbons by solvent extraction and extractive distillation. US 3,707,575, 1972.

168. Ushio, S. Extract isoprene with DMF. *Chem. Eng.* **1972**, *79*, 82-83.

169. Ogorodnikov, S. K.; Kogan, V. B.; Nemtsov, M. S.; Burova, G. V. Separation of C_5 hydrocarbons by azeotropic and extractive distillation. VII. Liquid-vapor equilibrium in binary and ternary systems formed by C_5 hydrocarbons with Acetonitrile. *Zh. Prik. Khim.* **1961**, *34*, 1096-1102.

170. Howatt, III, C. S. Acetylenes removal from diolefin streams by extractive distillation. US 4,134,795, 1979.

171. Lybarger, H. M. Recovery of isoprene. US 3,947,506, 1976.

172. Whited, G. M.; Feher, F. J.; Benko, D. A.; Cervin, M. A.; Chotani, G. K.; McAuliffe, J. C.; LaDuca, R. J.; Ben-Shoshan, E. A.; Sanford, K. J. Development of a gas-phase bioprocess for isoprene-monomer production using metabolic pathway engineering. *Ind. Biotechnol.* **2010**, *6*, 152-163.

173. Sanford, R. A.; Patinkin, S. H. Tertiary amylene recovery using sulfuric acid and hydrocarbon extractants. US 2,958,715, 1960.

174. ChemSystems. *Isoprene*; 1999; pp 40-43.

175. Dixon, R. E.; Hann, D. Isoamylenes from butenes. US 4,085,158, 1978.

176. Arpe, H.-J. *Industrial Organic Chemistry* 5th Ed.; Wiley-VCH: Weinheim, 2010; pp 119-122.

177. Anhorn, V. J.; Frech, K. J.; Schaffel, G. S.; Brown, D. Isoprene from propylene. *Chem. Eng. Prog.* **1961**, *57*, 43-45.

178. De Malde, M. New industrial process for isoprene. *Chim. Ind. (Milan)*, **1963**, *45*, 665-673.

179. Dumitriu, E.; Hulea, V.; Fechete, I.; Catrinescu, C; Auroux, A.; Lacaze, J.-F.; Guimon, C. Prins condensation of isobutylene and formaldehyde over Fe-silicates of MFI structure. *Appl. Catal. A: Gen.* **1999**, *181*, 15-28.

180. Blomquist, A. T.; Verdol, J. A. The thermal isobutylene-formaldehyde condensation. *J. Am. Chem. Soc.* **1955**, *77*, 78-80.

181. Reis, T. Isoprene production. 2. Synthesis based on isobutylene. *Chem. Process. Eng.* **1972**, *53*, 68-71.

182. Thiele, D.; Fernando de Souza, R. Oligomerization of ethylene catalyzed by iron and cobalt in organoaluminate dialkylimidazolium ionic liquids. *Catal. Lett.* **2010**, *138*, 50-55.

183. Sazo, V.; Lopez, C. M.; Gonzalez, G.; Arregui, A.; Gomes, M. E.; Urbina, C. Transformation of 1-butene over AlSBA-15 synthesized at different conditions of pH and hydrolysis. *Appl. Catal. A: Gen.* **2010**, *380*, 118-124.

184. Sigl, M.; Schubert, M.; Stephan, J.; Poplow, F. Method for producing propene from 2-butene and isobutene-rich feeding flows. US 2008/0200745 A1, 2008.

185. Guenther, A.; Karl, T.; Harley, P.; Wiedinmyer, C.; Palmer, P. I.; Geron, C. Estimates of global terrestrial isoprene emissions using MEGAN (Model of Emissions of Gases and Aerosols from Nature). *Atmos. Chem. Phys.* **2006**, *6*, 3181-3210.

186. Kuzma, J.; Nemecek-Marshall, M.; Pollock, W. H.; Fall, R. Bacteria produce the volatile hydrocarbon isoprene. *Curr. Microbiol.* **1995**, *30*, 97-103.

187. Fall, R. R.; Kuzma, J.; Nemecek-Marshall, M. Materials and methods for the bacterial production of isoprene. US 5,849,970, 1998.

188. Sivy, T. L.; Shirk, M. C.; Fall, R. Isoprene synthase activity parallels fluctuations of isoprene release during growth of *Bacillus subtilis. Bioch. Biophy. Res. Comm.* **2002**, *294*, 71-75.

189. Miller, B.; Oschinski, C.; Zimmer, W. First Isolation of an isoprene synthase gene from poplar and successful expression of the gene in *Escherichia coli*. *Planta*, **2001**, *213*, 483-487.

190. Yang, J.; Xian, M.; Su, S.; Zhao, G.; Nie, Q.; Jiang, X.; Zheng, Y. Liu, W. Enhancing production of bio-isoprene using hybrid MVA pathway and isoprene synthase in E. coli. *PLoS One.* **2012**, *7*, e33509.

191. Bouvier, F.; Rahier, A.; Camara, B. Biogenesis, molecular regulation and function of plant isoprenoids. *Prog. Lipid Res.* **2005**, *44*, 357-429.

192. Anthony, J. R.; Anthony, L. C.; Nowroozi, F.; Kwon, G.; Newman, J. D.; Keasling, J. D. Optimization of the mevalonate-based isoprenoid biosynthetic pathway in *Escherichia coli* for production of the anti-malarial drug precursor amorpha-4,11-diene. *Metab. Eng.* **2009**, *11*, 13-19.

193. Rohmer, M. The discovery of a mevalonate-independent pathway for isoprenoid biosynthesis in bacteria, algae, and higher plants. *Nat. Prod. Rep.* **1999**, *16*, 565-574.

194. Xiao, Y.; Zahariou, G.; Sanakis, Y.; Liu. P. IspG Enzyme activity in the deoxyxylulose phosphate pathway: Roles of the iron-sulfur cluster. *Biochem*. **2009**, *48*, 10483-10485.

195. De Guzman, D. Green Chemicals Blog: Global Bioenergies partners with Arkema. http://greenchemicalsblog.com/2013/06/08/global-bioenergies-partners-with-arkema/ (accessed on Feb. 27, 2015).

196. GlycosBio: Isoprene. http://www.glycosbio.com/products-overview/isoprene/ (accessed on Feb. 27, 2015).

197. Aemetis Business Update, March 2012. http://www.aemetis.com/wp-content/uploads/2012/05/Aemetis-Business-Summary-Website.pdf. (accessed on Feb. 27, 2015).

198. LanzaTech: Chemicals. http://www.lanzatech.com/innovation/markets/chemicals/. (accessed on Feb. 27, 2015).

199. De Guzman, D. ICIS Green Chemicals: Ajinomoto, Bridgestone in bio-isoprene. http://www.icis.com/blogs/green-chemicals/2012/06/ajinomoto-bridgestone-in-bio-i/. (accessed on Feb. 27, 2015).

200. Goodyear Corporate: Bio-based Tires Edge Closer to Reality/Collaboration between The Goodyear Tire Rubber Company and DuPont Industrial Biosciences results in breakthrough technology for tires made with renewable raw materials. http://www.goodyear.com/cfmx/web/corporate/media/news/story.cfm?a_id=646 (accessed on Feb. 27, 2015).

201. Williams, D. CHEManager International: News & Opinions; Braskem Join Amyris and Michelin in Renewable Isoprene R&D. http://www.chemanager-online.com/en/news-opinions/headlines/braskem-joins-amyris-and-michelin-renewable-isoprene-rd. (accessed on Feb. 27, 2015).

202. Feher, F. J; Whited, G. M.; Chotani, G. K.; Valle, F.; Fioresi, C.; Sanford, K. J.; McAuliffe, J.; Cervin, M.; Puhala, A. S.; Miasnikov, A.; Aldor, I. S. Polymers of isropene from renewable resources. US 8,420, 759 B2, 2013.

CHAPTER TWO

1. INTRODUCTION

With a global capacity of 47 million tons per year in 2012,[5] terephthalic acid (PTA) is an important commodity chemical. From clear beverage bottles to polyester fabrics, the chief downstream product of this commodity chemical, poly(ethylene terephthalate) (PET), is one of the most widely used polymer resins. Current production technology is highly efficient but suffers from some limitations. Firstly, commercial synthesis of PTA does not produce isophthalic acid (IPA) concurrently. Since PET contains 3-5% IPA, it would be advantageous and cost effective to develop a synthesis that does just that. Another limitation is the fact that production relies solely on fossil fuel feedstocks. Commercializing a process that can utilize petroleum, shale gas, as well as biobased materials would facilitate carbon feedstock diversification in a world with wildly fluctuating prices for current carbon inputs into chemical manufacture.

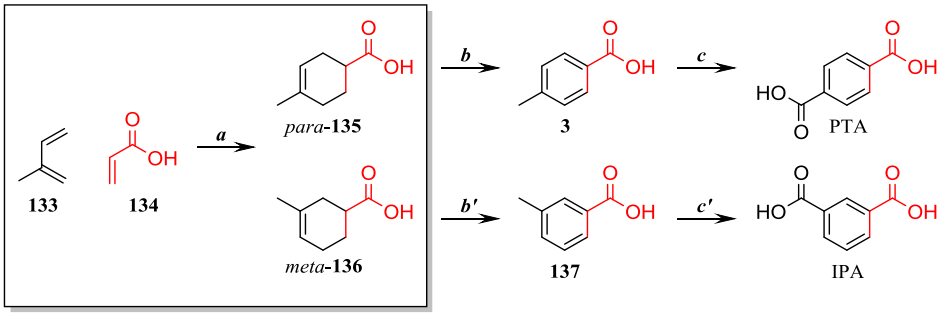

Scheme 38. Proposed synthesis of terephthalic acid and isophthalic acid from isoprene **133** and acrylic acid **134**, a) 2 mol% $TiCl_4$, rt; b)/b') 0.2 mol% Pd/SiO_2, 240°C; c)/c') 0.5 mol% $Co(OAc)_2$, $Mn(OAc)_2$, *N*-hydroxysuccinimide, AcOH, 1 bar O_2.

This work seeks to provide a synthetic route that produces both PTA and IPA, takes advantage of biological sources of starting materials as well as shale gas and petroleum

feedstocks. The proposed reaction scheme is shown in Scheme 38. A cycloaddition between acrylic acid **134** and isoprene **133** affords a pair of regioisomers (*para*-**135**, *meta*-**136**) that are aromatized to *p*-toluic acid **3** and *m*-toluic acid **137**, respectively. Aryl methyl oxidation utilizes a modified Amoco Mid-Century process to afford high yields of PTA and IPA in a ratio suitable for the manufacture of PET. The cycloaddition, discussed in this chapter, occurs with an abundant and inexpensive catalyst at low concentrations under solvent-free reaction conditions at ambient temperature. Vapor phase aromatization, discussed in the next chapter, is selective with moderate yields, and the modified methyl group oxidation operates under mild conditions. Furthermore, both acrylic acid **134** and isoprene **133** can be made from petroleum, shale gas, and biobased sources of carbon (Chapter 1, sections 6 and 7).

2. SOLVENT-FREE CYCLOADDITION OF ACRYLIC ACID AND ISOPRENE

The cycloaddition between isoprene **133** and acrylic acid **134** to produce *para*-**135** and *meta*-**136** was performed in 1952 by Kurt Alder.[136] Acrylic acid **134** was used to trap the isoprene formed from ring-opening of methylenecyclobutane **132** (Scheme 26). Upon aromatization and oxidation, PTA and IPA were observed. Though yields were not reported, this research was the first to demonstrate a PTA synthetic route that also affords IPA.[136] Later, this cycloaddition was conducted in the absence of solvent by reacting the two substrates in a high pressure autoclave at 95°C for 2 h to achieve a high yield of a 3:1 mixture of 4-methylcyclohex-3-enecarboxylic acid (*para*-**135**) and 3-methylcyclohex-3-enecarboxylic acid (*meta*-**136**).[203] The importance of this cycloaddition between isoprene **133** and acrylic acid **134** lies in its ability to generate both *para*-**135** and *meta*-**136** regioisomers. Following aromatization and aryl methyl group oxidation, both PTA and IPA are obtained. This reaction sequence is the only one reported in the literature that is capable of producing both PTA and IPA necessary for the manufacture of PET.

2.1. Titanium catalysis

Because PET contains only 3-5% by weight IPA, it is necessary for the cycloaddition between acrylic acid **134** and isoprene **133** to be more selective toward *para*-**135**. This is achieved by reacting a 1:1 mole/mole ratio of acrylic acid **134** and isoprene **133** in the presence of a catalytic amount of a Lewis acid under neat conditions at or below ambient temperature. Most Lewis acids are unsuccessful at catalyzing the cycloaddition between free acrylic acid **134** and isoprene **133** because of the increased acidity of acrylic acid **134** when complexed to a Lewis acid. Lewis acid complexation to the carbonyl moiety facilitates a violent Lewis-promoted

Brønsted acid-catalyzed reaction in which all of the starting materials are consumed resulting in a dark, tacky mass. Encouragingly, titanium tetrachloride ($TiCl_4$) was able to avoid unwanted, vigorous side reactions while achieving high yields and selectivities in the cycloaddition.

As shown in Scheme 38, the cycloaddition between acrylic acid **134** and isoprene **133** affords two regioisomers: *para*-**135** and *meta*-**136**. Relative to a 1:1 mol/mol ratio of isoprene **133**:acrylic acid **134** under solvent-free conditions at room temperature, 2 mol% $TiCl_4$ catalyzed a 94% yield of cycloaddition products consisting of a 23:1 ratio of *para*-**135**:*meta*-**136**. Selectivity can be further enhanced by operating at lower temperatures without any loss of yield (Table 9).

Table 9. Effect of temperature on $TiCl_4$-catalyzed cycloaddition of isoprene **133** and acrylic acid **134**.[a]

Entry	Catalyst	Temperature (°C)	Yield product	*para*-**135**/ *meta*-**136**
1	$TiCl_4$	rt	94%	23 : 1
2[b]	$TiCl_4$	0°C	94%	37 : 1
3[c]	$TiCl_4$	-20°C	94%	50 : 1

[a]2 mol% $TiCl_4$, 1:1 molar ratio of isoprene **133** to acrylic acid **134**; [b]48 h reaction; [c]100 h reaction.

Lewis acidity can be modulated by altering the ligands surrounding a metal center.[204] Triflate groups are more electron withdrawing than bromide groups, for instance, and thus produce a harder, more electrophilic metal atom.[205] In our study, only $TiCl_4$ was successful in catalyzing a selective and high-yielding cycloaddition (entry 2, Table 10; entry 17, Table 11). Changing the chloride ligands to fluoride groups (entry 3, Table 10) produced a catalyst that was selective to *para*-**135** but catalyzed a violent oligomerization reaction that quickly consumed the starting materials to afford <1% yield of cycloaddition products. Attempts to soften the metal center by replacing chloride ligands with bromide ligands (entry 4, Table 10) were met with

reduced yield. Neither the highly active Zeigler-Natta catalyst titanocene dichloride ($[\eta^5\text{-}C_5H_5]_2TiCl_2$) (entry 6, Table 10), nor titanium tetraisopropoxide ($Ti(O\textit{i}Pr)_4$) (entry 7, Table 10) were active in this cycloaddition. Even changing the electrophilicity of the titanium center by replacing two of the four chlorine groups with triflate groups (entry 5, Table 10) afforded a catalyst with marginal selectivity and a yield comparable with that of the uncatalyzed cycloaddition (entry 1, Table 10).

Table 10. Effect of counteranion on titanium-catalyzed cycloaddition of isoprene **133** and acrylic acid **134**.[a]

Entry	Catalyst	Yield product	*para*-**135**/ *meta*-**136**
1	none	27%	3 : 1
2	$TiCl_4$	93%	23 : 1
3	TiF_4	1%	14 : 1
4	$TiBr_4$	58%	18 : 1
5	$Ti(O_3SCF_3)Cl_2$[b]	23%	5 : 1
6	$Ti(\eta^5\text{-}C_5H_5)_2Cl_2$	13%	3 : 1
7	$Ti(O\textit{i}Pr)_4$	8%	4 : 1

[a]2 mol% catalyst, 1:1 molar ratio of isoprene **133** and acrylic acid **134**, rt, 24 h, [b]0.1 mol% catalyst.

2.2. Combined acid catalysis

The central challenge in developing a catalyst for the cycloaddition between isoprene **133** and acrylic acid **134** is controlling the increase of acidity of the catalyst-complexed carboxylic acid. When a Lewis acidic metal coordinates to the carbonyl oxygen of acrylic acid **134**, electron density about the hydroxyl oxygen decreases significantly which raises the acidity of the hydroxyl proton.[206,207] This Lewis assisted-Brønsted acidity is substantial enough to catalyze a violent oligomerization of substrate upon the addition of isoprene to an acrylic acid **134**-Lewis acid pre-complex.

The most common solution to the problem of increasing acidity with carboxylic acid substrates upon coordination to a metal center is esterification of the substrate. While this does

eliminate the problem of Brønsted acidity completely, esterification would not be desirable in a route to PTA. Esterification of acrylic acid **134** prior to the cycloaddition followed by hydrolysis of the DMT product introduces two extra steps in the synthesis. Extra steps reduce overall yields and increase process costs in commercial applications. Due to the commercial scale of PTA synthesis, methanol must be recaptured after hydrolysis of DMT so the overall process costs do not become prohibitively expensive. Methanol also presents a fire hazard which further limits the attractiveness of esterification steps.

Acyloxyborane and acylboronate intermediacy are potential alternative solutions for enhancing selectivity favoring *para*-**135** in the cycloaddition between acrylic acid **134** and isoprene **133** while avoiding unwanted oligomerization due to increased Brønsted acidity of acrylic acid **134** (Scheme 39).[208-211] Use of borane (BH_3) (10 mol%) in the cycloaddition between acrylic acid **134** and isoprene **133** affords a 70% yield of cycloaddition products in DCM, while Hall reports that *o*-bromophenylboronic acid ($BrC_6H_4B(OH)_2$) (20 mol%) affords a 91% yield of *para*-**135** with selectivities of around 95% in DCM. Despite these encouraging results, all attempts at replicating Hall's results in our laboratory were unsuccessful. Intermediate **218** in Scheme 39 shows how electrophilic activation of the carboxylate group of acrylic acid is provided by boron conjugation and hydrogen bonding in the acylboronate intermediate **218**.[209]

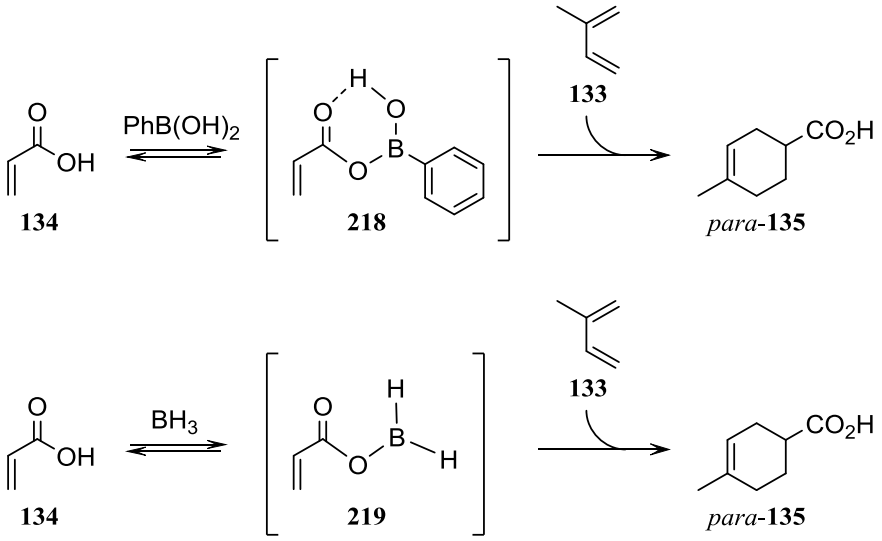

Scheme 39. Activation of acrylic acid **134** by phenylboronic acid and borane in a [4+2] cycloaddition with isoprene **133**.

The acyl-boronate strategy is of limited commercial use. High catalyst loading, the solvent (DCM) requirement, and the multiple steps involved in the synthesis of *o*-bromophenylboronic acid diminishes the usefulness of an acylboronate strategy in the synthesis of commodity chemical such as PTA. Lewis acid catalysts, on the other hand, are a more abundant and a more inexpensive alternative for commodity chemical synthesis. Titanium tetrachloride, for example, is an intermediate in the Kroll process for refining titanium ore and is a starting material for commercial manufacture of titanium dioxide (TiO_2).[212] Due to their low cost and lack of expensive ligands, many Lewis acids were tested for their propensity to catalyze the cycloaddition between isoprene **133** and acrylic acid **134**.

Lewis acids were screened using a 1:1 molar ratio of acrylic acid **134** and isoprene **133** under solvent free reaction conditions to identify a candidate that was able to increase cycloaddition yields with a high degree of selectivity toward *para*-**135**. Due to their ability to tune electrophilicity about a transition metal, bromides, chlorides, and triflates were examined as counteranions. In a prior report of a Lewis acid-catalyzed cycloaddition between β-acylacrylic

acids and various dienes, the addition of diisopropylethylamine was found to improve yields and selectivities in various solvents.[213] However, this previous work employed an excessive amount of catalyst (150-200%). Despite the high catalyst loading, this previous study suggested that the presence of an amine base might be helpful in catalyzing a cycloaddition with acrylic acid **134**.

Non-nucleophilic amine bases, diisopropylethylamine, triethylamine, and 2,6-lutidine were added to the reaction medium at 10 mol% relative to acrylic acid **134** (1:1 molar ratio of catalyst to base). Lewis acids such as Cu^{2+}, Fe^{3+}, and Sn^{2+} with triflate ligands were most active in catalyzing the unwanted violent oligomerization upon the addition of isoprene **133** to the reaction medium when run without added base. When an amine was added, this vigorous side-reaction was not observed, indicating effective buffering of the Lewis-assisted Brønsted acidity. However, only modest increase in yields were observed in the presence of these additives. Increasing the steric bulk around the nitrogen atom by using 3,5-di-*tert*-butylpyridine or removing some of the steric bulk by using pyridine did not affect cycloaddition yields substantially when compared to 2,6-lutidine.

Table 11. Effect of metal on cycloaddition of isoprene **133** and acrylic acid **134**.[a]

Entry	Catalyst	[b]Yield product	[c]*para*-**135**/ *meta*-**136**
1	none	27%	3 : 1
2	CuCl	8%	3 : 1
3	$CuCl_2$	8%	3 : 1
4	$NiCl_2$	11%	3 : 1
5	YCl_3	11%	4 : 1
6	$FeCl_2$	11%	4 : 1
7	$AlCl_3$	15%	6 : 1
8	$FeCl_3$	17%	7 : 1
9	$ZnCl_2$	20%	5 : 1
10	$MgCl_2$	21%	4 : 1
11	$TiCl_3$	34%	8 : 1
12	$SnCl_4$	37%	11 : 1
13	$ScCl_3$	48%	8 : 1
14	$SnCl_2$	59%	15 : 1
15	$HfCl_4$	73%	12 : 1
16	$ZrCl_4$	76%	12 : 1
17	$TiCl_4$	94%	23 : 1

[a]2 mol% catalyst, 1:1 molar ratio of isoprene **133** to acrylic acid **134**, rt, 24 h; [b]determined by NMR; [c]determined by GC.

Unwanted oligomerization was avoided in the absence of added base with the use of chloride counteranions (Table 11). Most of the Lewis acid chlorides afforded low to modest yields and selectivities (entries 2-16, Table 11). Significant improvement of yield and selectivity for *para*-**135** was seen with the early transition metals, Hf^{4+} (entry 15, Table 11) and Zr^{4+} (entry 16, Table 11), as well as Sc^{3+} (entry 13, Table 11). Interestingly, Sn^{2+} (entry 14, Table 11) and Sn^{4+} (entry 12, Table 11) was also active in the cycloaddition favoring *para*-**135**. However, unlike all other metals examined the lower oxidation state, Sn^{2+}, proved more active than the higher oxidation state, Sn^{4+}. As seen in Table 11, $TiCl_4$ was singular in its ability to catalyze a high yielding, highly selective cycloaddition between acrylic acid **134** and isoprene **133**.

Moreover, this reaction occurs without the use of solvent or other additives at room temperature with a low concentration (2 mol%) of a relatively inexpensive catalyst.

2.3. Acrylic acid-titanium tetrachloride complexes

Titanium tetrachloride has a square planar geometry that, upon coordination to two carbonyl compounds, develops an octahedral structure (**2:1**, Figure 15).[214-216] Alternatively, at low substrate concentrations, a substrate-catalyst dimer complex may develop (**2:2**, Fig. 15). Theoretical calculations and crystal structures have shown that the most favorable configuration for $TiCl_4$ complexed with two molecules of formaldehyde, acetaldehyde, acetone, or ethyl acetate places the carbonyl compounds *syn* to one another.[214-216] Initial coordination of one carbonyl compound affords a trigonal bipyramidal structure wherein the carbonyl presents a bent mode of coordination at the apical position (**1:1**, Fig. 15).[214-216] A second molecule of substrate binds in an equatorial position to afford a stable octahedral complex.[214-216]

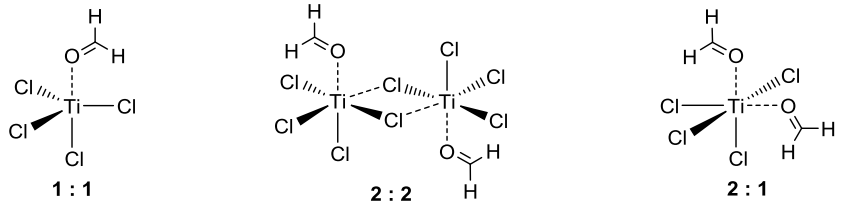

Figure 17. Structures of the complexes between formaldehyde and $TiCl_4$.

Efforts to understand acrylic acid **134** binding to $TiCl_4$ under catalytic concentrations of titanium were undertaken. Complexes between acrylic acid and $TiCl_4$ were prepared at varying concentrations of substrate relative to catalyst. These samples were analyzed using ^{13}C NMR. Results from this study are presented in Figure 16.

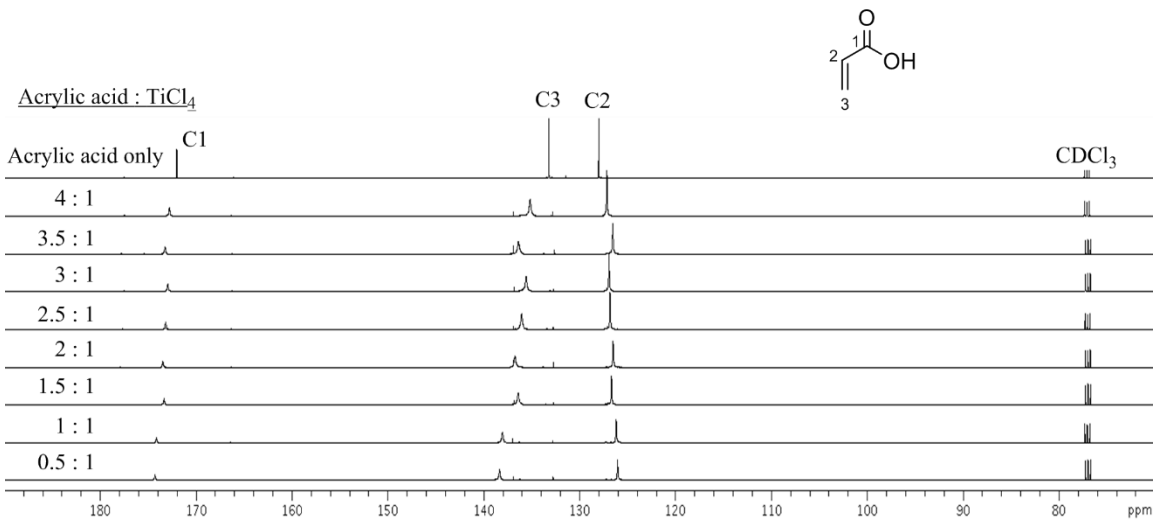

Figure 18. ^{13}C NMR titration study on the complex between $TiCl_4$ and acrylic acid **134**.

It is unclear from the spectra obtained what the precise mode of binding is for varying concentrations of acrylic acid **134**. Coordination of titanium to the carbonyl oxygen of acrylic acid **134** lowers the LUMO energy, thus allowing effective overlap with the HOMO of isoprene **133**. A side effect of this coordination and LUMO energy lowering is the increase in size of the orbital coefficients for carbons 1 and 3, while decreasing the LUMO coefficient on carbon 2. This parallels the decrease or increase of electron density about a particular carbon atom. Due to this change of electron density relative to an uncoordinated molecule of acrylic acid **134**, NMR signals should shift downfield for carbons 1 and 3, and upfield for carbon 2. This effect is observed in the ^{13}C NMR spectra when $TiCl_4$ is added to acrylic acid **134** (Figure 16). It appears that carbon 3 exhibits a larger shift in position than either carbon 1 or carbon 2. This suggests that carbon 3 is most sensitive to changes in orbital coefficients upon complexation with $TiCl_4$.

2.4. Heterogeneous catalysis of the cycloaddition between acrylic acid and isoprene

For most commercial synthesis of commodity chemicals the catalyst must be removed from the reaction medium and is typically recycled. This practice not only reduces unwanted waste thus saving money in the long term, but also affords materials that are of high purity. Catalyst separation is most easily accomplished if the catalyst is heterogeneous. In the cycloaddition between acrylic acid **134** and isoprene **133**, $TiCl_4$ is homogeneous and is thereby removed upon quenching with heptane and isopropanol and heated to 70°C for 1 h. The resulting solution is washed with 10% dilute H_2SO_4 once and H_2O twice, which removes the titanium and isopropanol from the organic layer. Upon concentration of the heptane solution, the cycloaddition products are isolated in good yields (94%) but $TiCl_4$ is converted to an unrecyclable compound. In order for this synthetic route to PTA to become commercially viable, the catalyst must be recovered in an active form.

2.4.1. Heterogeneous Lewis acids

Three Lewis acids were observed to remain heterogeneous in the cycloaddition between acrylic acid **134** and isoprene **133**: indium trichloride ($InCl_3$), lanthanum trichloride ($LaCl_3$), and lanthanum triflate ($La(OTf)_3$). As such, these were the first candidates for a heterogeneous cycloaddition at ambient temperature (Table 12). Of the lanthanum catalysts, the triflate ligands afforded a more catalytically active Lewis acid than the chloride ligands and, advantageously, like chlorides, did not promote violent oligomerization of the substrates. At 10 mol% concentration of catalyst, $La(OTf)_3$ (entry 2, Table 12) was about five times more active than $LaCl_3$ (entry 1, Table 12) but was only marginally more selective.

Table 12. Heterogeneous Lewis acids screened in the cycloaddition between isoprene **133** and acrylic acid **134**.[a]

Entry	Catalyst	Yield product	*para*-**135**/*meta*-**136**
1	none	27%	3 : 1
2	10 mol% $LaCl_3$	5%	4 : 1
3	10 mol% $La(OTf)_3$	24%	6 : 1
4	10 mol% $InCl_3$	1%	--[b]
5	1 mol% $InCl_3$	13%	10 : 1

[a]1:1 molar ratio of isoprene **133** and acrylic acid **134**, rt, 24 h; [b]no *meta*-**136** detected by NMR.

Though violent oligomerization was avoided with $La(OTf)_3$, the reaction medium gradually became more viscous. This indicates that polymerization may occur over extended reaction times. Indium trichloride, on the other hand (entry 3, Table 12), was active in the cycloaddition and was more selective to *para*-**135** than either of the lanthanum catalysts. Increased yields of cycloaddition products were observed upon a decrease of $InCl_3$ loading but even at 1 mol% (entry 5, Table 12), yields did not equal the yield of the uncatalyzed reaction (entry 1, Table 12).

2.4.2. Zeolite supports

Because $TiCl_4$ was singular in its ability to catalyze high yields of cycloaddition products with high levels of selectivity, attempts at finding a heterogeneous catalyst focused on finding an appropriate support for Ti^{4+}. Zeolites are commonly used as mild acidic heterogeneous catalysts or as supports for metal catalysts.[217,218] Zeolites are porous clays made from SiO_2 and Al_2O_3 with surface hydroxyl groups that affect the surface acidity of the zeolite material. Figure 17 shows a three dimensional representation of the channels and cages inside a commercial zeolite, H-ZSM-5. Different zeolites will have different sizes of channels and cages, as well as different ratios of SiO_2 to Al_2O_3 which changes the Brønsted acidity of the surface hydroxyl groups. Both acidity, and the size of cages and channels can affect how a reaction proceeds.

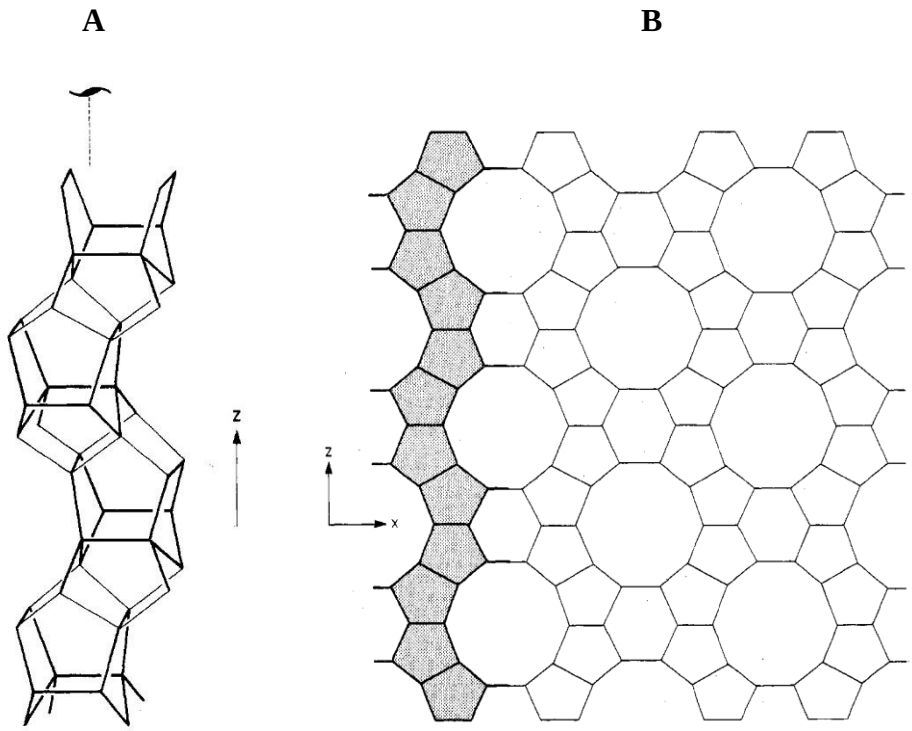

Figure 19. Three dimensional channels and cages of ZSM-5 zeolite, **A**) chain-type channel; **B**) skeletal diagram of ZSM-5 layer with chains of part **A** shaded in grey.

Several different zeolites were tested for their ability to bind $TiCl_4$ in an active form, thus providing a heterogeneous catalyst (Table 13). Silicoaluminophosphate (SAPO) zeolites are a unique class of molecular sieves that are synthesized by substitution of SiO_2 into aluminophosphate frameworks.[219,220] These present milder Brønsted acidity compared to conventional aluminosilicates like H-ZSM-5. Zeolites were chosen over a range of channel and cage sizes to study the influence of a three dimensional framework on catalytic activity.

Titanium tetrachloride was impregnated onto the zeolite supports via incipient wetness impregnation. After drying under vacuum, catalysts were screened in the cycloaddition between acrylic acid **134** and isoprene **133** at 20% by weight both in the presence and absence of solvent. No catalytic activity was observed at room temperature for any of the zeolite catalysts. Heating to 50°C and extending the reaction time from 24 h to 48 h showed minimal increase of yield and

selectivity (Table 13). Moreover, stoichiometric loading of the catalysts offered no improvement in either yield or selectivity at either temperature.

Table 13. Titainum tetrachloride-doped zeolites screened in the cycloaddition between isoprene **133** and acrylic acid **134**.[a]

Entry	Catalyst	Volume (Å^3)	Accessible volume	Yield product	*para*-**135**/*meta*-**136**
1	Zeolite β	4,178.43	22.5%	13%	3.3 : 1
2	Zeolite Y	14,428.77	27.6%	13%	3.3 : 1
3	ZSM-5	5,211.28	9.9%	14%	3.7 : 1
4	SAPO-5	1,420.64	14.1%	11%	3.0 : 1
5	SAPO-11	2,084.81	6.8%	16%	4.3 : 1
6	SAPO-34	2,391.59	17.3%	14%	3.7 : 1

[a]1:1 molar ratio of acrylic acid **134** to isoprene **133**, 20 wt% catalyst, 50°C, 48 h.

2.4.3. Polymer supports: polystyrene, Nafion, and Dowex

With the lack of catalytic activity from any of the zeolite catalysts, our attention turned to polymeric materials. Kobayashi and Nagayama discovered that a Nafion supported scandium chloride ($ScCl_3$) catalyst was effective in promoting a Diels-Alder cycloaddition between 3-acryloyloxazolidin-2-one **219** and cyclopentadiene **220** in DCM at room temperature in 92% yield (Scheme 40).[221] Scandium triflate supported on polystyrene was equally effective for a variety of allylation reactions of aldehydes, ketones, and esters.[222] Inspired by these encouraging results, polystyrene and Nafion were selected as supports for the cycloaddition between acrylic acid **134** and isoprene **133**.

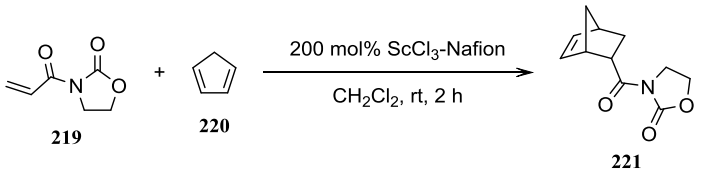

Scheme 40. Diels-Alder cycloaddition between 3-acryloyloxazolidin-2-one **219** cyclopentadiene **220** catalyzed by Nafion-supported scandium.

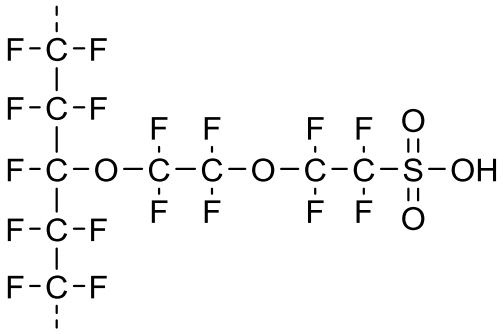

Figure 20. Structure of Nafion.

Polystyrene-supported $Sc(OTf)_3$ is commercially available and was purchased from Sigma-Aldrich. Polystyrene-supported $TiCl_4$ was prepared by wetness impregnation and dried overnight under vacuum.[223] Catalysts were screened in the presence and absence of a solvent. Surprisingly, reactions performed without added solvent showed higher yields than those conducted with a solvent (entries 3 and 4, Table 14). As such, the majority of screening was conducted in the absence of solvent. Polystyrene-supported $Sc(OTf)_3$ showed increased selectivity toward *para*-**135** at 10 mol% loading but suffered from low product yields (entry 2, Table 14). At 20 mol% loading, $TiCl_4$ affords good product yields but did not show selectivity favoring *para*-**135** above that of the uncatalyzed cycloaddition (entry 1, Table 11). Stoichiometric concentrations of polystyrene-supported $TiCl_4$ showed reduced activity without any change of selectivity (entry 5, Table 14).

Table 14. Heterogeneous catalysts screened in the cycloaddition between isoprene **133** and acrylic acid **134**.[a]

Entry	Catalyst	Conditions	Yield product	*para*-**135**/*meta*-**136**
1	10 mol% $TiCl_4$/Dowex-50	rt, neat	77%	10 : 1
2	10 mol% $Sc(OTf)_3$/PS	rt, neat	10%	8 : 1
3	20 mol% $TiCl_4$/PS	rt, neat	57%	3 : 1
4	20 mol% $TiCl_4$/PS	rt, heptane	26%	3 : 1
5	100 mol% $TiCl_4$/PS	rt, neat	24%	3 : 1
6	20 mol% $TiCl_4$/Nafion	rt, neat	3%	--[b]
7	30 mol% BCl_3/Nafion	rt, neat	5%	--[b]

[a]1:1 molar ratio of isoprene **133** to acrylic acid **134**, rt, 24 h; [b]no *meta*-**136** observed in NMR spectrum.

Unlike polystyrene, Nafion is a perfluorosulfonic acid resin which does not possess aromatic moieties present in polystyrene.[224] Titanium tetrachloride and boron trichloride (BCl_3) were both supported on Nafion and tested at 20 mol% and 30 mol% respectively (entries 6 and 7, Table 14). For both catalysts, no *meta*-**136** was observed suggesting a high degree of selectivity, however yields were very low. It is not clear whether the absence of *meta*-**136** in NMR spectra is due to high selectivity or low yields. Because the yields of Nafion-supported $TiCl_4$-catalyzed cycloadditions were significantly lower than those of polystyrene-supported $TiCl_4$ (entries 3 and 6, Table 14), Nafion was discarded as a potential catalyst support.

Dowex-50 is an aryl sulfonic acid typically used as an ion exchange resin.[225] Wetness impregnation with a solution of $TiCl_4$ in toluene was used to impregnate titanium on Dowex-50 beads. At 10 mol% titanium on Dowex-50 in the absence of solvent, a 77% yield of cycloaddition products was achieved (entry 1, Table 14). This yield is higher than any other supported Lewis acid catalyst. Advantageously, selectivity favoring *para*-**135** is quite high (10:1 *para*-**135**:*meta*-**136**). Upon completion of the cycloaddition, the Dowex-50 catalyst was washed with toluene and dried under vacuum before being recycled into a second reaction. Unfortunately, catalytic activity decreased upon a second use. A 24% yield of *para*-**135** and *meta*-**136** was achieved in a 4:1 mol ratio. This suggests either the $TiCl_4$ leached into solution during the first reaction or that the catalytic sites degraded during the catalyst regeneration. It is likely that a more robust catalyst preparation is necessary for the catalyst to be used multiple times. Though not as active as the homogeneous catalyst, $TiCl_4$ on Dowex-50 is the most successful heterogeneous catalyst developed so far for the cycloaddition between acrylic acid **134** and isoprene **133**. Current efforts continue to develop cost effective heterogeneous catalyst that affords high yields of cycloaddition products with a selectivity to *para*-**135** isomer on par

with that of the homogeneous reaction. Moreover, this catalyst should be able to be reused without loss of catalytic activity.

3. CONCLUSIONS

The first cycloaddition step in a synthetic route to biobased PTA and IPA has been elaborated. This route is inspired by Alder's investigation of trapping isoprene **133** with acrylic acid **134** followed by aromatization and methyl group oxidation to obtain PTA and IPA. The proposed synthesis uniquely provides access to both PTA and IPA required for PET manufacture. It also makes use of starting materials that are obtainable from petroleum, shale gas, or biological sources, thereby diversifying available feedstocks for industrial production of PTA.

Our work has been successful in developing a solvent-free cycloaddition between acrylic acid **134** and isoprene **133** that affords high yields (94%) of *para*-**135** and *meta*-**136** with a selectivity favoring *para*-**135** of 96% at room temperature. Furthermore, this cycloaddition makes use of a low concentration (2 mol%) of an inexpensive and abundant catalyst, $TiCl_4$, which helps make this route commercially attractive. Future work seeks to provide a heterogeneous catalyst that will be easily recovered from the reaction medium and reused without loss of activity. Initial attempts at finding such a catalyst suggest an ion-exchange resin such as Dowex-50 may be a suitable support for $TiCl_4$. However, the loss of activity upon recycling this catalyst indicate that a more robust impregnation technique may be necessary. Other Lewis acids besides $TiCl_4$ may prove to be active heterogeneous catalysts when impregnated on an appropriate support. This work is ongoing in our laboratory.

REFERENCES

REFERENCES

203. Cahiez, G.; Rivas-Enterrios, J.; Clery, P. Organomanganese (II) reagents XIV: a short and efficient synthesis of diastereoisomeric (±)-α-bisabolols and (±)-chlorophenoxamine. *Tetrahedron Lett.* **1988**, *29*, 3659-3662.

204. Pindur, U.; Lutz, G.; Otto, C. Acceleration and Selectivity Enhancement of Diels-Alder Reactions by Sepecial and Catalytic Methods. *Chem. Rev.* **1993**, *93*, 741-761.

205. Corey, E. J.; Shibata, T.; Lee, T. W. Asymmetric Diels-Alder Reactions Catalyzed by a Triflic Acid Activated Chiral Oxazaborolidine. *J. Am. Chem. Soc.* **2002**, *124*, 3808-3809.

206. Li, P.; Yamamoto, H. Bifunctional acid catalysts for organic synthesis. *Top. Organomet. Chem.* **2011**, *37*, 161-183.

207. Yamamoto, H.; Futatsugi, K. "Designer acids:" combined acid catalysis for asymmetric synthesis. *Angew. Chem. Int. Ed.* **2005**, *44*, 1924-1942.

208. Furuta, K.; Miwa, Y.; Iwanaga, K.; Yamamoto, H. Acyloxyborane: an activating device for carboxylic acids. *J. Am. Chem. Soc.* **1988**, *110*, 6254-6255.

209. Al-Zoubi, R.; Marion, O.; Hall, D. G. Direct and waste-free amidation and cycloadditions by organocatalytic activation of carboxylic acid at room temperature. *Angew. Chem. Int. Ed.* **2008**, *47*, 2876-2879.

210. Hall, D.; Marion, O.; Al-Zoubi, R. Method for the organocatalytic activation of carboxylic acids for chemical, reactions using orthosubstituted arylboronic acids. US 2010/0197960, 2010.

211. Wang, F.; Tong, Z. Dehydro-aromatization of cyclohexene-carboxylic acids by sulfuric acid: critical route for bio-based terephthalic acid synthesis. *RSC Adv.* **2014**, *4*, 6314-6317.

212. Imam, M. A.; Froes, F. H.; Housley, K. L. Titanium and titanium alloys. In Kirk Othmer Encyclopedia of Chemical Technology; John Wiley & Sons: 2010.

213. Miles, W. H.; Cohen, E. M.; Naimoli, B. J. Diels-Alder reactions of β-acylacrylic acids. *Synth. Commun.* **2013**, *43*, 1980-1991.

214. Branchadell, V.; Oliva, A. Complexes between formaldehyde and titanium tetrachloride. An ab initio study. *J. Am. Chem. Soc.* **1992**, *114*, 4357-4364.

215. Branchadell, V.; Oliva, A. Formation of 1:1, 2:1, and 2:2 complexes between carbonyl compounds and titanium tetrachloride. An ab initio study. *Inorg. Chem.* **1995**, *34*, 3433-3439.

216. Brun, L. The crystal structure of ($TiCl_4$, $CH_3COOC_2H_5$)$_2$. *Acta Crystallog.* **1966**, *20*, 739-749.

217. Narayana Murthy, Y. V. S.; Pillai, C. N. Diels-Alder reactions catalyzed by zeolites. *Synth. Commun.* **1991**, *21*, 783-791.

218. Zendehdel, M.; Gaykani, Z. Diels-Alder reaction with transition metal/zeolites. *J. Incl. Phenom. Macro. Chem.* **2005**, *53*, 47-49.

219. Olson, D. H.; Kokotailo, G. T.; Lawton, S. L.; Meier, W. M. Crystal structure and structure-related properties of ZSM-5. *J. Phys. Chem.* **1981**, *85*, 2238-2243.

220. Lok, B. M.; Messina, C. A.; Patton, R. L.; Gajek, R. T.; Cannan, T. R.; Flanigen, E. M. Silicoaluminophosphate molecular sieves: another new class of microporous crystalline inorganic solids. *J. Am. Chem. Soc.* **1984**, *106*, 6092-6093.

221. Kobayashi, S.; Nagayama, S. A polymer-supported scandium catalyst. *J. Org. Chem.* **1996**, *61*, 2256-2257.

222. Kobayashi, S; Nagayama, S. A microencapsulated Lewis acid. A new type of polymer-supported Lewis acid catalyst of wide utility in organic synthesis. *J. Am. Chem. Soc.* **1998**, *120*, 2985-2986.

223. Rahmatpour, A.; Mohammadian, S. Polystyrene-supported $TiCl_4$ as a novel, efficient and reusable polymeric Lewis acid catalyst for the chemoselective synthesis and deprotection of 1,1-diacetates under eco-friendly conditions. *C. R. Chimie.* **2013**, *16*, 912-919.

224. Product Information: DuPont Nafion PFSA Superacid Resins NR-40 and NR-50. http://www.ion-power.com/res/Nafion_and_XL_MEA/NAFION_NR40_NR50.pdf (accessed on Mar. 4, 2015).

225. Dow Water Solutions; DOWEX Fine Mesh Spherical Ion Exchange Resins, http://msdssearch.dow.com/PublishedLiteratureDOWCOM/dh_006f/0901b8038006f232.pdf?filepath=liquidseps/pdfs/noreg/177-01509.pdf&fromPage=GetDoc. (Accessed on February 16, 2015).

CHAPTER THREE

1. INTRODUCTION

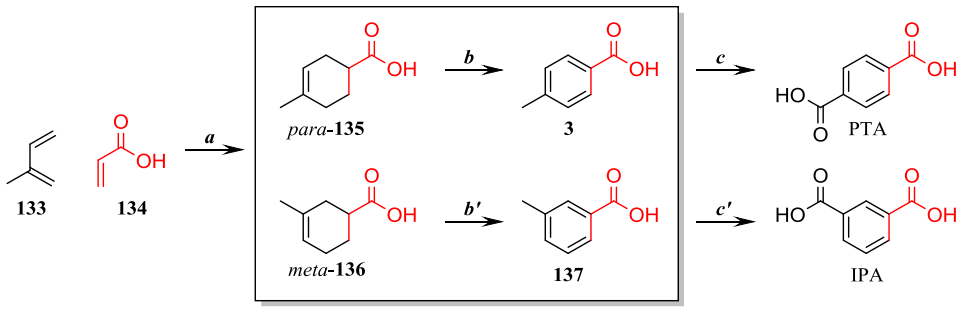

Scheme 41. Proposed synthesis of terephthalic acid and isophthalic acid from isoprene **133** and acrylic acid **134**, a) 2 mol% $TiCl_4$, rt; b)/b') 0.2 mol% Pd/SiO_2, 240°C; c)/c') $Co(OAc)_2$, $Mn(OAc)_2$, *N*-hydroxysuccinimide, AcOH, 1 bar O_2.

The next step in the Alder route to terephthalic acid (PTA) and isophthalic acid (IPA) is an aromatization of the cycloaddition products *para*-**135** and *meta*-**136** to *p*-toluic acid **3** and *m*-toluic acid **137**. Alder utilized H_2SO_4 as the solvent, catalyst, and oxidant for the aromatization of *para*-**135** and *meta*-**136** (Scheme 26, chapter 1).[136] Concentrated H_2SO_4 has been shown to facilitate aromatization of a variety of substituted cyclohexenes and is more effective than other acidic oxidants such as HNO_3.[211] Attempts in our laboratory to aromatize *para*-**135** in concentrated H_2SO_4 resulted in a 79% yield of *p*-toluic acid **3** where the fate of the remaining 21% of substrate could not be resolved. Furthermore, when *meta*-**136** was introduced as a substrate, only a 9% yield of *m*-toluic acid **137** was obtained where the fate of 91% of *meta*-**136** could not be determined (unpublished results). A synthesis cannot reach commercial stages without a near quantitative mass balance. Previous research in our laboratory took advantage of the favorable vapor pressures of *para*-**135**, *p*-toluic acid-**3**, *meta*-**136**, and *m*-toluic acid **137** which allowed *para*-**135** and *meta*-**136** to be distilled at 240°C and 0.11 bar through a plug

reactor containing Pd/C dispersed in SiO_2.[135] Such a system afforded a 77% yield of toluic acid **3** from *para*-**136** along with *cis*-4-methylcyclohexanoic acid **222** and *trans*-4-methylcyclohexanoic acid **223** in 9% and 12% yields respectively (Scheme 42). Advantageously, a 69% yield of *m*-toluic acid **137** was achieved from *meta*-**136** along with *cis*-3-methylcyclohexanoic acid **224** and *trans*-3-methylcyclohexanoic acid **225** in 13% and 10% yields respectively. The vapor phase catalytic dehydrogenation of *para*-**135** and *meta*-**136** is attractive due to the absence of solvent, high accountability of mass balance, and prospects for continuous flow aromatizations.

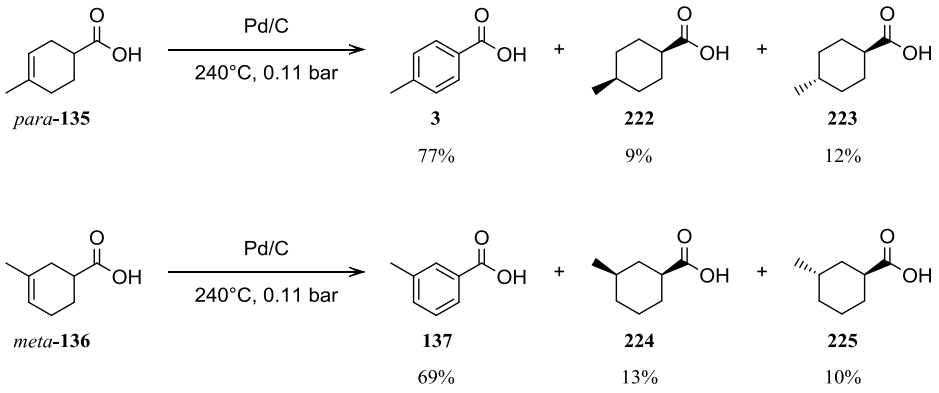

Scheme 42. Vapor phase catalytic dehydrogenation of *para*-**135** and *meta*-**136** over Pd/C.

Though the vapor phase aromatization of *para*-**135** and *meta*-**136** consumes all of the cyclohexene substrate and 98% of *para*-**135** could be accounted for between *p*-toluic acid **3** and cyclohexane byproduct, the 77% yield of *p*-toluic acid **3** achieved is not an improvement over the 79% yield attained in H_2SO_4. In order to reach high yields of *p*-toluic acid **3** in the vapor phase aromatization of *para*-**135**, the formation of cyclohexane byproducts must be avoided. The presence of saturated cyclohexanes in the product stream of cyclohexene dehydrogenative aromatizations has been an enduring problem in synthetic organic chemistry. This challenge has been addressed by Bercaw,[226] Sheldon,[227] Trost,[228] and others,[229] but a generally applicable

solution has not been identified to the problematic generation of cyclohexane byproducts during dehydrogenative aromatizations.

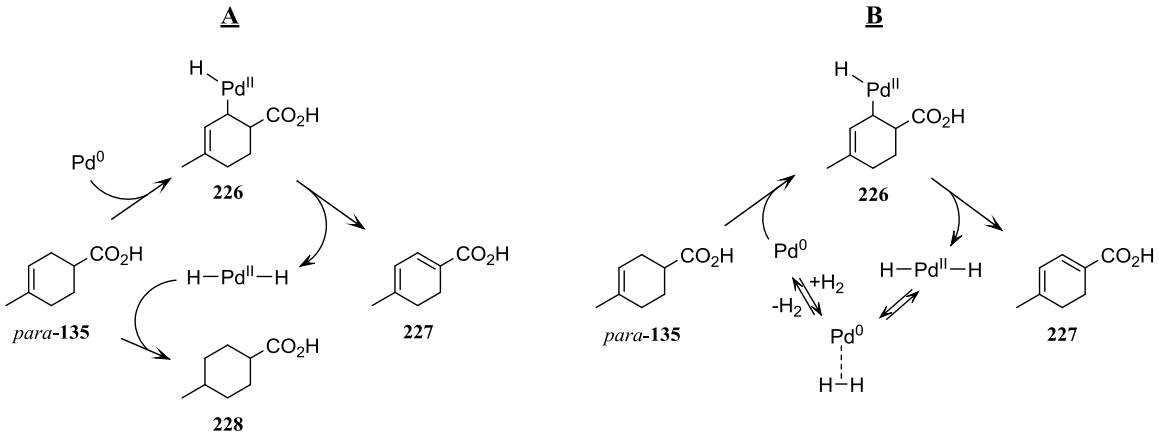

Scheme 43. Palladium hydride intermediacy in dehydrogenative aromatization of *para*-**135**.

A mechanism for cyclohexene byproduct formation is shown in Scheme 43A. Palladium insertion into an allylic C-H bond in *para*-**135** is followed by elimination to afford a conjugated diene **227** and palladium hydride (H-Pd-H). This H-Pd-H species may reduce the π bond of *para*-**135** to afford cyclohexane byproduct **228**. The fundamental obstacle in the formation of aromatics and cyclohexanes from cyclohexenes lies in controlling the metal hydride intermediate. For high yields of aromatics, H-Pd-H should release H_2 generating fully reduced Pd^0, which can then be available for another allylic C-H insertion as shown in Scheme 43B. However, *para*-**135** may be reduced to cyclohexane **228** by the H-Pd-H intermediate if the rate of H_2 dissociation is slow. As shown in Scheme 43B, release of H_2 from H-Pd-H has two stages: interconversion of H-Pd-H and Pd^0 with adsorbed H_2, and the interconversion of Pd^0 with adsorbed H_2 to free Pd^0 and H_2 generation. Enhancing the rates associated with H_2 dissociation from H-Pd-H is key to achieving high yields and selectivity toward aromatized products.

Alternate strategies to control the hydride intermediate would be to remove the H_2 by reaction of H_2 with O_2, or to avoid the generation of H_2 altogether.

2. CONTROLLING H-Pd-H INTERMEDIACY

2.1. Effect of heterogeneous support

In order to reduce the amount of cyclohexane formed in the Pd/C-catalyzed dehydrogenation of *para*-**135** to *p*-toluic acid **3**, various materials were investigated as supports for Pd^0. Changing the solid support may influence the rate of H-Pd-H conversion to Pd^0 by altering the Lewis acidity of the support cation.[230] Palladium at 3% by weight was impregnated on γ-Al_2O_3, SiO_2, TiO_2, and ZrO_2 using incipient wetness impregnation with tetraamine palladium(II) hydroxide ($Pd(NH_3)_4(OH)_2$). An advantage of $Pd(NH_3)_4(OH)_2$ over other Pd^{II} salts is the acid-base reaction with acidic supports that eliminates the need for multiple impregnations to achieve the desired Pd^0 loading. After calcination in air and reductive activation under a flow of 0.5% H_2 in N_2, supported Pd^0 catalysts were examined at 0.2 mol% in the catalytic dehydrogenation of *para*-**135** to *p*-toluic acid **3** (Table 15).

Table 15. Effect of support on the Pd-catalyzed aromatization of *para*-**135**.[a]

Entry	Catalyst	Yield toluic acid **3**	Conversion	Toluic acid **3** : cyclohexane **228**
1	Pd/C[b]	73%	94%	3 : 1
2	Pd/Al_2O_3	36%	50%	3 : 1
3	Pd/SiO_2	83%	>99%	5 : 1
4	Pd/TiO_2	6%	12%	1 : 1
5	Pd/ZrO_2	11%	16%	3 : 1

[a]0.2 mol% Pd, 240°C, 0.11 bar, [b]0.4 mol% of 5 wt% commercial Pd/C.

Results presented in Table 15 indicate that changing the Pd^0 support has a pronounced effect on the yield and selectivity favoring **3**. Relative to Pd/C (entry 1, Table 15), γ-Al_2O_3 (entry 2, Table 15), TiO_2 (entry 4, Table 15), and ZrO_2 (entry 5, Table 16) had a detrimental effect on the conversion of *para*-**135** as well as the selectivity favoring *p*-toluic acid **3**. The Ti^{4+} cation of TiO_2 is known to be a strong Lewis acid.[231] Not only did Pd/TiO_2 afford the lowest yield of *p*-

toluic acid **3** among the examined supports but it also was the least selective, affording a 1:1 mol ratio of *p*-toluic acid **3** to cyclohexane byproduct **228** (entry 4, Table 15). Encouragingly, less Lewis-acidic macroporous SiO_2 (150Å) (entry 3, Table 15) proved to be the best support for Pd^0 in the aromatization of *para*-**135**. Palladium impregnated onto SiO_2 achieved a nearly complete conversion of *para*-**135** thus affording a higher yield of *p*-toluic acid **3** than any other supported Pd^0 catalyst.

2.2. Oxidative dehydrogenation

As an alternative strategy to improving the yields of *p*-toluic acid **3** by eliminating the formation of byproduct cyclohexane, oxidative dehydrogenation was examined as a means to sweep away the H_2 from the Pd^0 with adsorbed H_2 intermediate (Scheme 43A) by reaction of H_2 with O_2. We investigated different ways of promoting an oxidative dehydrogenation of *para*-**135** to *p*-toluic acid **3**. One approach was inspired by Sheldon's use of sodium anthraquinone-2-sulfonate in the Pd/C-catalyzed dehydrogenative aromatization of cyclohexene to benzene.[227] Another strategy involved co-impregnation of Pd^0 with a metal that was not effective for dehydrogenation of *para*-**135**, but is known to catalyze the reaction of H_2 and O_2. Finally, a different type of oxidative dehydrogenation was studied with vanadia (V_2O_5), which is known to catalyze dehydrogenations via a Mars van Krevelen mechanism, which does not produce hydrogen during dehydrogenations.[232]

2.2.1. Oxidative dehydrogenation with dopants

In 1991, Sheldon and Sobczak reported the successful use of sodium anthraquinone-2-sulfonate **229** (Scheme 44) to suppress byproduct cyclohexane formation during the liquid-phase

Pd/C-catalyzed dehydrogenative aromatization of cyclohexene to benzene.[227] In the presence of the quinone, high conversions (85-100%) of cyclohexene and high selectivities favoring benzene (92-100%) were achieved. Control reactions in the absence of **229** only achieved 59-80% selectivity to benzene with a concomitant increase in cyclohexane formation. Sheldon proposed that the 5-10% Pd/C catalyzed the reaction of H_2 with the quinone, facilitating the reduction of H-Pd-H to Pd^0. The resultant dihydroquinone is subsequently reoxidized by O_2 which forms H_2O_2 as a byproduct. The Pd^0-catalyzed reaction of anthraquinone with H_2 followed by oxidation of dihydroanthraquinone by O_2 is the basis for commercial production of H_2O_2.[233]

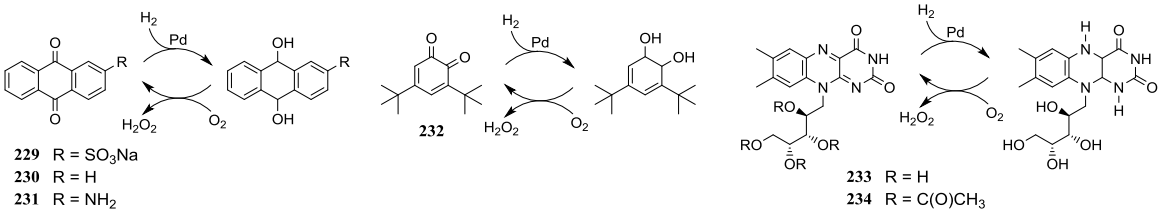

Scheme 44. Reactions of quinones with hydrogen with their reoxidation with O_2.

Inspired by Sheldon's work, a series of different quinones were studied to investigate their propensity to increase selectivity toward *p*-toluic acid **3** in the dehydrogenative aromatization of *para*-**135** (Scheme 44). It is possible that the chosen quinone will inhibit binding of *para*-**135** or *p*-toluic acid **3** to Pd^0 sites. Thus a variety of quinones were selected including Sheldon's sodium anthraquinone-2-sulfonate **229** for aqueous impregnation, anthraquinone **230** for impregnations in organic solvents, 2-aminoanthraquinone **231** to improve binding to acidic supports, 3,5-di-*t*-butyl-*ortho*-benzoquinone **232** to sterically hinder its binding and poisoning of catalyst surface, and riboflavin **233** or peracetylated riboflavin **234** to improve organic solubility during impregnation.

Early trials sought to apply Sheldon's methodology to the vapor phase aromatization of *para*-**135**. A commercially available 5 wt% Pd/C catalyst was impregnated with **229** (Scheme 44) via incipient wetness in H_2O. Different ratios and catalyst loadings were investigated to find suitable conditions for the vapor phase aromatization (Table 16). An improvement in selectivity in favor of *p*-toluic acid **3** over the cyclohexane byproduct was observed when **229** was used (Scheme 44). However, this improvement in selectivity was accompanied by a significant decrease in conversion (entries 3-5, Table 16).

Table 16. Impact of sodium anthraquinone-2-sulfonate **229** on the Pd/C catalyzed aromatization of *para*-**135**.[a]

Entry	Quinone : Pd	Pd loading	Yield toluic acid **3**	Conversion	Toluic acid **3** : cyclohexane **228**
1	0 : 1	0.1 mol%	15%	21%	3 : 1
2	0 : 1	0.4 mol%	73%	94%	3 : 1
3	1 : 1	0.1 mol%	40%	46%	7 : 1
4	3 : 1	0.1 mol%	24%	27%	8 : 1
5	1 : 1	0.4 mol%	34%	40%	6 : 1

[a]5 wt% Pd/C, 240°C, 0.11 bar.

Entries 1 and 2 show that Pd/C control reactions without a quinone benefit from an increase in catalyst loading. However, in the presence of **229**, an increase of Pd catalyst loading afforded a decrease in both conversion and selectivity (entries 3 and 5, Table 16). Unlike the results obtained by Sheldon, a 3:1 excess of quinone to Pd (entry 4, Table 16) did not significantly affect the selectivity toward *p*-toluic acid **3** relative to a 1:1 loading of quinone to Pd (entry 3, Table 16). Excess quinone did lead to a significant decrease in conversion of *para*-**135**. It appears that the presence of **229** has a poisoning effect on the activity of Pd/C, reflected in reduced conversions, but has a positive effect on selectivity. Following these studies, a 1:1 ratio of quinone to Pd was used for all experiments.

In order to determine whether a different quinone was more suitable for the catalytic dehydrogenative aromatization of *para*-**136**, Pd/C was impregnated with **230**, **231**, **232**, or **233** using ethanol as the impregnation solvent. After calcination and reductive activation, these catalysts were examined at 0.4 mol% catalyst loading relative to *para*-**135** (Table 17).

Table 17. Impact of varying quinone on Pd/C-catalyzed aromatization of *para*-**135**.[a]

Entry	Quinone	Yield toluic acid **3**	Conversion	Toluic acid **3** : cyclohexane **228**
1	none	73%	94%	3 : 1
2	anthraquinone **230**	27%	33%	4 : 1
3	2-aminoanthraquinone **231**	16%	20%	4 : 1
4	3,5-di-*t*-butyl-*o*-benzoquinone **232**	71%	96%	3 : 1
5	riboflavin **233**	61%	87%	4 : 1

[a]5 wt% Pd/C, 1:1 quinone:Pd, 0.4 mol% catalyst loading, 240°C, 0.11 bar.

It can be seen from Table 17 that Pd/C impregnated with either di-*t*-butyl-*o*-benzoquinone **232** or riboflavin **233** (entries 4 and 5, Table 17) are much more active in the aromatization with conversions approaching that of the control reaction (entry 1, Table 17). However, no improvement in selectivity was observed with any of the organic soluble quinones tested. It appears that only anthraquinone sulfonate **229** (Scheme 44) has any significant impact on the selectivity of the vapor phase aromatization with Pd/C.

Because Pd/SiO_2 is a more active catalyst for the aromatization of *para*-**135** than Pd/C, chosen quinones were impregnated onto Pd/SiO_2 in an attempt to determine whether the low yields achieved with quinones on Pd/C were due to the carbon support (Table 18). In order to improve solubility during wetness impregnation, riboflavin **233** was peracetylated before use.

Table 18. Impact of varying quinone in Pd/SiO_2-catalyzed aromatization of *para*-**135**.[a]

Entry	Quinone	Yield toluic acid **3**	Conversion	Toluic acid **3** : cyclohexane **228**
1	none	83%	>99%	5 : 1
2	anthraquinone **230**	23%	29%	4 : 1
3	2-aminoanthraquinone **231**	13%	17%	3 : 1
4	sodium anthraquinone-2-sulfonate **229**	46%	58%	4 : 1
5	3,5-di-*t*-butyl-*o*-benzoquinone **232**	58%	81%	3 : 1
6	acetylated riboflavin **234**	35%	44%	4 : 1

[a]0.2 mol% Pd, 1:1 quinone:Pd, 240°C, 0.11 bar, [b]aqueous impregnation of quinone onto Pd/SiO_2.

It can be seen from results in Table 18, that while unmodified Pd/SiO_2 is an active catalyst for the dehydrogenative aromatization of *para*-**135**, impregnation of a quinone onto Pd/SiO_2 (entries 2-6, Table 18) affords a decrease in conversion and no significant increase of selectivity favoring *p*-toluic acid **3** relative to the control (entry 1, Table 18). Unlike on Pd/C, sodium anthraquinone-2-sulfonate **229** (entry 4, Table 18) affords no increase in selectivity over the control reaction. Futhermore, though 3,5-di-*t*-butyl-*ortho*-quinone **232** affords the highest yield of all of the tested quinones, a modest decrease in selectivity is observed when impregnated onto Pd/SiO_2 (entry 5, Table 18). It appears that quinones may occupy dehydrogenative catalytic sites on Pd resulting in a decrease in yields of *p*-toluic acid **3** while binding tightly so as to be ineffective in a reaction with H_2.

In a modification of the oxidative dehydrogenation via co-impregnation of quinones onto Pd catalysts, the quinone component was replaced with Pt. Studies in our laboratory have shown that Pt^0 is ineffective in the vapor phase aromatization of *para*-**135**, however it is known to be an effective promoter of the reaction between H_2 and O_2 to form H_2O_2.[234] Macroporous SiO_2 was co-impregnated with $Pd(NH_3)_4(OH)_2$ and $Pt(NH_3)_4(OH)_2$ followed by calcination and reductive activation under H_2. Silica was chosen over activated carbon as a support due to the advantageous acid-base reaction during impregnation with the Pd^{II} and Pt^{II} amine salts. With a

Pt:Pd mol ratio of 1:1 at 0.2 mol% catalyst loading, Pd(Pt)/SiO_2 afforded a 57% yield of *p*-toluic acid **3** with a 3:1 selectivity. This is comparable to a Pd/SiO_2 catalyst impregnated with di-*t*-butyl-*o*-benzoquinone **232** (Scheme 44, Table 18).

It appears that co-impregnating Pd^0 catalysts with quinones capable of catalyzing an oxidative reaction of H_2 with O_2, is ineffective in improving the selectivity of the vapor phase dehydrogenative aromatization of *para*-**135** without reducing conversion. A different mode of impregnation may help to improve catalytic activity. Solid state synthesis whereby solid particulates are intermixed before heating to high temperatures to allow the dopant to diffuse into the host; sol-gel synthesis wherein precursors are chosen to achieve a gel with a uniform distribution of host and dopant cations; and coprecipitation methods wherein a solution of host and dopant salts are treated with a chemical that precipitates both cations, have yet to be studied.[235] Other supports, such as ceria (CeO_2) and niobia (Nb_2O_5) have also been overlooked and may prove to be more suitable to co-impregnation of Pd^0 and quinones than SiO_2.

2.2.2. Mars van Krevelen oxidative dehydrogenation

A different type of oxidative dehydrogenation may be accomplished using a catalyst that does not form a metal hydride intermediate. Without such a metal hydride intermediate, reduction of cyclohexene to cyclohexane as shown in Scheme 43A cannot proceed. Vanadia is known to promote the dehydrogenation of propane to propylene via a Mars van Krevelen mechanism that produces water as a byproduct rather than H_2 derived from a metal hydride intermediate.[232,236,237] Such a mechanism would be an ideal solution for the problem of competing cyclohexane byproduct formation in dehydrogenative aromatizations of cylcohexenes (Scheme 45).

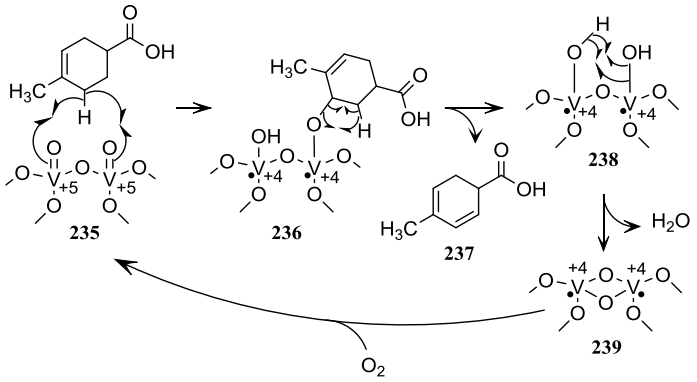

Scheme 45. Mars van Krevelen oxidative dehydrogenation of *para*-**135** over V_2O_5.

Vanadia was examined in the vapor phase aromatization of *para*-**135** to *p*-toluic acid **3**. It was discovered that no reaction occurs at the operating temperature of 240°C used for Pd^0-catalyzed aromatizations. Instead, reaction temperatures of 500°C were necessary and the reaction had to be conducted in a stainless steel flow reactor inside a muffle furnace. A series of experiments in which the loading of V_2O_5 was varied shows that a high concentration of V_2O_5 is necessary (Table 19). At low catalyst loading (entries 1 and 2, Table 19), V_2O_5 was dispersed in macroporous SiO_2 to prevent flow channeling. At high catalyst loading (entry 3, Table 19), V_2O_5 was the only species present in the plug reactor.

Table 19. Effect of catalyst loading on the V_2O_5-catalyzed aromatization of *para*-**135**.[a]

Entry	V_2O_5 loading	Yield toluic acid **3**	Toluic acid **3** : cyclohexane **228**
1	0.4 mol%[b]	4%	only **3**
2	20 mol%[b]	9%	only **3**
3	150 mol%	10%	21 : 1

[a]500°C, 0.11 bar, [b]dispersed in SiO_2.

Results presented in Table 19 show that even at high catalyst loading, conversion of *para*-**135** is low. This is a significant decrease compared to the >99% conversion in the Pd/SiO_2-catalyzed aromatization. However, V_2O_5 demonstrates a high degree of selectivity favoring *p*-toluic acid **3**. At low catalyst loadings, the only product observed was *p*-toluic acid **3** (entries 1 and 2, Table 19). Small amounts of cyclohexane byproducts were observed with an excess of V_2O_5 (entry 3, Table 19). However, the selectivity toward *p*-toluic acid **3** is greater than any of the Pd-catalyzed oxidative dehydrogenative aromatizations. Substrate conversions must be increased before a high yield of *p*-toluic acid **3** can be realized. This may be achieved by using other types of catalysts that react via a Mars van Krevelen mechanism such as MoO_3 or CrO_3. Increasing the reaction temperature may also have a beneficial effect on conversions of *para*-**135**, however, elevated temperatures may promote undesired cracking reactions.[238] This would have a detrimental effect on both the yield and selectivity of the aromatization. Developing a highly active catalyst for oxidative dehydrogenation via a Mars van Krevelen mechanism is an ongoing subject of research in our laboratory.

3. REACTOR DESIGNS

The aromatization of *para*-**135** to *p*-toluic acid **3** required the use of two types of apparatus. As shown in Figure 18, one type utilizes a glass tube filled with supported Pd^0 which is inserted between a distilling flask and receiving bulbs of a Kugelrohr apparatus. The distilling flask is charged with *para*-**135** and is placed, along with the catalyst plug, inside an oven and heated while the distillation train is connected to a water aspirator pump vacuum (0.11 bar). The water aspirator eliminates a fire hazard from evolved H_2. Throughout the reaction, the distillation train oscillates to avoid bumping of the liquid substrate, to ensure even heating of the catalyst and substrate, and to avoid flow channeling through the catalyst plug. Oscillation is provided by a pneumatic actuator.

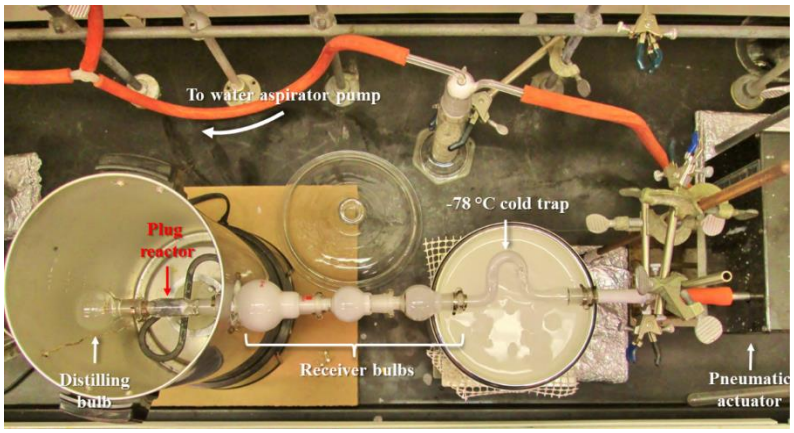

Figure 21. Apparatus design for vapor phase aromatization of *para*-**135** and *meta*-**136.** A furnace heats the distilling bulb and catalyst plug while aromatized products collect in a series of bulbs. A mild vacuum (0.11 bar) provided by a water aspirator pulls the effluent stream through the plug. Oscillation of the glassware is provided by a pneumatic actuator.

For experiments requiring temperatures above 250°C or when reactions were run under atmospheric pressure, a stainless steel continuous flow reactor heated in a muffle furnace was used (Figure 19A, B). A short tube near the outlet of the muffle furnace is filled with supported Pd^0 while the 250 mL cylinder is charged with *para*-**135** and the furnace is heated. The reactor is run near atmospheric pressure using a flow of N_2 connected via stainless steel tubing at the top

of the reactor. The N_2 gas sweeps across the surface of a pool of liquid *para*-**135** and carries the vapors through the apparatus and exits via the outlet. Vacuum tubing directs the effluent into a series of cold traps (-78°C) that condense the hot vapors.

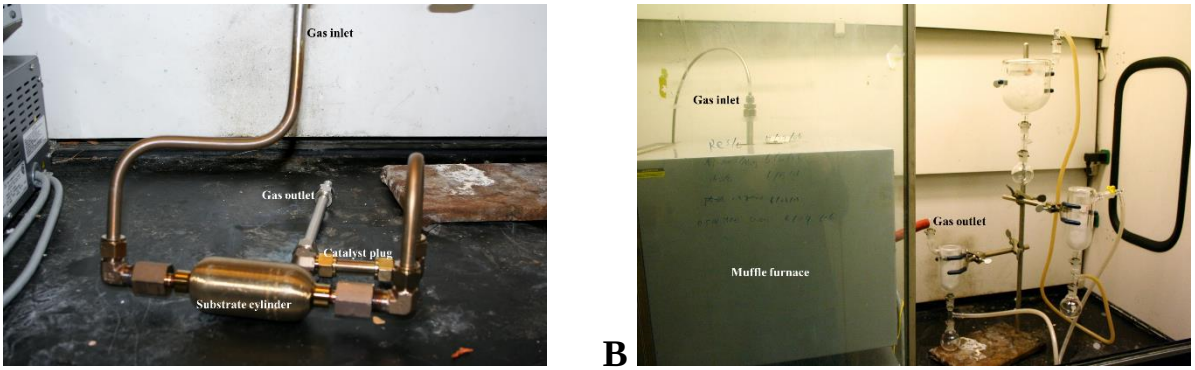

Figure 22. Continuous flow reactor, a) stainless steel reactor apparatus with substrate cylinder and catalyst plug equipped with gas inlet and outled; b) full reactor setup. Apparatus from Fig. 22A is housed inside a muffle furnace and connected to stainless steel gas line. Effluent is captured in series of cold fingers equipped with collection flasks.

4. CONCLUSIONS

An improvement over the liquid-phase H_2SO_4-catalyzed aromatization of *para*-**135** and *meta*-**136** used by Alder was found. An improved yield (83%) of *p*-toluic acid **3** was achieved in the vapor phase over a 3 wt% Pd/SiO_2 catalyst dispersed in macroporous silica. Conversions were near 100% and, importantly, all of the carbon from the cyclohexene substrate could be accounted for in *p*-toluic acid **3** and byproduct cyclohexane **224**. This is the major advantage of our vapor phase catalytic dehydrogenative aromatization over the H_2SO_4 aromatization used by Alder[136] and Tong[211]. Further improvement in *p*-toluic acid **3** yield will be a result of controlling the formation of byproduct cyclohexanes, which has been a long-standing problem in dehydrogenative aromatizations. Our attempts to eliminate formation of cyclohexane focused on increasing the rate of H-Pd-H conversion to Pd^0 by altering the catalyst support. Other experiments focused on removing H_2 by reacting with O_2 or a quinone that could be re-oxidized by O_2. A different type of oxidative dehydrogenation in which hydrogen is removed as H_2O instead of as H_2 via a metal hydride by exploiting a Mars van Krevelen mechanism was also investigated. The most encouraging results stem from a) the use of anthraquinone sulfonate **229**, Scheme 44 that has been impregnated onto Pd/C; and b) the use of V_2O_5 to promote a Mars van Krevelen mechanism. Both catalyst systems succeeded in decreasing the amount of cyclohexane byproduct but did so at the expense of *para*-**136** conversion. Research is continuing to find a catalyst that avoids the formation of cyclohexane while achieving high substrate conversions.

REFERENCES

REFERENCES

226. Bercaw, J. E.; Hazari, N.; Labinger, J. A. Oxidative aromatization of olefins with dioxygen catalyzed by palladium trifluoroacetate. *J. Org. Chem.* **2008**, *73*, 8654-8657.

227. Sheldon, R. A.; Sobczak, J. M. Catalytic oxidative dehydrogenation of cyclohexene. *J. Molec. Catal.* **1991**, *68*, 1-6.

228. Trost, B. M.; Metzner, P. J. Reaction of olefins with palladium trifluoroacetate. *J. Am. Chem. Soc.* **1980**, *102*, 3572-3577.

229. Horrillo-Martinez, P.; Virolleaud, M.-A.; Jaekel, C. Selective palladium-catalyzed dehydrogenation of limonene to dimethylstyrene. *ChemCatChem.* **2010**, *2*, 175-181.

230. Zhao, C.; Wachs, I. E. Selective oxidation of propylene over model supported V_2O_5 catalysts: influence of surface vanadia coverage and oxide support. *J. Catal.* **2008**, *257*, 181-189.

231. Farfan-Arribas, E.; Madix, R. J. Characterization of the acid-base properties of the TiO_2(110) surface by adsorption of amines. *J. Phys. Chem. B.* **2003**, *107*, 3225-3233.

232. Mars, P.; van Krevelen, D. W. Oxidations carried out by means of vanadium oxide catalysts. *Chem. Eng. Sci. (Suppl.)*, **1954**, *3*, 41-59.

233. Porter, D. H. Production of hydrogen peroxide by anthraquinone process in the presence of a fixed bed catalyst. US 3,009,782, 1961.

234. Veser, G.; Friedrich, G.; Freygang, M.; Zengerle, R. A simple and flexible micro reactor for investigation of heterogeneous catalytic gas phase reactions. *Stud. Surf. Sci. Catal.* **1999**, *122*, 237-245.

235. McFarland, E. W; Metiu, H. Catalysis by doped oxides. *Chem. Rev.* **2013**, *113*, 4391-4427.

236. Alexopoulos, K.; Reyniers, M.-F.; Marin, G. B. Reaction path analysis of propane selective oxidation over V_2O_5 and V_2O_5/TiO_2. *J. Catal.* **2012**, *289*, 127-139.

237. Doornkamp, C.; Ponec, V. The universal character of the mars and van krevelen mechanism. *J. Molec. Catal. A: Chem.* **2000**, *162*, 19-32.

238. van Goethem, M. W.; Barendregt, S.; Grievink, J.; Moulijn, J. A.; Verheijen, P. J. T. Ideal chemical conversion concept for the industrial production of ethene from hydrocarbons. *Ind. Eng. Chem. Res.* **2007**, *46*, 4045-4062.

EXPERIMENTAL

GENERAL

^{1}H NMR spectra were recorded on a 500 MHz spectrometer. Chemical shifts for ^{1}H NMR spectra are reported (in parts per million) relative to $CDCl_3$ (δ = 7.26 ppm). ^{13}C NMR spectra were recorded at 125 MHz and the shifts for those spectra are reported (in parts per million) relative to $CDCl_3$ (δ = 77.0 ppm). GC chromatograms were recorded on an Agilent 6890N chromatograph equipped with an autosampler. $MnBr_2$, $SnBr_2$, $Sn(OTf)_2$ and 5% Pd/C were purchased from Alfa Aesar while CuBr, $Cu(OTf)_2$, $Fe(OTf)_2$, $MgBr_2$, $ScCl_3$, and $Zn(OTf)_2$ were purchased from Strem. Palladium and platinum salts, $Pd(NH_3)_4(OH)_2$ and $Pt(NH_3)_4(OH)_2$, were purchased from Heraeus Precious Metals. All other reagents were purchased from Sigma-Aldrich. Chemicals were used as received without further purification.

PRODUCT ANALYSES

Cycloaddition of isoprene **133** and acrylic acid **134**

A weighed quantity of the cycloaddition reaction products 4-methyl-3-cyclohexenecarboxylic acid **135** and 3-methyl-3-cyclohexenecarboxylic acid **136** (50.0 mg, 0.357 mmol) was added to a 10 mL volumetric flask. Decane internal standard (0.02 mL, 0.1 mmol) and *N*,*O*-bis(trimethylsilyl)trifluoroacetamide (BSTFA) (1.5 mL, 5.59 mmol) were then added. Derivatization was complete upon mixing. The solution was then diluted with toluene to 10 mL. Syringe filtration (0.45 µm Whatman filter) was followed by GC analysis to determine the ratio of *para*-**135** and *meta*-**136**. Derivatized samples were analyzed using an Agilent HP-5 ((5%-phenyl)-methylpolysiloxane) coated capillary column (30 m x 0.32 mm i.d. x 0.25 µm film thickness) to determine the ratio of *para*-**135** and *meta*-**136**. A second sample was prepared for

GC analysis without BSTFA derivatization and analyzed using an Agilent DB-FFAP nitroterephthalic acid modified polyethylene glycol coated capillary column (30 m x 0.32 mm i.d. x 0.25 μm film thickness), which allowed the determination of unreacted acrylic acid **134** and the sum of *para*-**135** and *meta*-**136** cycloaddition products, which co-eluted.

Aromatization of 4-methyl-3-cyclohexenecarboxylic acid **135**

Following the vapor phase aromatization of 4-methyl-3-cyclohexenecarboxylic acid **135**, white solid that accumulated on the sides of the apparatus was collected with EtOH washes. All of the EtOH washes were combined and diluted with clean EtOH to 200 mL. A measured quantity of solution (2.0 mL) was transferred to a 1 dram glass vial and 3-methylcyclohexanone internal standard (10 μL, 0.081 mmol) was added. Syringe filtration (0.45 μm Whatman filter) was followed by GC analysis using an Agilent DB-FFAP nitroterephthalic acid modified polyethylene glycol coated capillary column (30 m x 0.32 mm i.d. x 0.25 μm film thickness).

$TiCl_4$-CATALYZED CYCLOADDITION OF ISOPRENE **133** AND ACRYLIC ACID **134**

A 350 mL glass pressure vessel (10.3 bar max) equipped with a magnetic stir bar was charged with $TiCl_4$ (3.04 g, 16.0 mmol) at rt under Ar in a glove bag. The flask was sealed with a rubber septum in the glove bag and acrylic acid **134** (57.7 g, 800 mmol) was added to the sealed pressure vessel via syringe. After mixing $TiCl_4$ with acrylic acid **134**, the Ar atmosphere was not required. The resulting red-brown solution was cooled in an ice bath followed by addition of isoprene **133** (54.5 g, 800 mmol) via syringe. The rubber septum was replaced by a pressure vessel screw cap (15 mm PTFE bushing with Viton® O-ring). After removing the ice bath 2 h following the addition of isoprene **133**, the reaction mixture was allowed to warm to rt.

The heterogeneous reaction crude containing substantial solid precipitate was transferred to a round bottom flask equipped with a side-arm and a magnetic stir bar. After addition of heptane (600 mL) and isopropanol (80 mL), the dissolved reaction crude was heated to 80°C with stirring for 1 h. This clear amber homogeneous solution was extracted with 10% dilute aqueous H_2SO_4 (1x160 mL) followed by water (2x160 mL). The organic layer was dried over $MgSO_4$ and concentrated to afford 105 g (94%) of a white solid containing 4-methyl-3-cyclohexenecarboxylic acid **135** and 3-methyl-3-cyclohexenecarboxylic acid **136** as a 23:1 mixture. This solid was dissolved in a minimal amount of hot hexanes, crystallized at rt, filtered and dried to afford 90.3 g (81%) of purified **135** as needle-like crystals. ^{1}H NMR (500 MHz, $CDCl_3$) for 4-methyl-3-cyclohexenecarboxylic acid **135**: δ = 1.63 (s, 3H), 1.70 (m, 1H), 1.92-2.26 (comp, 3H), 2.16-2.28 (m, 2H), 2.50 (m, 1H), 5.40 (s, 1H).[239] ^{13}C NMR (125 MHz, $CDCl_3$) δ = 23.5, 25.2, 27.4, 29.1, 39.0, 119.0, 138.8, 182.5.[239]

UNCATALYZED CYCLOADDITION OF ISOPRENE 133 AND ACRYLIC ACID **134**[203]

Acrylic acid **134** (71.4 g, 0.991 mol) was added to isoprene **133** (77.5 g, 1.14 mol) under N_2 in a Parr Series 4575 high pressure reactor interfaced with a Series 4842 temperature controller. The reactor was flushed with N_2 and then pressurized to 8.3 bar with N_2. Heating the reactor to 95°C with stirring (100 rpm) for 2 h led to an initial increase in pressure to 13.8 bar followed by a decrease of pressure to 9.7 bar. After allowing the reactor to cool, a yellow heterogeneous reaction crude was obtained containing a 79% yield of a 3:1 ratio of *para*-**135**:*meta*-**136** (83.2 g of 4-methyl-3-cyclohexenecarboxylic acid **135** and 26.9 g of 3-methyl-3-cyclohexene carboxylic acid **136**). ^{1}H NMR (500 MHz, $CDCl_3$) for 3-methyl-3-cyclohexenecarboxylic acid **136**: δ = 1.63 (s, 1H), 1.72 (m, 1H), 1.95-2.02 (m, 3H), 2.23-2.24

(m, 2H), 2.49 (m, 1H), 5.36 (m, 1H).[239] ^{13}C NMR (125 MHz, $CDCl_3$) δ = 23.8, 24.8, 25.0, 31.2, 40.1, 121.0, 132.4, 183.1.[240] Crude product was submitted to repeated crystallizations from hexanes to obtain 37.5 g (27% yield) of pure 4-methyl-3-cyclohexenecarboxylic acid **135**.

SCREENING OF LEWIS ACID CYCLOADDITION CATALYSTS

Screening of Lewis acids as catalysts for the cycloaddition of isoprene **133** and acrylic acid **134** employed a 15 mL glass pressure vessel (10.3 bar max) equipped with a magnetic stir bar that was charged with 0.5 mmol of Lewis acid under N_2 in a glove bag and sealed with a rubber septum. For reactions requiring a solvent, solvent (4 mL) was then added to create a suspension. Acrylic acid **134** (0.36 g, 5 mmol) was added via syringe. A color change was often observed (sometimes immediately, sometimes delayed) after addition of acrylic acid **134** to the Lewis acid. When added, triethylamine, diisopropylethylamine, or 2,6-lutidine (0.5 mmol) were introduced following the addition of acrylic acid **134**. Isoprene **133** (0.41 g, 6 mmol) was finally added via syringe and the rubber septum replaced by a pressure vessel screw cap (15 mm PTFE bushing with Viton® O-ring). The reaction mixture was allowed to stir at rt for 24 h and the resulting crude analyzed by NMR and GC.

SCREENING OF HETEROGENEOUS LEWIS ACID CYCLOADDITION CATALYSTS

Screening of supported Lewis acids as heterogeneous catalysts for the cycloaddition of acrylic acid **134** and isoprene **133** employed a 15 mL glass pressure vessel (10.3 bar max). The vessel was charged with catalyst (1 mmol) under N_2 and sealed with a rubber septum. For reactions requiring a solvent, solvent (5 mL) was added to create a suspension. Acrylic acid **134** (0.36 g, 5 mmol) was then added via syringe. Isoprene **133** (0.34 g, 5 mmol) was added via

syringe and the rubber septum was replaced by a pressure vessel screw cap (15 mm PTFE bushing with Viton® O-ring). The sealed pressure vessel was inserted into an orbital shaker set to 250 rpm for 24 h and the resulting crude analyzed by NMR and GC.

IMPREGNATION OF $TiCl_4$ ON POLYSTYRENE[223]

A 50 mL three-neck round bottom flask equipped with a magnetic stir bar was charged with polystyrene (2% divinylbenzene, 30-60 mesh, 5.0 g) and carbon disulfide (15 mL) and placed under a flow of N_2. The mixture was stirred and $TiCl_4$ (2.0 g, 10.5 mmol) was added under N_2 before being heated to reflux and allowed to stir under reflux conditions for 2 h. After 2 h, the mixture was allowed to cool to rt before water (25 mL) was added. The mixture was stirred until the red-brown color disappeared and a cloudy white liquid with orange polymer beads was observed. The polymer beads were collected by filtration and washed with water (150 mL) and then with diethyl ether (15 mL) and finally with $CHCl_3$ (15 mL). The catalyst was dried in a vacuum oven (50°C, 0.015 bar) overnight prior to use.

IMPREGNATION OF $TiCl_4$ ONTO NAFION NR40[221]

A three-neck 50 mL round bottom flask equipped with a magnetic stir bar was charged with Nafion NR40 beads (5.0 g) and placed under a flow of N_2. $TiCl_4$ (0.38 g, 2.0 mmol) was added under N_2 followed by the addition of dry hexanes (10 mL). The mixture was heated to reflux while stirring and remained under reflux conditions for 40 h. After allowing the mixture to cool to rt, the polymer beads were filtered and washed with hexanes (3x20 mL). The beads were then dried under reduced pressure for 24 h.

IMPREGNATION OF $TiCl_4$ ONTO ZEOLITES

A stock solution composed of $TiCl_4$ in dry toluene (0.05 M) was prepared. A three-neck flask equipped with magnetic stir bar was charged with a zeolite (0.1 g) and connected to a flow of N_2. The zeolites investigated are as follows: zeolite β, zeolite Y, ZSM-5, SAPO-5, SAPO-11, SAPO-34. The $TiCl_4$-containing stock solution (10 mL) was then added under N_2 and a small release of gas was observed. The mixture was stirred and heated to 100°C for 1 h. After 1 h at 100°C, the mixture was allowed to cool to rt and the toluene was removed under reduced pressure. The resulting solids were dried in a vacuum oven overnight (100°C, 0.015 bar) prior to use.

IMPREGNATION OF $TiCl_4$ ONTO DOWEX-50

Dowex 50Wx8 sulfonic acid resin (hydrogen form, 50-100 μm mesh, 8% divinylbenzene, 25.0 g) was added to a 3 cm x 13 cm glass chromatography column equipped with a frit. A dilute solution of 5% H_2SO_4 in water (4x50 mL) was eluted through the column followed by water (20x50 mL) and toluene (4x50 mL). The Dowex beads were then suspended in toluene (90 mL) and concentrated under reduced pressure before drying overnight in a vacuum oven (100°C, 0.015 bar). A stock solution of $TiCl_4$ in toluene (0.9 M) was prepared and the dried Dowex 50Wx8 beads were returned to a 3 cm x 13 cm glass chromatography column equipped with a frit. The Dowex was eluted with the $TiCl_4$-containing stock solution (3x50 mL) followed by toluene (3x50 mL). The catalyst was dried overnight in a vacuum oven (100°C, 0.015 bar) prior to use.

GENERAL PROCEDURE FOR SUPPORTED Pd-CATALYZED VAPOR PHASE AROMATIZATION OF 4-METHYL-3-CYCLOHEXENECARBOXYLIC ACID **135**

Davisil Grade 643 macroporous (150 Å, 35-70 μm mesh) silica gel (1.35 g) was dried in a vacuum oven (150°C, 0.015 bar) overnight. Commercially available Pd/C containing 50 wt% water was dried for 3 h under reduced pressure at 70°C prior to use while freshly prepared 3% Pd/SiO_2, Pd/Al_2O_3, Pd/TiO_2, and Pd/ZrO_2 were used immediately following their preparation. Supported Pd catalysts that had been modified with quinones were used immediately following impregnation.

A supported Pd catalyst (0.072 mmol) was thoroughly mixed with dried silica gel and packed into a 9 cm x 1.7 cm glass tube using glass wool to immobilize the plug reactor material. 4-Methyl-3-cyclohexenecarboxylic acid **135** (5.0 g, 36 mmol) from a $TiCl_4$-catalyzed cycloaddition was placed in a 25 mL, 14/20 round bottom flask. Vaporization/aromatization of 4-methyl-3-cyclohexenecarboxylic acid **135** employed a Kugelrohr apparatus assembled as follows: the 25 mL flask containing **135**, the 9 cm x 1.7 cm glass tube comprising the plug reactor, three 50 mL collection bulbs in series, a U-shaped tube, and finally a straight gas adaptor connected to a water recirculating aspirator pump. The flask containing **135** and plug reactor were inserted into the Kugelrohr oven. The U-shaped tube was cooled to -78°C. Vaporization/aromatization proceeded at 240°C under vacuum (0.11 bar) with reciprocal oscillating agitation. White solid accumulated in the collection bulbs and U-shaped tube which was collected by washing with EtOH. The plug reactor contents were suspended in EtOH followed by filtration to remove the catalyst and silica gel. All of the EtOH washes were combined and analyzed by NMR and GC. ^{1}H NMR (500 MHz, $CDCl_3$) for *p*-toluic acid **3**: δ = 2.45 (s, 3H), 7.29 (d, *J* = 8 Hz, 2H), 8.02 (d, *J* = 8 Hz, 2H), 11.2-12.8 (s br., 1H).[241] ^{13}C NMR (125 MHz, $CDCl_3$) δ = 21.8, 126.5, 129.2, 130.2, 144.6.[241]

GENERAL PROCEDURE FOR CONTINUOUS FLOW AROMATIZATION OF 4-METHYL-3-CYCLOHEXENECARBOXYLIC ACID **135**

Both Pd/SiO_2 and V_2O_5 were examined in the vapor phase aromatization of 4-methyl-3-cyclohexenecarboxylic acid using an N_2 or compressed air flow. V_2O_5 was heated to 400°C under air for 4 h prior to use while Pd/SiO_2 was used directly after preparation. Macroporous silica gel (Davisil Grade 643, 150 Å, 35-70 mesh, 1.30 g) was dried overnight in a vacuum oven (150°C, 0.015 bar). Pd/SiO_2 (0.27 g, 0.072 mmol) or V_2O_5 (0.026 g, 0.144 mmol) was mixed with the dried silica gel and packed into a 8 cm x 1.2 cm stainless steel tube using glass or quartz wool to immobilize the plug reactor material. The use of a gas stream required a stainless steel continuous flow apparatus as follows: a gas inlet tube, a 14 cm long 50 mL cylinder containing 4-methyl-3-cyclohexenecarboxylic acid **135** (4.0 g, 36 mmol), a U-shaped tube, an 8 cm x 1.2 cm tube containing the catalyst plug, a gas outlet tube, and three cold traps equipped with collection flasks in series. All connections between steel reactor components were provided by Swagelok fittings. The final cold trap was equipped with a side vent to prevent a buildup of pressure. The stainless steel reactor was placed in a muffle furnace with the gas inlet and outlet tubes directed through openings in the top and back of the furnace respectively. Stainless steel tubing connected the gas inlet tube to a gas cylinder containing either compressed air or N_2 via a flowmeter. The reactor was heated to the reaction temperature (240°C with Pd/SiO_2, 500°C with V_2O_5) and the flow of gas was initiated (0.5 L/min). The flow of gas was turned off and the reactor was allowed to cool to rt. The white solid that accumulated in the cold traps was collected with EtOH washes. The components of the stainless steel reactor were also washed with EtOH. The plug reactor contents were suspended in EtOH and filtered to remove the catalyst. All of the EtOH washes were combined and analyzed by GC and NMR. ^{1}H NMR (550 MHz, $CDCl_3$) for *m*-toluic acid **137**: δ = 2.44 (s, 3H), 7.38 (t, 1H), 7.44 (m, 1H), 7.93-7.95 (m,

2H), 11.6-12.6 (s br., 1H).[242] ^{13}C (125 MHz, $CDCl_3$) δ = 21.3, 127.4, 128.4, 129.1, 130.7, 134.6, 138.3.[242]

IMPREGNATION OF Pd ONTO OXIDE SUPPORTS

Prior to impregnation, γ-Al_2O_3 (100-200 μm mesh), TiO_2 (anatase, 325 μm mesh), ZrO_2 (5 μm mesh), and macroporous SiO_2 (Davisil Grade 643, 150 Å pore size, 35-70 μm mesh) were dried overnight in a vacuum oven (150°C, 0.015 bar).

A 150 mL quartz round bottom flask was charged with an oxide support (5.0 g) and 5 wt% aqueous $Pd(NH_3)_4(OH)_2$ solution (5.5 mL) in air and stirred to combine. The bright yellow mixture was allowed to rest without stirring for 2 h at rt before it was placed in a muffle furnace and heated to 110°C at a rate of 3°C/min. After 4 h at 110°C, bright yellow solids were observed. The temperature was increased to 350°C at a rate of 3°C/min and held at 350°C for 3 h at which point black solids were observed in the quartz flask. The black solids were allowed to cool to rt before transferring to a fritted quartz U-tube with a gas inlet and outlet and placed in a muffle furnace. The U-tube and associated glassware is shown in Figure 20. The inlet end of the U-tube was connected to a stainless steel gas line while the outlet was connected to a quartz air condenser that exits through the top of the muffle furnace. N_2 was passed through the U-tube for 1 h at a rate of 0.4 L/min at rt before 5% H_2 in N_2 was passed through for 30 min at a rate of 0.4 L/min at rt. The flow of 5% H_2/N_2 was increased to 0.8 L/min and the furnace was heated to 350°C at a rate of 3°C/min. After holding the temperature at 350°C for 3 h the heater was turned off and the U-tube containing the supported Pd was allowed to cool to rt under a 0.8 L/min flow of 5% H_2/N_2. After the temperature decreased below 100°C, N_2 was passed through the U-tube overnight at a rate of 0.2 L/min. A dry black powder was obtained.

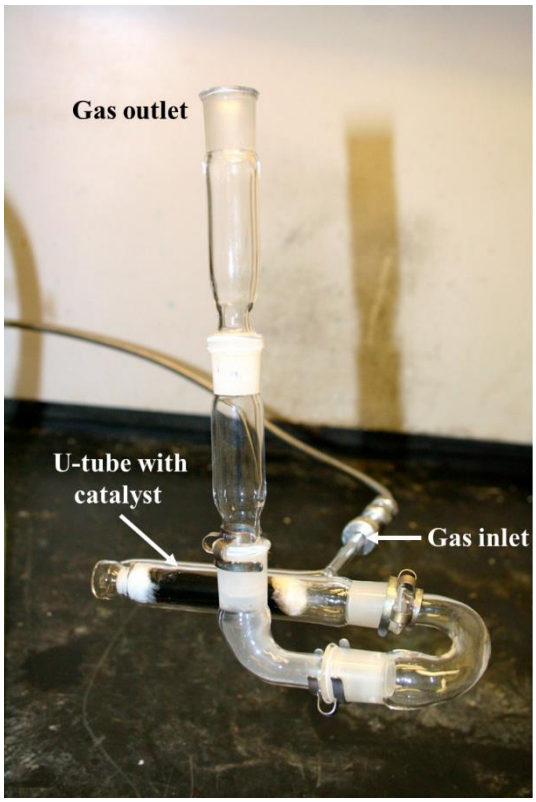

Figure 23. Apparatus used in preparing supported palladium catalysts.

CO-IMPREGNATION OF Pd AND Pt ONTO OXIDE SUPPORTS

Co-impregnation of Pd and Pt onto SiO_2 followed the procedure described above but employed $Pd(NH_3)_4(OH)_2$ (5.5 mL) along with $Pt(NH_3)_4(OH)_2$ (5.5 mL) mixed with macroporous silica gel (Davisil Grade 643, 150 Å pore size, 35-70 μm mesh, 5.0 g). The mixture was calcined as described above for the impregnation of Pd onto oxide supports.

IMPREGNATION OF QUINONES ONTO Pd/C OR Pd/SiO_2

Quinones were used as received while commercial 5% Pd/C containing approximately 50 wt% water was dried for 3 h under reduced pressure at 70°C. Freshly prepared 3% Pd/SiO_2 was used directly after preparation as described above. A 20 mm x 250 mm disposable glass test tube

was charged with 0.03 mmol of a chosen quinone. Water was selected as the solvent for sodium anthraquinone-2-sulfonate **224** while organic soluble quinones employed EtOH. A measured amount (5 mL) of the appropriate solvent was added to the test tube to dissolve the quinone. Meanwhile, a round bottom flask was charged with 0.03 mmol Pd/C or Pd/SiO_2 which was suspended in 1.5 mL of the same solvent used to solubilize the quinone. The quinone solution was added to the suspended catalyst and stirred to mix, after which the mixture was allowed to rest at rt for 20 min. The solvent was removed under reduced pressure until a wet paste was observed in the round bottom flask. This solid was allowed to dry overnight in a vacuum oven (70°C, 0.015 bar) overnight.

REFERENCES

REFERENCES

239. Akkari, R.; Calmès, M.; Escale, F.; Iapichella, J.; Rolland, M.; Martinez, J. (R)- or (S)-4-(3-hydroxy-4,4-dimethyl-2-oxopyrrolidin-1-yl)benzoic acid as a new chiral auxiliary for solid phase asymmetric Diels-Alder reactions. *Tetrahedron: Asymmetry*, **2004**, *15*, 2515-2525.

240. Kuehne, M. E.; Horne, D. A. Photochemical cyclization of olefininc *N*-chloroamides. *J. Org. Chem.* **1975**, *40*, 1287-1292.

241. Schmidt, A.-K. C.; Stark, C. B. W. TPAP-catalyzed direct oxidation of primary alcohols to carboxylic acids through stabilized aldehyde hydrates. *Org. Lett.* **2011**, *13*, 4164-4167.

242. Yavari, I.; Karimi, E. *N*-hydroxyphthalimide-catalyzed oxidative production of phthalic acids from xylenes using O_2/HNO_3 in an ionic liquid. *Synth. Commun.* **2009**, *39*, 3420-3427.